UNIVERSITÀ DEGLI STUDI DI PADOVA

DIPARTIMENTO DI INGEGNERIA CIVILE, EDILE E AMBIENTALE

Department Of Civil, Environmental and Architectural Engineering

Master Degree in Environmental Engineering

Master thesis

Maritime and geotechnical modeling of the stability of coastal dikes in the Po river Delta lagoons

Supervisor:

Chiar.mo Prof. Giampaolo Cortellazzo

Co-supervisor:

Chiar.mo Prof. Piero Ruol

Graduate student: Nicolò Lucidi

2021416

ACADEMIC YEAR 2021-2022

ABSTRACT

The Po Delta region is characterized by a great value from an environmental and economic point of view but also by a huge hydrogeological fragility and a high hydraulic risk. These will increase due to the effects of climate change, the consequent sea level rise and the increase in the frequency with which extreme events occur. This fragility affects the development of the area, with the possible loss of landscape and economic resources such as fishing, shellfish farming and tourism.

This work aims to analyze the coastal dikes stability in the Po River Delta region, studying the main meteo-marine forcings and the geotechnical characteristics, to identify the critical sections, in a current scenario (2020) and in a future one (2070). The data used for this purpose regards the mean sea level rise, the wave set-up, the subsidence, and the geotechnical characteristics. The data related to the mean sea level rise come from the studies conducted by the IPCC, updated to the latest report provided (SROCC, 2019). While the geotechnical data are referred to the boreholes conducted by the AIPO in 2021. Thanks to the in situ and laboratory tests it was possible to characterize the soil and starting from these data perform the geotechnical modelling in PLAXIS 2D.

The result is the identification of the most critical areas but also the possible design interventions that must consider a series of elements, such as hydraulic-maritime (tidal level, wave run-up and overflow), geotechnical (seepage, piping and erosion) and socio-economic (maintenance and costs) aspects. The need to raise the coastal dikes is also demonstrated considering the effect of subsidence and the sea level rise. This is required to obtain a sufficient freeboard and guarantee a safety condition. It will be necessary also to proceed with a more detailed analysis especially in the lagoons where this has not been done in the past and where the geotechnical safety coefficient is higher than the limit indicated by law.

INDEX

INTRODUCTION

The aim of this study is to identify the critical aspects that characterize the coastal dike in the Po Delta region from a hydraulic, maritime, and geotechnical point of view. This to provide indications for the technical adaptation of the sections of the embankments, considering current and long-term risk scenarios. Deltas are transitional environments between land and sea created by the deposition of sediments transported by rivers. The morphology of this area is very dynamic since it depends on the variability of natural forces but also on the human activities. The investigated area is the Po Delta region, characterized by 60,000 hectares and includes the five lagoons analyzed: the Sacca degli Scardovari, the Caleri Lagoon, the Vallona Lagoon, the Barbamarco Lagoon, and the Canarin Lagoon. These areas are characterized by the presence of coastal dikes that separate the lagoon from the cultivated fields, which are almost completely below the sea level. Furthermore, following some extreme events, including those that occurred in the Venetian littoral in October 2018 and November 2019, localized erosions and instability of the coastal dikes occurred. These have also caused the reduction of the low sandy barrier, with a consequent repercussion on the lagoon system. The Po Delta in fact is an extremely sensitive area but of great value from an environmental and economic point of view. The economy of this region is based on activities like the agriculture, the fishing, the shellfish farming, and the tourism especially in the coastal area. There is also a strong value from an environmental point of view with the presence of coasts, lagoons, fishing valleys, floodplains, and sandy dunes.

The study was divided into several phases. First, the available data on lagoons and on the coastal dikes were collected. Then different scenarios were chosen to describe a current condition (2020) and a future one (2070). The scenarios were defined by selecting the wind intensity and the sea level, including the phenomenon of subsidence and forecasts of mean sea level rise. The data used are collected by the survey stations located in the territory. The data referred to the future sea level rise, instead, are provided by the IPCC, within the latest report (SROCC, 2019). The coastal dikes are subdivided in different sections, considering the location and the presence of systems like low crest structure, rock riprap protection and low sandy barrier. Then through a numerical modeling, the marine forcings (waves and levels) were evaluated. Subsequently, thanks to the use of the PLAXIS 2D software, it is possible to study the evolution of the system from a geotechnical point of view, highlighting the failure mechanisms and the seepage processes. These analyses allow to characterize each different sections, evaluating the most critical situation in terms of hydraulic-maritime and geotechnical conditions. Finally, the design indications for the adaptation of the coastal dikes, in the future scenario, have been identified.

The following thesis work is divided into six chapters. The first provides a general description of the coastal dikes, considering the structural characteristics, the materials used and the possible failure mechanisms. The second chapter describes the area of interest. In particular, its extension, the hydraulic and geotechnical problems and also its economic and environmental value. In this chapter the characteristics of all the lagoons studied are further described. The third one focuses on the meteo-marine forcings (level and wind), sea level rise and numerical modeling. Thanks to this, it was possible to identify the levels and the waves that impact on the coastal dikes. The geotechnical investigation, on the other hand, is described in the fourth chapter where the results of the in situ and laboratory tests are presented. However, it should be emphasized that these measurements were carried out only for the Sacca degli Scardovari while for the other lagoons it was necessary to introduce some assumptions. Finally, the geotechnical modeling, the study of the failure mechanisms and the seepage processes are described in chapter five. Thanks to this research it was possible to identify the criticalities in the system both in the current and future scenario. The results will be detailed exposed in the final conclusions of this thesis.

1. COASTAL DIKES

A sea dike is an artificial structure designed to protect the coastal areas from flooding. Their design is based on the structure's ability to resist against the actions of water, waves, and seepage condition. The coastal dike is made by different components like a crest, the top part of the structure that limits the wave run-up, a central part that can be subjected to wave impact during storms and a lower area that instead experiences constant water action.

1.1 A general overview

Coastal areas are among the most productive areas in the world for tourism, fishing and the environment characterized by different habitats and ecosystem services. However, especially in recent years, they are also the most vulnerable areas to climate change and natural hazards.

The main problems are related to the coastal erosion and the coastal flooding. The first one indicates the long-term loss of the shore material relative to fixed reference line and it is always accompanied with the shoreward recession of the shoreline. This can be done due to the action of the sea level rise, waves action, currents, tides, and human activities like changes in the river courses, alteration of the usual pattern of coastal currents and land subsidence (extraction of water and gas). The flooding instead occurs in coastal areas when high water levels due to storm surges, tide and the waves action, inundate the hinterland**.**

The most important works to defend the coastal areas can be separated into hard or soft measures depending on the construction materials and the impact on the shoreline. The hard measures are for example the coastal dike itself, groins, detached breakwaters and revetment, while the soft measures instead are related to the beach nourishment the low-crest structure like breakwaters but also the possibility to plant seagrass on the sea bottom.

In any case, it is important to note that both structural remedies against beach erosion and protection against flooding are very expensive. Therefore, they are used in many cases only when the socio-economic benefits outweigh the costs involved.

Italy with its approximately 8,300 km of shoreline (ISPRA) is a very sensitive area to these problems and in the future, this may be even more accentuated due to the sea level rise. One of the most endangered areas is the Po River Delta Region, also due to the subsidence resulting from the

extraction of water and gas in the past. After the flood of 1966 it was established that this site should be protected from the sea with two levels of dikes, that are, the first at sea and a second one instead backward. In addition, the most exposed sections must be protected through a breakwater, placed in front of the dike itself.

Figure 1.1: Vallona Lagoon.

1.2 Construction and materials

Dikes can be built in earth or concrete. Although this last one is more resistant to erosive actions due to currents, the structure is often made up with homogeneous silty and clayey earth, between type A6 of the CNR-UNI10006 classification with minimum sand content of 15% and type A4 with maximum sand content of 50% (Da Deppo, Datei, Salandin, 2019).

Generally, the materials are sand for the dike core and clay and clayey soils for the revetment, these last ones are used due to their low permeability and appreciable mechanical resistance.

The material used must be characterized by a high specific weight to ensure slip stability, a permeability not exceeding $10^{-6} \div 10^{-8}$ to contain filtration processes and good compaction to improve stability and tightness of the structure.

The lateral parts are then covered with grass to protect the dike from erosion induced by the current on the waterside and from runoff due to rainwater on the landside.

During construction it is necessary to proceed in suitably compacted layers with a thickness of $30 \div 40$ cm and verify the soil bearing capacity. The subdivision into several phases allows to obtain a better compaction through the mechanical equipment used today, moreover if the construction takes place too quickly there could be problems related to the stability of the structure. Before the construction of a new dike, it is very important to verify that the mechanical properties of the ground on which it will rest are like those of the embankment itself. If this does not happen, before the construction, it is possible to remove the surface layer and replace it with a more suitable material. While if the embankment already exists, it is possible to introduce other system such as those summarized below:

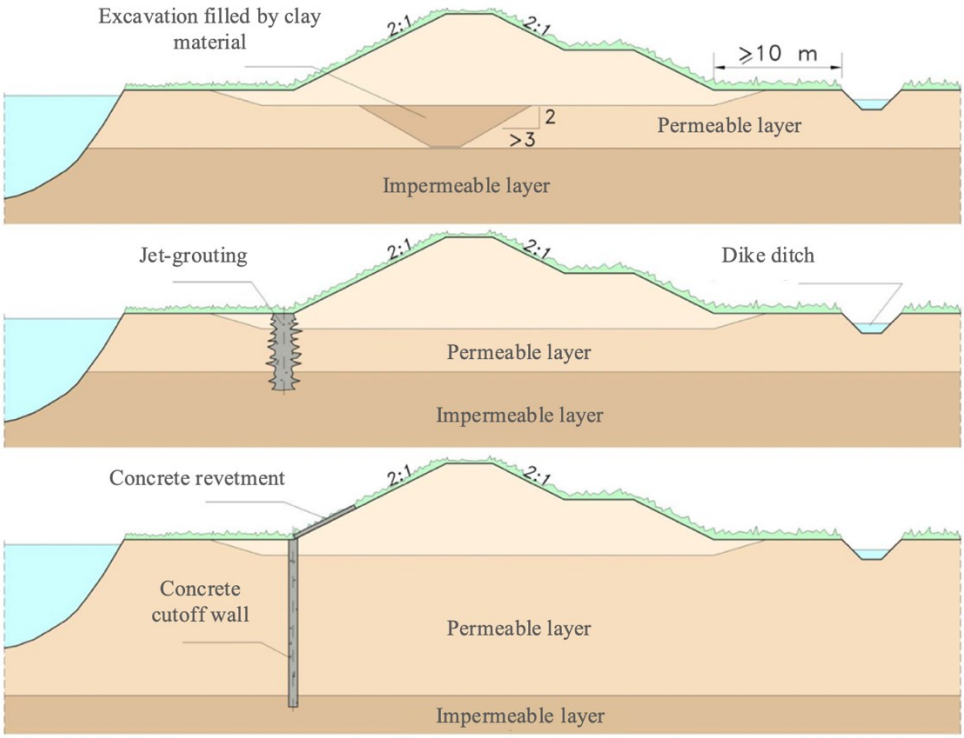

Figure 1.2: Excavation with clay filling, jet-grouting and concrete cutoff wall, translated by [Da Deppo, Datei, Salandin, 2019].

Another very important aspect is related to the fact that the upper level of a coastal dike, in the design phase, must be characterized by a greater value than what is expected to occur after a long period of exercise. Generally, a height greater of about 10% is considered (Da Deppo, Datei, Salandin, 2019). This obviously to remedy the possible failures that will characterize the structure over time, or the subsidence phenomenon.

A typical example is given by the Po Delta region, in fact, the extraction of methane and water from the subsoil between 1940 and 1960, led to a process of subsidence with the consequent lowering of the top, compared to the water level.

In absence of suitable material to create homogeneous embankments, often, it is necessary to introduce internal layers made by more impermeable materials or with other techniques. Typical examples are the presence of internal cores and impermeable cutoff walls (Figure 1.3):

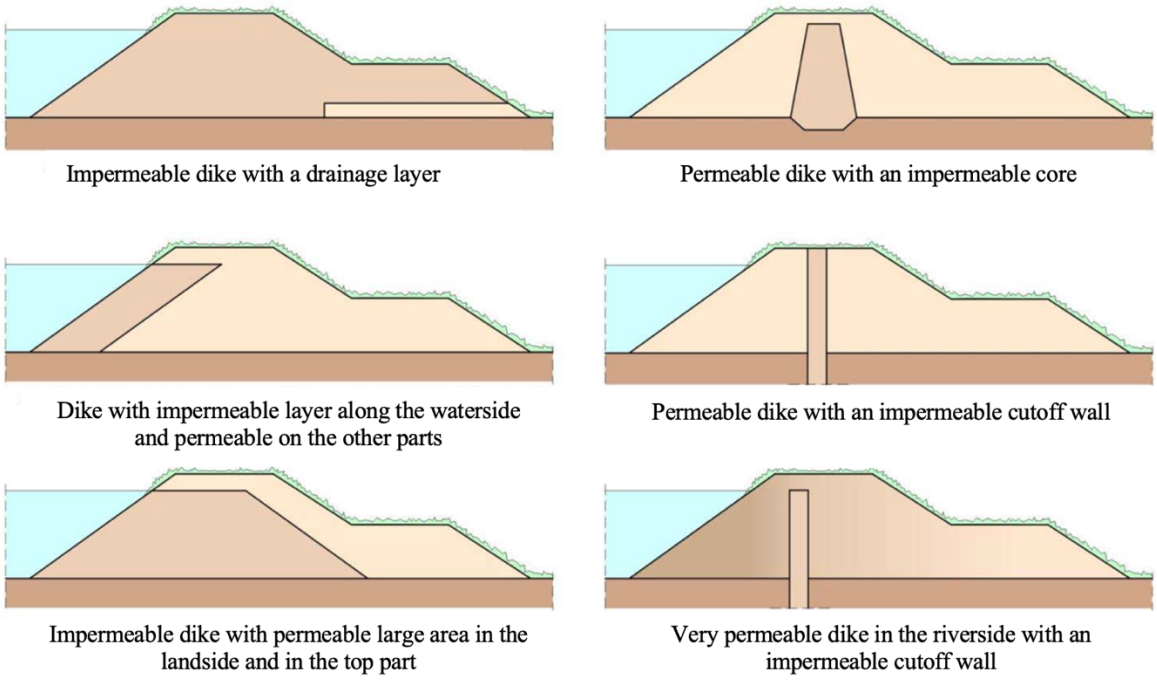

Figure 1.3: Construction with materials of different nature, translated by [Da Deppo, Datei, Salandin, 2019].

1.3 Structural characteristics

In the design phase, the height of the coastal dike is defined on the expected flood events and with reference to a return period (T_r) that varies according to the importance of the work but generally it is set as T_r = 200 years. It is important, however, to note that in the specific case of the Po River, as established by the Basin Authority within the *'Progetto di Piano stralcio per l'Assetto Idrogeologico'* (PAI), the return time for the design must be at least 200 years.

The maximum height of the coastal dike is then determined starting from the maximum flood level added to the water run-up and a safety factor called freeboard. Is important to note that the water run-up is the maximum onshore elevation due to the presence of the waves respect to the shoreline position without the waves. The freeboard, instead, is normally set equal to 1.00 m; however higher levels may be required based on the conditions of the environment and the hydraulic risk.

A very important aspect is related to the geometry of the coastal dike and the elements that compose it. These can be summarized as follows:

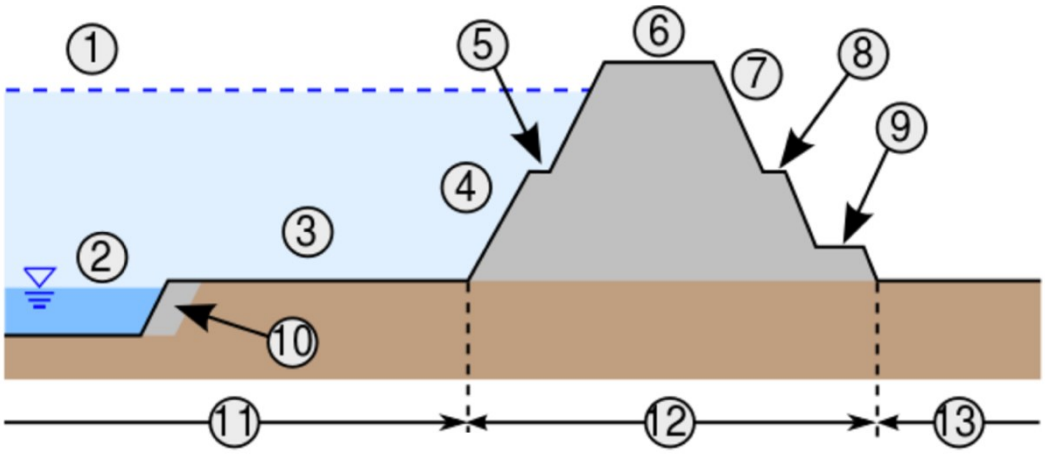

1. Design High Water Level
2. Low water level and foreland
3. Flood area
4. Waterside slope
5. Waterside banquette
6. Crown
7. Landside slope
8. Landslide banquette
9. Berm
10. Low water revetment
11. Seaward
12. Coastal dike core
13. Protected lowland

Figure 1.4: Coastal dike nomenclature.

First, it is possible to distinguish between the waterside that is the region between the dike and the sea, that can be flooded during storm surges, and the landside that instead is the area that must be protected by the work.

The top of the embankment called crown must have a minimum width of 4 ÷ 5 meters to ensure the passage of machinery for the construction and for the system compaction. The crown is not flat but convex with a slope ranging from 2% to 4% to facilitate the flow of water, thus avoiding accumulation and seepage problems.

The mean seaside or riverside slope (vertical : horizontal) must be at least 1:1,5 but generally for the stability is required a value of 1:2. The mean landside slope, instead, must be always higher than 1:2 and sometimes good values can be 1:3 or 1:4.

However, in the design phase, one of the most important elements to be considered is the costs. This aspect is not related to the soil itself and therefore of the material but rather its transport, which is why in some situations the material located in the surrounding area and, where possible, small dimensions works are preferred.

When the height of the dike exceeds 5 meters it is also necessary to build structures called banquette to ensure the stability. They must have a width, like that of the crown, that is 4÷5 m. The lateral banquette must be inclined towards the outside in such a way as to convey the water in the opposite direction from the structure. They must be no more than 5 m away from each other in a vertical direction and a cross slope of 5%.

To access the crown and the underlying banquette, up to the ground level, service ramps are set up with a slope of 10% and located every 500 m (Da Deppo, Datei, Salandin, 2019).

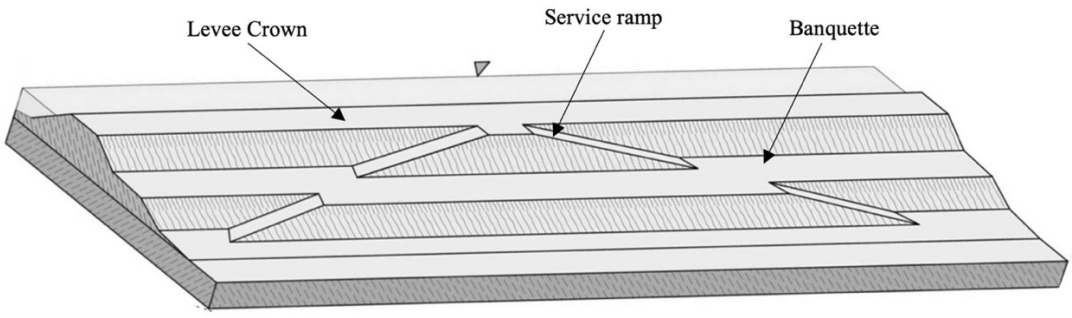

Figure 1.5: Service ramp to connect the crown and the banquette to the ground level.

1.4 Instability processes

There are many different causes that can lead to the instability of the system, some of which are induced by infiltration processes, others by localized erosion due both to the action of waves or currents and to the action of animals such as otters. One of the possible classifications concerns the distinction between the collapse mechanisms that occur landside or seaside (or riverside).

1.4.1 Landside failure mechanisms

The main causes that lead to the breaking of the dike on the landside are:

1) Overtopping: occurs when the water level exceeds the embankment itself. The causes are many, including a wrong design in terms of the maximum height, the presence of waves (overtopping by waves) or phenomena of subsidence due to withdrawals of water or gas from the subsoil. Following the overflow, the water flows towards the landside, hitting the base of the embankment and triggering an erosive phenomenon. The possible interventions concern the positioning of sandbags to limit it and the subsequent embankment rise as soon as possible.

2) Piping: this is the formation of a preferential path below the embankment through which the water passes, starting from the river side up to the landside. This can be related to multiple causes such as the presence of more permeable soil layers, wrong compaction of the embankment or the action of animals such as otters. To overcome this problem, it is possible to build an emergency structure downstream through sandbags whose height must be such as to ensure the exit of clean water. In fact, if the water is cloudy, it means that there is a phenomenon of removal of sand and earth below the structure itself. If, on the other hand, we want to solve the problem in a more lasting way, it will be possible to build a cutoff wall located in such a way as to interrupt the preferential path followed by the water. This can be built in concrete or by get-grouting.

3) Sliding: it consists in the movement of the slope towards the landside, following a very significant flood. This phenomenon can occur not only during the flood event but also during the decreasing phase, especially if this last one is very fast. Among the countermeasures we have the possibility of placing sandbags on the landside while on the waterside we can place boulders, pebbles, and waterproof sheets.

Other possible failure mechanisms are related to translation, rotation, and micro-instability movements.

Figure 1.6 summarizes the phenomena previously described.

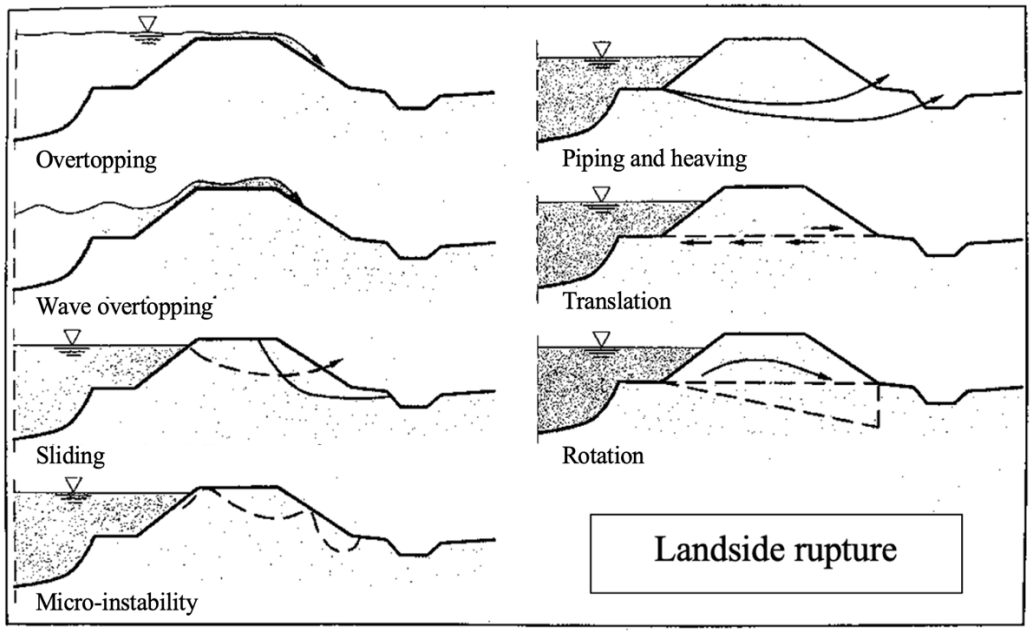

Figure 1.6: Landslide instability processes and collapse [Da Deppo, Datei, Salandin, 2019].

1.4.2 Seaside and riverside failure mechanisms

The main causes that lead to the rupture of the seaside or riverside dikes are:

1) Erosion: it can occur during floods when the strength of the current or waves that touch the surface of the dike exceeds the resistance of the earthy material that compose the structure itself. To limit this phenomenon and to avoid the collapse it is possible, immediately, to place stone or plastic sheets, while for long-term protection grass coverings, stones, or concrete plates are used.

2) Lifting due to erosion: occurs at the foot of a dike and can be caused by the erosive processes induced by the current. Recognizing this problem is difficult and consequently also the interventions, but one of the main signs that can be identified is related to the turbidity of the water in this region.

3) Sliding: consists in the movement of the lateral portion of the dike, in the waterside and it can occur with a reduction in the level of the flood after the maximum phase, especially if this has been prolonged in time. This can also be related to high tide which can slow down a rapid outflow of water into the sea. The saturation of the embankment soil and the simultaneous absence of hydrostatic thrust of the water causes an imbalance with consequent possible instability.

4) Wave impacts: due to the waves breaking against the main structure, erosive phenomena are formed with consequent instability of the system. To limit this process, it is possible to introduce a rock riprap made by boulders whose dimensions depend on the speed and amplitude of the waves. To avoid the sinking of the boulders it is necessary to stretch a geotextile layer.

Other significant processes can be the mechanical impact that occurs when objects such as boats collide against the dike, deterioration due to freezing and liquefaction, that is a loss of shear strength caused by dynamic loads, for example induced by a seismic event.

Figure 1.7 summarizes the phenomena previously described.

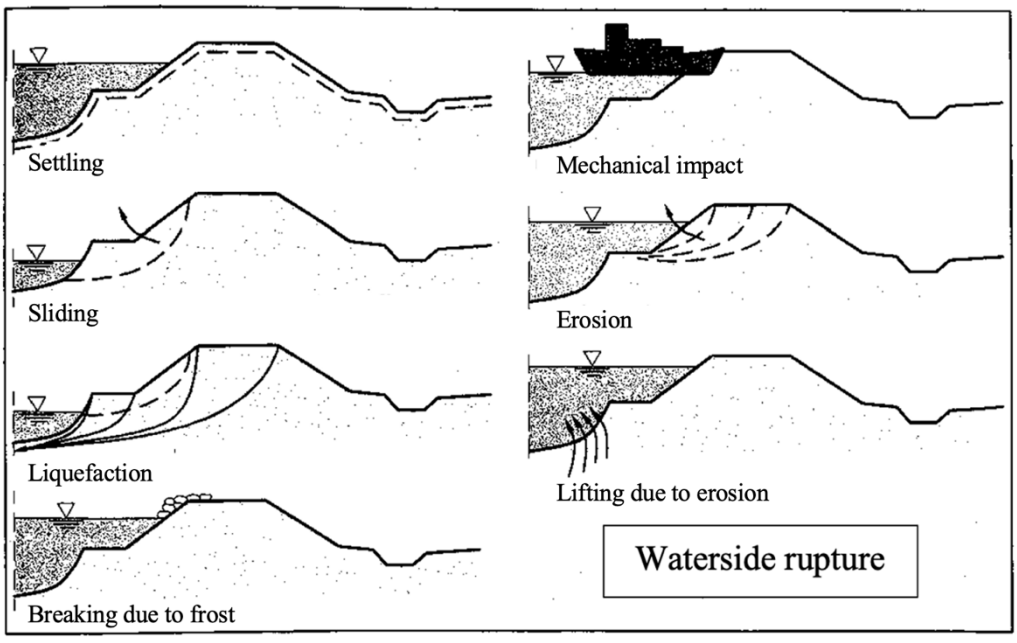

Figure 1.7: Waterside instability processes and collapse [Da Deppo, Datei, Salandin, 2019].

1.4.3 Infiltration processes

The presence of a filtration process across a coastal dike can remarkably affect the stability of the structure. One of the most important studies related to the seepage condition through an embankment was conducted by Pavlovsky, who assumed the presence of a trapezoidal embankment, made by homogeneous and uniform material, placed on an impermeable layer.

The most important characteristics of the structure are: b the length of crown, the slope angle α and β respectively in the upstream and downstream part, and the maximum height H. But are known also the water level h_0, h_1 and h_2, and the difference in height a_0, a_1 and a_2. This means that are known not only the geometric conditions but also the boundary ones. All the previous characteristics are summarized in the following schema:

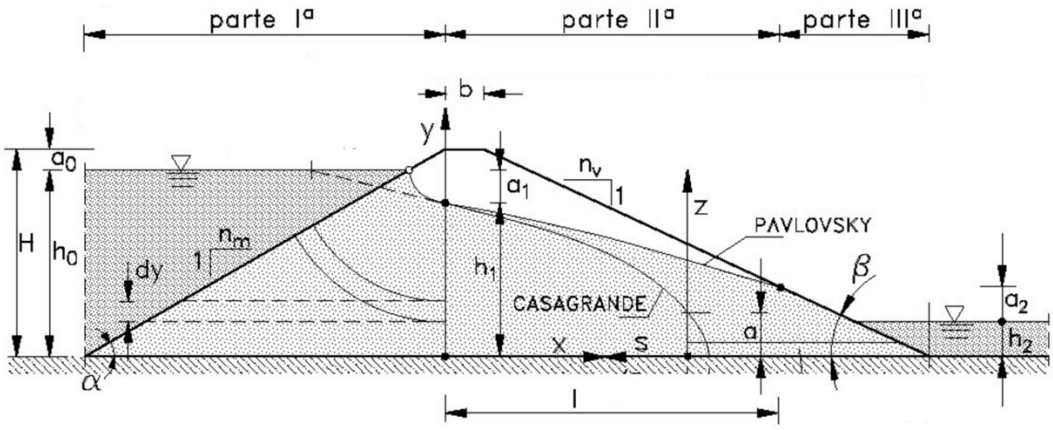

Figure 1.8: Pavlovsky filtration process.

The most important hypothesis are:

1. Homogeneous material
2. Steady state process so it is not time dependent
3. 2-D analysis
4. Dupuit hypothesis → vertical velocity is limited respect to the horizontal one, this is the reason why, generally it is neglected and as a consequence a hydrostatic pressure distribution take place along the vertical.

Once the x and y axes are fixed, the idea is to subdivide the body in 3 portions. The first one in the upstream part (I), the second one between the y axis and the vertical passing through the point where

the water table emerges (II) and the last in the downstream part (III). The aim now is to define the specific discharge q in each different section.

In the first part (I) is important to note that each generic flow path starts orthogonally from the upstream face and then progressively reduces its inclination. Pavlovsky hypothesized to replace this generic flow path with the horizontal one (dashed in Figure 1.9), that is characterized by the same width (*dy*), and it ends exactly in the same point of the previous (x = 0). At this point, defined as K the hydraulic conductivity and as v the Darcy velocity, the infiltration discharge is defined as:

$$dq = v \cdot dy \quad with \quad v = -K\frac{dh}{dx} \qquad \text{Eq. 1.1}$$

By substitution:

$$dq = -K\frac{dh}{dx}dy = K\frac{a_1 tg\alpha}{H-y}dy \qquad \text{Eq. 1.2}$$

To obtain the final discharge is necessary to integrate the previous function between 0 and h_1:

$$q_I = K(h_0 - h_1)tg\alpha \int_0^{h_1} \frac{1}{H-y}dy = K(h_0 - h_1) \cdot tg\alpha \cdot ln\frac{H}{H-h_1} \qquad \text{Eq. 1.3}$$

In the second part (II) instead the Dupuit relationship $q = -Ky(\frac{dy}{dx})$ must be integrated for x between 0 and l that is the length of the second part and for y between h_1 and $h_2 + a_2$:

$$q_{II} = K\frac{h_1^2 - (h_2 + a_2)^2}{2l} \qquad \text{Eq. 1.4}$$

The third part (III) can be instead separated into 2 different portions, the first one between h_2 and $h_2 + a_2$ and the second one that instead in characterized by a height lower than h_2:

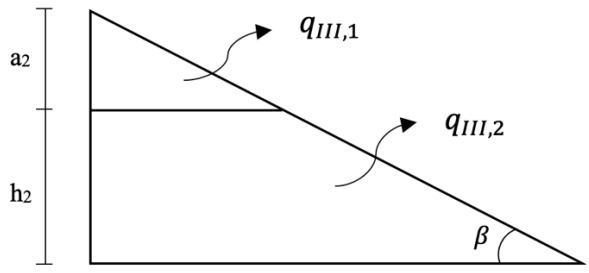

$$q_{III,1} = K \cdot tg\beta \cdot a_2$$

$$q_{III,2} = K \cdot tg\beta \cdot a_2 \cdot ln\frac{a_2 + h_2}{a_2} \qquad \text{Eq. 1.5}$$

Figure 1.9: Third part subdivision.

At this point of the problem, the unknowns are 4 (h_1, a_2, L and q) where, by continuity:

$$q = q_I = q_{II} = q_{III,1} + q_{III,2} \qquad \text{Eq. 1.6}$$

as consequence another equation is needed to complete the system, this is a geometrical relationship:

$$l = b + [H - (a_2 + h_2)] \frac{1}{tg\beta} \qquad \text{Eq. 1.7}$$

Now, there are four equations and four unknowns so the problem can be solved.

Is possible also to introduce a simplify approach, considering a homogeneous system without water downstream. In that case the Pavlovsky solution can be approximated through a straight line with a slope 1/5 ~ 1/6, starting from the water level upstream.

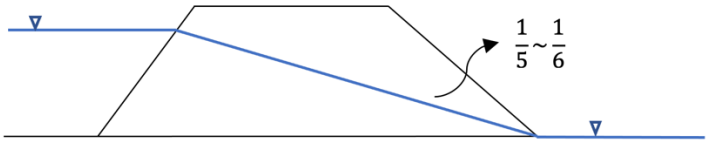

Figure 1.10: Pavlovsky solution in a simplify approach.

However, if we try to apply this solution to the real world, we can have a problem related to the formation of a seepage phase downstream, and a trigger for piping. Then the structure may collapse, due to a continuous deterioration.

1.4.4 Piping phenomenon

Piping is a phenomenon that consists in the progressive development of internal erosion by seepage, that leads to the formation of a hole downstream of the structure, through which the water can flow. Due to the effect of the difference in elevation between the water during flood condition and the outlet section of the system, the dissipation of energy along the flow path may not be sufficient to contain the value of the piezometric gradient below the critical value that gives rise the removal of the smallest soil particles.

The first sign of this phenomenon is linked to the presence of water emerging on the surface on the landside. Subsequently, the process leads to the lifting of the soil due to the action of underpressures,

furthermore, due to the swelling that is created, the water begins to filter through the raised grassy layer. The final state then occurs when the flow causes the removal of soil particles from the foundations of the structure and the consequent instability. The removed material is then deposited at the outlet forming an accumulation whose colors depend on the transported material.

Figure 1.11: Piping phenomenon below the levee of the Po River.

Due to this phenomenon, the consequent lowering of the crown can occur with the danger in terms of overtopping and landslide conditions.

Among the main causes we have the wrong sizing of the cross section, the inappropriate choice of building materials, wrong preparation of the foundation material on which the dike is then build, the presence of plants and roots in decomposition and finally the action of animals such as otters that dig their burrows inside the structure.

One of the most important interventions is based on the possibility to introduce sandbags that are placed in a proper way, in order to surround the point where the water comes out. This structure is called *coronella*. The height of this system must be such as to guarantee the flowing of clean water in the downstream part of the dike. The increase in height into the sandbags system reduces the hydraulic head difference between the river and the threshold of the structure and produces a velocity reduction. The consequence of this is that also the removal of earthy material is stopped.

It is important to note that it will be completely useless to obstruct the water outlet with sandbags or impermeable sheets because the result would simply be to move the water outlet in another location.

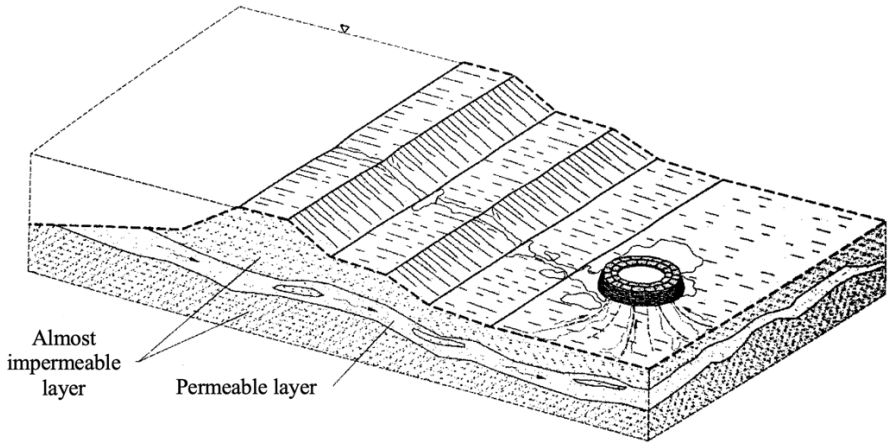

Figure 1.12: Piping phenomenon and sandbags protection system, translated by [Da Deppo, Datei, Salandin, 2019].

1.4.5 Heaving phenomenon

It is related to the possibility of lifting a portion of land in the area downstream of the work. The main discussion derives from Terzaghi's studies conducted on the filtration processes acting on a cutoff wall driven into the ground up to a depth S_0. The process is then studied comparing the forces acting on a control volume located downstream of the structure and with a height equal to S_0 and a width instead equal to $S_0/2$. In particular, the contributions involved are the vertical forces exerted by the water flow and oriented from the bottom up (uplift pressure) and the weight force of the ground which instead acts in the opposite direction.

Then defined the critical slope (i_c) and the exit slope (i_e) as:

$$i_c = \frac{\gamma_{sat} - \gamma_w}{\gamma_w} \qquad i_e = \frac{\bar{h}}{S_0} \qquad \text{Eq. 1.8}$$

where γ_{sat} is the soil specific weight in saturated condition, γ_w is the specific weight of water, $\bar{h}$ is the mean value of the hydraulic head along the length equal to $S_0/2$, and finally S_0 is the distance between the ground and the point of maximum depth that characterize the structure.

Heaving check can be considered satisfied if the safety factor F is greater than a reference value, proposed by Terzaghi, of 4÷5.

$$F = \frac{i_c}{i_e} \geq 4 \div 5 \qquad \text{Eq. 1.9}$$

2. THE PO RIVER DELTA REGION

This chapter presents the main aspects that characterize the Po and its Delta. The Po River is the main Italian river as far as length, about 652 kilometers, flow and surface are concerned. This last one extends for about 74,000 km^2 and is the largest river basin in Italy. It originates from Monviso, in Piemonte, crosses the Po Valley and flows into the Adriatic Sea, with a delta of 400 km^2 (ARPAV). The territory of the Po Delta extends over a very large area between the Adige River (Rosolina Mare) in the north and the Sacca degli Scardovari in the south.

2.1 Localization and characterization of the area

The actual coastal morphology of the Po Delta is very complex and is the result of both natural and anthropic events that have developed over the years and is divided into seven active branches, named Po di Levante, Po di Maistra, Po di Pila (Busa di Tramontana, Busa Dritta and Busa di Scirocco), Po di Tolle, Po di Gnocca, Po di Goro. The Po Delta extends over four municipalities in the province of Rovigo. Furthermore, due to the continuous supply of sediments, the system is still evolving.

Figure 2.1: Subdivision into branches of the Po Delta.

It is a very sensitive environment subjected to the variations induced by the river itself and the action of the waves and currents coming from the sea. However, its conservation is essential for its ecological and economic value, being the ideal place for fishing, tourism, and the habitat for numerous species of plants and animals.

One of the most important elements that characterize the studied lagoons is the presence of the low sandy island. These barriers, in the lagoon systems, represents the separation line between the lagoon and the sea. It is a sandy formation originating from the sediments transported by the rivers and then modeled over time by the action of the sea waves. Generally, this portion of land is characterized by the presence of a lush vegetation, especially on the lagoon side. This is very important to reinforce the low sandy islands. The Po Delta sandy barriers are characterized by a narrow and elongated shape, they are disconnected from the mainland, bathed to the east by the sea and in the internal part by the lagoon.

Their formation is very complex and require a considerable supply of sediments as well as their transport (longshore sediment transport). This movement is mainly due to the non-perpendicular direction with which the waves impact on the shoreline. In particular the sand, carried by the Po River, tends to accumulate in the area of the mouth, and then be transported along the shore by the action of waves and currents. However, these structures are not stable but undergo constant changes depending on the conditions of the surrounding environment, due to factors such as wind and waves. In the Po Delta region, the low sandy barrier protecting the lagoons studied are:

- Scanno del Palo (Sacca degli Scardovari)
- Scanno Cavallari (Vallona Lagoon)
- Scanno di Boccasette e Scanno del Gallo (Barbamarco Lagoon)
- Scanno Canarin (Canarin Lagoon)

They are the first natural defense for the lagoons from the sea. In fact, these protect the mainland from storm events and the wave action, but they are also a very important ecosystem for many species. The dunes and the vegetation on the low sandy island absorb the energy of the waves before that these hits the mainland. This means not only small waves but also fewer floods on the coast. A reduction of this protection can therefore lead to a greater action of waves and currents that can impact on the stability of the coastal dikes protecting the lagoon.

However, in recent years, these systems have suffered erosion caused by human activity such as vessel traffic and the construction of works along the upstream regions of the rivers which have

significantly reduced the contribution of sediments downstream. The effects of climate change are also of considerable importance, including the rapid sea level rise and the extreme weather conditions, which lead to a strong and continuous erosion of the low sandy barriers.

The current degradation from a hydrological point of view can be partly traced back to the phenomenon of subsidence linked to the extraction of methane and water from the subsoil starting from 1950. In the past, the area was characterized by deep canals and salt marsh that emerged only during the high tide; however, later there was a flattening and a change in the water conditions that negatively affected the recirculation and, as consequence, also the quality of the water itself. Starting from the 1990s, several works were carried out which led to an improvement in the environmental conditions of the area, thanks also to the PIM (Mediterranean Integrated Programs). Subsequently, the Veneto Region entrusted the Po Delta Reclamation Consortium with the implementation of measures to improve the hydraulic regime of the lagoons involved. Since 2006, a Scientific Committee has been established which, together with the Consortium itself, still has the task of identifying the most suitable methodologies and interventions in order to guarantee the management of the territory and protection from a hydraulic and environmental point of view. Among the main measure, the most important ones are the dredging of the canals and the formation of sandbanks in such a way as to partially recreate the diversity of the seabed and the passage of tidal currents.

Periodically, the Consortium carries out measurements regarding the hydrodynamic aspects in the lagoons, in particular the flow rates and the tide levels in different points of the region, starting from the sea inlets and the internal sections of greater importance, in order to have an indication of the trend of tides towards the lagoon margins. The investigations carried out in the past are not only fundamental for the maintenance of the works already built but also for the realization of new structures to limit the danger due to storm surges. With the rising of the sea, in fact, this region could be subject to high tide phenomena and the continuous impact of waves, which could make the existing structures unable to protect an area with such a high environmental and economic impact.

Indeed, already in the past, due to the reduction of the freeboard and the increase in depth of the seabed in front of the dikes, these last ones were insufficient to face with a marked impact related to the wave motion. Extreme storm events occurred along the Venetian coastline in 1957 and 1958. The combination of high storm surges and extreme waves caused extensive flooding and damages to the inland area. Furthermore, in November 1966, extreme sea levels caused a large breach along the Scardovari lagoon dikes. Particularly strong was the flood of 4 November 1966 during which the Po Delta was hit by extreme weather conditions with the concomitance of a significant flood event of

the Po River and the sirocco wind on the coast that did not allow the river to discharge its waters in the Adriatic Sea. A violent storm thus affected the area of Porto Tolle causing the destruction of its protective dikes, flooding the surrounding fishing valleys and the entire Isola della Donzella. Among the main causes that led to the breaking of the dikes, fundamental is the presence of extreme weather conditions with the persistence of low pressure which led to the sea level rise and the wave action from the sea. Furthermore, other causes are: the lack of suitable defenses from the wave, the erosion of the low sandy barrier in front of the Sacca degli Scardovari and the lowering of the top of the defense dike located between the Sacca degli Scardovari and the valleys from fishing areas, due to subsidence.

DATE	LOCATION	REASON	FLOODED AREA (he)
14/2/1952	Rosolina	Rotta arginale	580
04/12/1952	Isola Camerini	Rotta arginale	100
15/02/1953	Forti Maddalena	Overtopping	800
15/04/1953	Valle Ripiego	Overtopping	100
25/10/1953	Isola Camerini	Overtopping	1.900
05/01/1954	Busa Bastimento	Overtopping	330
31/01/1954	Busa Bastimento	Piping	300
05/07/1954	Sacca Scardovari	Piping	100
29/10/1955	Pila Barbamarco	Rotta arginale	150
29/11/1956	Sottobacino Pila	Wave action	300
10/04/1957	Isola Camerini	Rotta e piping phenomena	2.700
10/11/1957	Isola Camerini	Storm surge	3.500
11/11/1957	Valli Boccara e Raniera	Rotta arginale	6.000
12/11/1958	Sacca Scardovari	Sliding	100
04/11/1966	Sacca Scardovari	Storm surge and high tidal	10.000
04/11/1966	Valle Pozzatini	Storm surge and high tidal	360
04/11/1966	Porto Tolle	Storm surge and high tidal	150
04/11/1966	Valle Capitania	Storm surge and high tidal	300
04/11/1966	Boccasette	Storm surge and high tidal	150

Table 2.1: Main dikes failure between 1951 and 1966 (*Piano per la valutazione e gestione del rischio di alluvione*, 2016).

Table 2.1 summarizes the main dike failure due to the sea flood events in Po River Delta Region, between 1951 and 1966. It is important to note that the last significant see flood that affected the Po Delta area was that of November 4, 1966. After this event, in fact, thanks to the construction of reinforced dikes, that phenomena have been limited.

2.2 Po Delta lagoons

The Po Delta is characterized by 60.000 hectares, divided into approximately 42.000 ha of agricultural and inhabited land and 18.000 ha of wetlands. It is also divided into seven lagoons and "*sacche*", namely: Caleri Lagoon, Vallona Lagoon, Barbamarco Lagoon, Burcio Lagoon, Basson Lagoon, Sacca del Canarin and Secca degli Scardovari.

Figure 2.2: (a) Different Lagoons in the Po River Delta Region , (b) River levees and coastal dikes in Po River Delta Region (*Piano per la valutazione e gestione del rischio di alluvione*, 2016).

The area of interest is for the most part located lower than the mean sea level, on average 2 m, (but with peaks reaching 4 m), obviously excluding embankments and dunes. The Po Delta can then be divided into two parts: an external region that includes the lagoons and humid environments separated from the sea by coastal dunes and a more internal and closed region because it is included between levees as protection from the river and the coastal dikes.

The main characteristics for each specific lagoon are introduced in the next paragraphs.

2.2.1 Scardovari Lagoon

Located between the Po di Gnocca and the Po di Tolle, Scardovari Lagoon occupies an area of approximately 3300 he. In the past, until 1997, it communicated with the Adriatic Sea through a single 1700-meter-wide inlet placed perpendicularly to the south-east direction, subsequently a second inlet was opened near the Po di Tolle estuary. The seabed is not uniform especially in the region closest to the inlet due to the presence of both natural and artificial canals, while the central part is characterized by deeper and more uniform bottoms.

The formation of this lagoon can be dated back to the early 1600s mainly due to the works promoted by the City of Venice to avoid that the solid transport coming from the Po River, discharged into the Adriatic Sea, and pushed northward by the currents, could have had a negative impact on the Venetian lagoon. Really important was also the deviation of the main flow of the Po River, towards the east and south, which leads to a rapid expansion of the river Delta itself, originating the lagoons present today.

One of the most important studies related to the morphology of this lagoon were conducted on the initiative of the Po Delta Reclamation Consortium and summarized in the "Quaderno 0 Ca'Vendramin". Thanks to the maps and topographies, it is possible to observe the evolution of this region from 1950, as regards the lagoon itself and its seabed, the strip of land that separates it from the sea and the salt marsh. The possibility nowadays to use GIS system (Geographic Information System) allows not only to have more precise data but also to identify the areas where the interventions are most urgent. The bathymetric data of 1950, 1967, 1990 and 2008 are collected in the Geographic Archive of the Lagoons.

Considering Figure 2.3 it is possible to observe how in 1950 the Sacca Scardovari seabed was articulated with considerably different heights depending on the region analyzed, in particular it is important to note the presence of a single channel that become narrow as it flows into the lagoon. On the other hand, in the northern part and along the lateral banks it is possible to notice the presence of areas characterized by salt marsh and partially emerged areas depending on the tidal conditions. Instead, the sandbar *("scanno")* that separates the lagoon from the sea is clearly visible.

In addiction comparing the bathymetry of 1950 with the subsequent one in 1967, the differences are remarkable, starting from the lower visibility of the central channel following a more general increase in the water level. Furthermore, the areas covered by salt marsh in the region disappear not only in the central but also in the lateral part of the lagoon. This overall leads to a reduction in the

heterogeneity that instead characterized the region in previous decades, as well as the significant reduction of the sandbar between the lagoon and the sea. Among the main causes of this phenomenon, it is important to underline the subsidence and the storm surges that hit the area especially between 1950 and 1967, including that of 1966. A concomitance of factors therefore leads on the one hand to the attachment of large areas and on the other hand to a further erosion of the seabed especially in the central part of the lagoon which had already been deepened by subsidence. The action of the waves into the lagoon is also of considerable importance, especially in conditions of Scirocco wind, which can have an impact not only on the lagoon itself but also on its defense works.

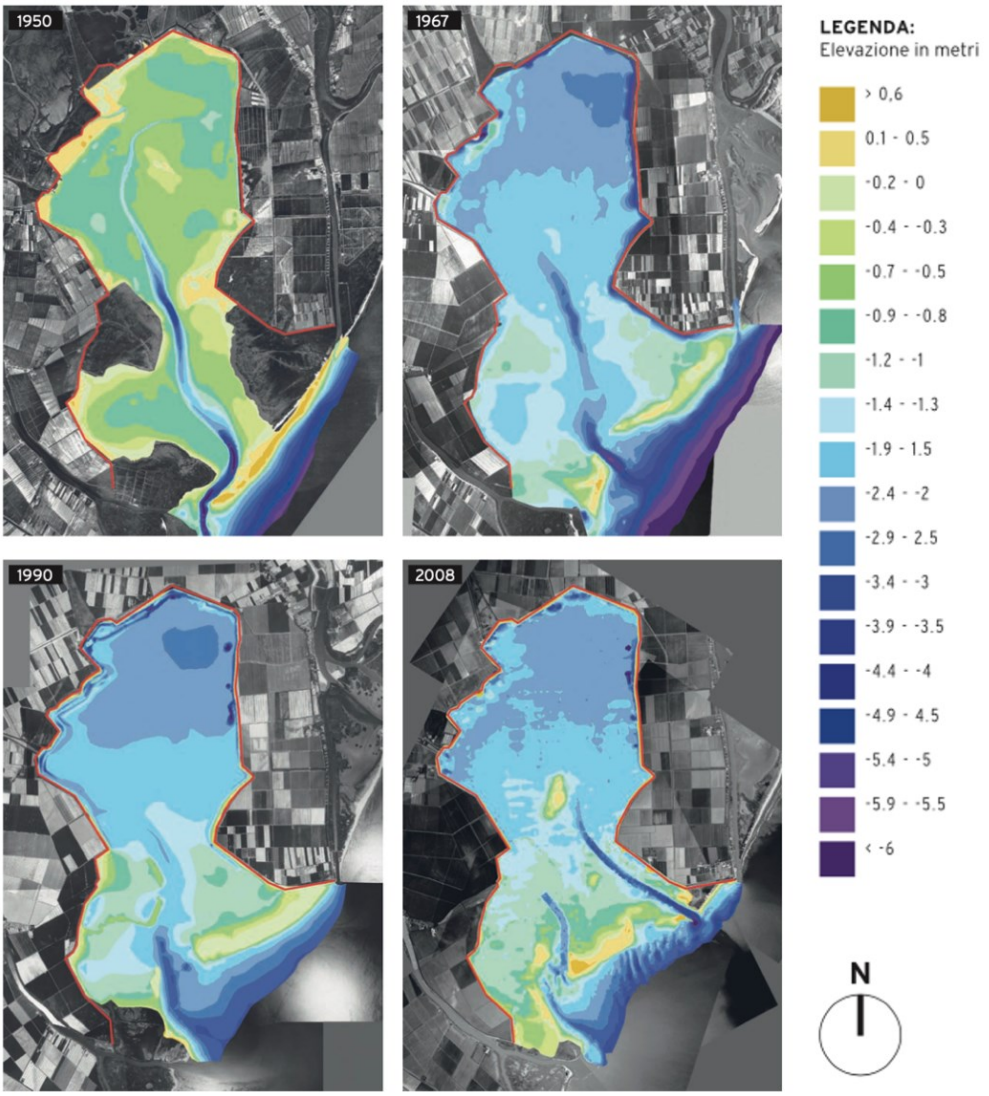

Figure 2.3: Altimetric models of the Sacca Scardovari built based on the bathymetric surveys available superimposed on aerial photos, in 1950, 1967, 1990 and 2008 *(Mattichio, Quaderni Ca'Vendramin, Evoluzione morfologica recente della Sacca degli Scardovari, 2009).*

In the following years, as confirmed by the bathymetry performed in 1994 and 2008, this process is characterized by a less visible variations than in the previous case. Of considerable importance, as shown in the bathymetry of 2008, is the excavation of the second inlet, which has significantly changed the morphology of the region. In particular, two channels, separated by the central sandbar, penetrate into the lagoon and also an emerged area appear at the center of the lagoon.

One of the most significant variations in the last 50 years involves the salt marshes *("barene")*, the structures rich in halophilic vegetation, so able to withstand high levels of salinity that characterize this region. The salt marshes are also located at higher level than the middle sea but strongly influenced by the tides, consequently they can be emerged or completely submerged. The Sacca degli Scardovari was characterized by a large area with the presence of salt marshes, however, nowadays, the extension has been significantly reduced especially in the central part. This is mainly due to subsidence and in the southern region due to the effect of storm surges. Furthermore, with the increase of this last one and the sea level rise, these areas are destined to be submerged.

Also, the low sandy barrier that separates the Lagoon from the sea, called as "*Scanno del Palo"*, has undergone significant transformations both in terms of size and position, due to the coastal sediment dynamics that affect this area. The evolution can be studied using the topographic maps of the IGM (Military Geographical Institute) GAI and ReVen, in the time between 1950 and 1990 as shown in the Figure 2.4:

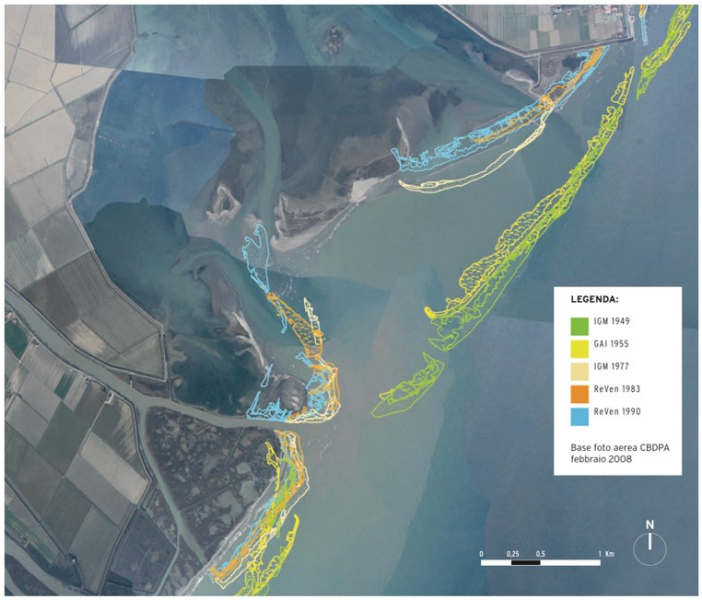

Figure 2.4: Scanno del Palo and salt marsh evolution in 1949, 1955, 1977, 1983 and 1990 *(Mattichio, Quaderni Ca'Vendramin, Evoluzione morfologica recente della Sacca degli Scardovari, 2009).*

In particular, it is important to observe how, between 1949 and 1955, the southern part of the sandbar disappeared, thus increasing the size of the inlet that connects the lagoon to the sea. However, the most important modification dates back to the period between 1955 and 1970, always linked, as in the case of salt marshes, to the combined action of subsidence and the coastal dynamic. In this period, in fact, the portion further to the sea disappears, thus limiting the division between the lagoon and the sea itself, thus reducing the protection against waves in the same way. Overall, we have a setback of the land strip and a decrease in terms of size, a conformation very similar to the current one. In fact, the only significant changes, in the following years, are a slight slub, especially around 1990, linked to the defense interventions, and in 1996 for the construction of a new inlet in the North.

2.2.2 Caleri Lagoon

The Caleri Lagoon is located between the Po di Levante and the Adige River. This region extends over an area of about 4000 he of which 1000 he of lagoon and 3000 he of fishing valley. It is in communication with the sea through the Caleri inlet and with the Vallona Lagoon (Bocca Pozzatini). Furthermore, the Caleri Lagoon receives a small amount of freshwater from a pumping station in the northern part.

Among the main activities that take place in the area, fishing and shellfish farming are certainly important, but also seaside tourism and environmental impact, with the establishment of the Botanical Garden. Also, for these reasons, the lagoon has always been subject to interventions aimed at maintaining its environmental conditions, including the expansion of the Bocca Pozzatini to allow greater recirculation of water, the construction of an artifact for regulating the tide and dredging of the channels. It is a constantly evolving area whose morphology has evolved thanks to the sea action, the accumulation of sediments transported by the river and anthropogenic activities.

2.2.3 Vallona Lagoon

The Vallona Lagoon is located south of the Caleri Lagoon, between the Island of Albarella and the Po di Maistra. It has an area of about 1150 hectares; in the region there are also nine fishing valleys which constitute a further extension of 3700 ha. The Lagoon is connected to the sea through the inlet of the Po di Levante, to the north, but also through a second inlet to the south, much smaller than the previous one and called “Bocchetta”. Furthermore, it is connected to the Caleri lagoon through the Pozzatini inlet. The lagoon is strongly affected by the river, in fact the Po di Levante flows directly into it, while the mouth of the Po di Maistra is only a few meters away. Consequently, these last ones

significantly influence the hydrodynamic of the area both in terms of water quality and morphology. The Vallona lagoon has shellfish farming as its main productive resource.

2.2.4 Barbamarco Lagoon

The Barbamarco Lagoon is located between the Po di Maistra and the Po Busa di Tramontana, with an extension of about 800 ha. In the region there are also four fishing valleys which constitute a further extension of 1800 ha. It is connected with the Adriatic Sea through the north and south inlets, whose extension is similar. The south inlet is more recent, and it is protected by a rock rip-rap. Fresh waters enter in the north part of the lagoon from the Po di Maistra and in the south corner from the Busa di Tramontana. The most important activities in this area are the shellfish farming and fishing. To safeguard these aspects, the Reclamation Consortium has conducted a series of projects such as the formation of new salt marshes, the excavation of canals and the refurbishment of the shoreline, on which psammophilous species, capable of strengthening the dunes, have been planted.

Figure 2.5: Aerial view of Barbamarco Lagoon (*Consorzio di Bonifica Delta del Po, Atlante lagunare costiero del Delta del Po, 2015).*

2.2.5 Canarin Lagoon

Canarin Lagoon is the southernmost lagoon of those analyzed, and in the past (especially in the 1970s), it was studied for the construction of the ENEL thermoelectric plant. The lagoon is limited to the north by the Po di Scirocco and to the south by the Busa di Bastimento. Fresh water enters into the lagoon from the north through an opening in the embankment and to the south through a narrow channel. In the past it was characterized by two inlets, one to the north and the other to the south;

however, around 1980 the south inlet began to reduce until it closed completely. The result of this phenomenon is the complete modification of the area with a decrease in water circulation. Furthermore, the seabed, previously sandy, has gradually become covered with a layer of fine clay and silt and has risen compared to the past. In the summer and winter periods the typical phenomena of biological and environmental problems with prolonged anoxia are present.

Figure 2.6: Northern part of the Canarin Lagoon on the left side while on the right the drainage channel of the ENEL plant *(Consorzio di Bonifica Delta del Po, 1950 – 2010 - 60 anni di bonifica del delta del Po, 2011).*

Table 2.2 summarizes the main characteristics of the lagoons, considering the total area, the average depth, the inlets cross section width and inlets average depth. It is important to note that the Sacca degli Scardovari is the largest in terms of surface and with the largest and deepest section. Vice versa, the Canarin Lagoon has the smallest total area and average depth.

Lagoon	Total area (km^2)	Average depth (m)	Inlet cross section width (m)		Inlet average depth (m)	
			North	South	North	South
Scardovari	28,1	1,6	225	845	4,4	0,9
Caleri	9,8	1,4	100		4,2	
Marinetta-Vallona	11,1	1,8	400		3,6	
Barbamarco	6,8	1,0	55	70	1,5	4,6
Canarin	6,4	0,9	200		1,2	

Table 2.2: Main Po lagoons features *(Maicu et al., Hydrodynamics of the Po River Delta Sea system, 2018).*

2.3 Hydraulic and geotechnical problems in the area of interest

Deltas are transitional environments between land and sea created by the deposition of sediments transported by rivers. The morphology of this area is very dynamic since it depends on the variability of natural forces like the sediment transport but also on the human activities. These last ones include, for example, the overexploitation of the natural resources, the agricultural land use, and the hydrological system alternation like the construction, along the river basin, of levees and hydropower plant. The Po delta region is subject to numerous natural and anthropogenic problems, some of which are linked to the past and others that could occur in the future.

One of the most important phenomena that have changed the conformation of the delta, in a definitive way, is the subsidence, which occurred especially in the period between 1940 and 1960, due to the extraction of methane and water from the subsoil. This phenomenon, which consists in the lowering of the soil, originated mainly from three factors. First of all, it is essential to consider the subtraction of water from the subsoil; in fact, the consequent decrease in water pressure causes the deformation of the soil, especially if these are characterized by clayey layers. In the Po Delta Region, the extraction concerned not only water but also methane, especially between the years 1950 and 1960. In this period, decreases of the order of 20-30 cm were observed every year. In fact, during the 1950s the gas was extracted from about 400 wells with an average depth of 350 m and with annual volumes extracted of hundreds of millions of cubic meters. This phenomenon continued until 1963, the date on which the Ministry of Industry suspended the extractions.

The second aspect, also this of considerable importance, is the drainage and modification of the most superficial layers of the soil following the reclamation events of lagoon areas and marshes, the presence of organic material exposed to the air has also led to the degradation of this last one and a strong reduction in terms of volume. In some reclamation areas with a huge presence of vegetable organic material, there have been reductions of tens of centimeters.

Finally, a third cause is related to the geological aspect linked to the consolidation of the materials that characterize the quaternary, however these phenomena contribute to subsidence with lowering rates of less than 1 cm per year, consequently very limited compared to the previous factors.

These phenomena have led to new problems in the delta and imposed the design and implementation of a series of defense and land management works, from river to marine ones, from reclamation to irrigation.

The lowering of the area produced, firstly, the complex instability of the reclamation and irrigation works. Furthermore, the river embankments underwent a modification in the filtration processes compared to those of the project, with greater and lasting water loads. Subsequently, due to the lowering of the coastal strip, there was a significant reduction in the sandbars that formed a defense system against the action of the waves. Consequently, with the increase in wave energy, erosive phenomena have also increased. This is the reason why it was necessary to reinforce the embankments and rebuild the sandbar as a protection system.

Until 1950 the sea defenses in the Po Delta mainly concerned the protection of reclaimed areas, fishing areas and the inhabited areas, thanks to the presence of small embankments lined with stones.

Between 1950 and 1968 the problem of defense from the sea becomes more significant especially due to the subsidence that had reduced or canceled the defense works freeboard, exposing the structures to the waves action. From 1950 to 1965 considerable works were carried out to modify the existing embankments with enlargements and rises to altitudes of +1.50 and +3.50 on the average sea, as well as the construction of breakwater and new coastal dikes.

Nowadays, the decision to reactivate the gas extraction in the upper part of the Adriatic Sea can determine the start of a new sequence of phenomena also with serious consequences for the coastal areas not only in the Po Delta Region but also in the Venice Lagoon. For this reason, since the late 1990s, institutions and technicians have focused their attention on the problem, setting up a monitoring system. However, it should also be noted that this last one may not always be adequate as the phenomenon of subsidence is not immediate but postponed over time with respect to the causes that generated it, and therefore lead to a late and irreversible response. According to Article 8 of the law of August 6, 2008, n. 133, it is also imposed that:

"Il divieto di prospezione, ricerca e coltivazione di idrocarburi nelle acque del golfo di Venezia…si applica fino a quando il Consiglio dei Ministri, d'intesa con la regione Veneto, su proposta del Ministro dell'ambiente e della tutela del territorio e del mare, non abbia definitivamente accertato la non sussistenza di rischi apprezzabili di subsidenza sulle coste, sulla base di nuovi e aggiornati studi, che dovranno essere presentati dai titolari di permessi di ricerca e delle concessioni di coltivazione, utilizzando i metodi di valutazione più conservativi e prevedendo l'uso delle migliori tecnologie disponibili per la coltivazione" (Conversione in legge, con modificazioni, del decreto-legge 25 giugno 2008, n. 112, recante disposizioni urgenti per lo sviluppo economico, la

semplificazione, la competitività, la stabilizzazione della finanza pubblica e la perequazione tributaria, agosto 2008).

Another very important problem that occurs in that region is the salt wedge intrusion. It is defined as the movement of water from the sea towards the hinterland through the subsoil, measured in p.s.u. (practical salinity unit) that is the ratio (K) between the electrical conductivity of a sample of sea water (T = 15 °C and p = 1 atm) and the conductivity of a solution of known concentration and under the same conditions of temperature and pressure. By a practical point of view, instruments such as conductivity probes are used.

In the Po Delta Region this problem has been considerably accentuated in recent years, particularly between 1950 and 1960. According to studies conducted by the Po Delta Reclamation Consortium, this phenomenon occurred no more than 2-3 km from the inlet, in the years 1970-1980 there was a rise up to about 10 km towards the internal part. Nowadays, on the other hand, in some cases the presence of the salt wedge intrusion was detected 20 km from the sea (*Po Delta Reclamation Consortium*). The Po Delta lagoons are in fact characterized by river branches connected by small channels whose contribution in terms of water volumes is essential for establishing the salinity trend in the lagoons. This is obviously strongly influenced by the exchange of water between the lagoons and the Adriatic Sea and mainly depends on the presence of fluvial inputs, sea currents and tides.

Thanks to the studies conducted by Maicu et al. and published in the "*Journal of Geophysical Research: Oceans" (2018)*, it is possible to have a more precise idea for each lagoon in the Delta system. In particular:

- Scardovari Lagoon: there is no evident salinity gradient because of the small freshwater input, mostly confined in the southern edge. Moreover, in front of the inlets, the surficial salinity is lower than inside the lagoon because of the buoyancy of the Po di Tolle outflow driven southward by the coastal current, so that the higher lagoon salinity comes mainly from deeper and mixed sea water (Maicu et al., 2018).
- Barbamarco Lagoon: the area between the two inlets has a slightly lower salinity than the sea.
- Vallona Lagoon: the scarce hydrodynamics confines freshwater in the inner basin (Maicu et al., 2018).
- Canarin Lagoon: the freshwater inputs are small, and the mixing between the freshwater coming from the Busa di Scirocco and sea water produce the variability of the salinity in the inlet region.

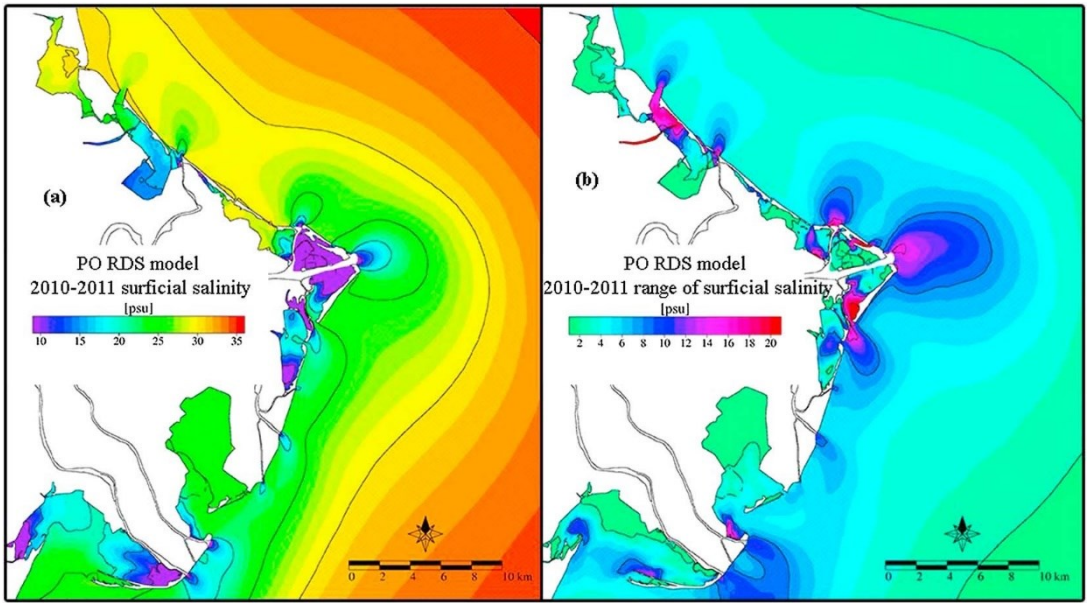

Figure 2.7: Calculated patterns of surficial salinity (a) and its variability (b) calculated as average of the daily range *(Maicu, F., De Pascalis, F., Ferrarin, C., & Umgiesser, G, Hydrodynamics of the Po River-Delta-Sea system. Journal of Geophysical Research: Oceans, 2018).*

Among the causes that led to this phenomenon, there are obviously some more general, that are related to the entire basin and other local ones, that are, associated with the Delta area itself. In particular, the general causes are, for example, the increase in the upstream flows for the hydropower production and the lowering of the riverbed due to the withdrawal of materials such as sand and gravel. Instead, the main local causes are the subsidence, the sea level rise, and the alteration of the Po Delta characteristics due to human activities.

Regardless of their nature, the salt wedge intrusion produces significant effects in the area, including the salinization of the underground water tables, and the inability to use water for drinking (aqueducts) and for agriculture. If the salt water penetrates through the coastal dike, it can cause a change in the surrounding ecosystem and a desertification of the area. To overcome these problems, therefore, it will be possible to intervene both locally with the construction of anti-salt barriers and storage basin and on the entire basin, in particular by increasing the releases of water downstream of hydroelectric works or lakes and the construction of mountain reservoirs.

The behavior of the Po delta lagoons has changed significantly in recent decades due to the reclamation and vivification processes. Starting from the 90s, thanks to the Integrated Mediterranean Programs (PIM), recovery works were carried out on the lagoons which led to an improvement in the environmental conditions and on the local economy. Subsequently, the Veneto Region entrusted the management of the Po delta lagoons to the Reclamation Consortium. The measures involved all the

lagoons. As for the Sacca degli Scardovari, with the PIM works carried out between 1995 and 1997, a second inlet was opened near the mouth of the Po di Tolle to obtain a better exchange of water in the lagoon. Furthermore, it was necessary to proceed with the dredging of the canals and the reconstruction of the salt marshes. At the end of the 1980s, the Caleri lagoon instead was characterized by a high condition of eutrophication with consequent damage to the local economy. For this reason, it was necessary to proceed with the dredging of the lagoon canals and to expand the Pozzatini estuary. The Vallona lagoon was also involved in these projects. In fact, the network of canals was modified, and four marshes were built. These last interventions were also carried out in the Barbamarco Lagoon. The material obtained from the dredging operations of the canals was reused to reinforce the low sandy barrier. The Canarin lagoon was the most studied environment. In fact, since the 1970s, ENEL carried out extensive research for the construction of the Polesine Camerini thermoelectric plant. These works became an important reference point for understanding the phenomena that characterize the area. Subsequently, the hydraulic adaptation and stabilization of the north inlet were also designed. As in the case of the other lagoons, it was necessary to proceed with the dredging of the canals.

The Po Delta Region is also subject to other phenomena and problems related to the sea such as waves action, persistence of tidal conditions and the mean sea level rise. All these events, which will be explored in Chapter 3 “Meteo-marine forcings”, can lead to erosive phenomena, floods, and failure mechanisms of the coastal dikes.

2.4 Economical and environmental value of the region

The Po Delta is an extremely sensitive area but of great value from an environmental and economic point of view. The area is characterized by a serious hydrogeological fragility and a high hydraulic risk, especially from the sea, attributable, as seen above, to the phenomenon of subsidence. This risk will be destined to increase due to the effects of climate change and the consequent sea level rise and the increase in terms of frequency with which storm surges occur. This fragility affects the development of the area both from an economic and social point of view, in particular about the construction of infrastructures, the quality of life and the efficiency of services.

The economy of this region is essentially based on activities such as agriculture, fishing, and shellfish farming but also tourism especially in the coastal area.

Agriculture represents an important source of income for the local economy, but the sector is threatened by the problem of the flooding of cultivated fields and by water shortages due to the reduction of the Po River flows along its path, and for the salt wedge intrusion. In this context, the Delta Po Reclamation Consortium guarantees drainage and irrigation activities for farms, making it possible to obtain excellent products such as rice from the Po Delta and "Radicchio di Chioggia", both recognized by the title IGP (Protected Geographical Indication).

Some other very important sources of income are fishing and aquaculture, especially if we consider the coastal area, the fishing valleys, and the lagoons where there are numerous mussel and clam farms. Fishing in this area can be carried out with fixed or mobile nets depending on the species caught and the trend in market prices. Among the main species that inhabit the area we have shrimps, crabs, eels, mullets, and sea bream. However, estimating fish production in the lagoon is very complex, especially due to the impossibility of quantifying the fish that is sold through alternatives to those of the large fish market. However, if we refer exclusively to the main fish markets (Scardovari, Pila and Donada) and sampling on the catch, the average productivity between 2007 and 2008 was estimated at 4.500 quintals, with variations related to the months of the year and biological cycles of the single species. Obviously the most productive seasons are spring and summer (monthly productions between 400 and 600 quintals per month), while the least productive is winter (between 50 and 150 quintals per month). Fishing is also fundamental not only in terms of earnings but also from an employment point of view, in fact, about 20% of workers in the Delta area, are involved in the primary sector (Consorzio di Bonifica Delta del Po, *Atlante lagunare costiero del Delta del Po*, 2015). However, this is a sector in crisis, above all due to the reduction of fish available in terms of quantity and variety of species.

Figure 2.8: Fishing and aquaculture systems in Sacca degli Scardovari *(Consorzio di Bonifica Delta del Po, Atlante lagunare costiero del Delta del Po, 2015).*

As for shellfish farming, production is mainly based on clams and mussels; in fact, the environment of the lagoons, characterized by the presence of variations in salinity due to the fresh water transported

by the Po River and the salt water of the sea, is ideal for their growth thanks to the presence of microalgae and phytoplankton. Aquaculture is also a very important economic activity for the area, both in terms of turnover and the number of people directly involved not only in the form of cooperatives operating in the sector but also of small families that obtain concessions or fishing permits.

Fishing areas (Tapas)	Water surface (ha)	Production area (ha)	Effective yield (kg/m^2)	%
Caleri - Marinetta	1.653	423,56	0,72	29
Vallona	703	111,36	0,79	8
Scardovari	3.000	320,00	1,52	32
Barbamarco	800	50,00	3,53	17
Canarin	850	50,00	2,99	14
Basson	375	0	0,00	0
Total lagoons	7381	854,92	1,23	100

Table 2.3: Tapas production in the Po Delta River (Donati, Le lagune del delta del Po, 2013).

In Table 2.3 it is possible to observe how the clams farming (Tapas decussatus) involves all the main lagoons in the Po Delta, with a total area of 7381 ha. The territories characterized by a greater production are the Sacca degli Scardovari and the Caleri-Marinetta Lagoon.

Regarding the tourism, the key aspect is linked to seaside tourism due to the presence of beaches such as Rosolina and Porto Tolle. According to the data provided by the Veneto Region (2016), these two locations respectively welcome approximately 1.6 million and 220.000 visitors each year, mainly concentrated during the summer period. The other municipalities that make up the area of interest, on the other hand, are affected by tourist flows especially on weekends and not only linked to the sea but also to river and lagoon navigation, trekking, food and wine and visits to protected sites, parks, and natural resources. The presence of numerous ecosystems such as the river itself, the lagoons and the Adriatic Sea has allowed a rich biodiversity and unique landscape offer, all elements that have favored the development of services and businesses. Obviously, the economic boost given by tourism was fundamental for the development of this region, with a continuous increase in the accommodation offer of hotels, holiday homes and farmhouses, and consequently also for the creation of new jobs.

In Table 2.4 are collect the data in terms of arrivals, attendance, and average stay period for the main municipalities of the area of interest.

MUNICIPALITY	TOTAL (HOTEL + ADDITIONAL)		
	Arrivals	Attendance	Average stay
Ariano del Polesine	1.076	5.144	4,8
Loreo	1.141	3.004	2,6
Porto Tolle	39.266	221.322	5,6
Porto Viro	3.330	14.037	4,2
Rosolina	217.077	1.673.659	7,7
Taglio di Po	6.554	18.752	2,9
Total	267.303	1.932.914	7,2

Table 2.4: Arrivals, attendance, and average stay period in the municipalities *(Area interna contratto di foce Delta del Po, 2019)*.

There is also a strong value from an environmental point of view with the presence of coasts, lagoons, fishing valleys, floodplains, and sandy dunes. To protect these territories and the species of plants and animals that populate them, the Veneto Regional Park of the Po Delta was established, which extends from the Adige River to the Po di Goro. This area has the largest wetland in Italy with thousands of different species, including numerous mammals and birds. In addition, on June 9, 2015, the Po Delta was recognized as a MAB Biosphere Reserve by UNESCO. This last one aims to identify terrestrial and marine ecosystems where, thanks to the management and respect for the territory, it is possible to enhance the ecosystem, biodiversity, and sustainable development. This in turn implies a commitment to landscape conservation, research and awareness raising. Finally, in the Po Delta region there are also sites belonging to the 2000 Network and Important Bird Areas.

Figure 2.9 : (a) Porto Caleri Botanical Garden, (b) Rosolina mare *(Parco Naturale Regionale Veneto del Delta del Po).*

The conservation of the area is therefore fundamental not only for an economic issue linked to fishing, shellfish farming and agriculture but also for the protection of such a delicate environment where different species of animals and plants live in unique landscapes. This means that is necessary to carefully study these environments and find solutions in order to protect them not only nowadays but also in the future taking into account climate change, the mean sea level rise and the consequent mutation of the lagoon, coastal and delta region.

3. METEO-MARINE FORCINGS

The coastal environment is a dynamic system constantly changing and subject to the action of terrestrial and marine forcings. The study of coastal defense works must, therefore, consider numerous aspects including the variation in the sea level, the tides, the wind and the storm surges. The intensity of these phenomena can be studied starting from the numerous data obtained from the monitoring stations in the area and their processing through mathematical and physical models.

3.1 The sea level forcings

The meteo-marine forcings are the wind and the sea level. This last one must consider not only the mean sea level rise but also the wave set-up. The concomitance of adverse events such as the occurrence of the astronomical maximum tide, the low pressure conditions and strong winds (Scirocco and Bora), have led in recent years to extreme tidal levels with significant damages to the Adriatic coast.

Among these, of great importance was the event of November 12, 2019, occurred in the Venetian littoral, with a maximum level equal to 187 cm, recorded at Punta della Salute at 22:50, the second highest value ever measured in this area. The event was characterized by exceptional conditions and a combination of factors. In particular, an astronomical tidal peak with a severe storm surge generated by a strong wind and a strong pressure drop occurred in that region. (*Favaretto C. et al., 2021*).

The region was then hit by a cyclonic vortex characterized by winds, which according to the data provided by the station at the CNR platform "Acqua Alta" (Venice), also reached speeds of 110 km/h (maximum wind gust 31.5 m/s). The combination of these phenomena, with the action of the waves and wind, has caused great damages to the city of Venice, the coastal area, and the regions of the Po Delta. Here, because of the exceptional level and wave conditions, considerable damages have occurred, especially in the Sacca degli Scardovari.

Considering that the sea level in the North Adriatic is 34 cm higher than the zero level of Punta della Salute (*Ferrarin et al., 2019*), the exceptional tide of 12 November was determined by the coincidence in time of the maximum of the astronomical tide, equal to 26 cm, and the meteorological maximum of about 127 cm.

In reality, the maximum peak of 187 cm was recorded only in the city of Venice. As can be seen in Figure 3.1, in fact, there is a considerable difference between the level recorded at the Punta della

Salute station (187 cm), Chioggia and the north lagoon, depending on the direction and intensity of the wind.

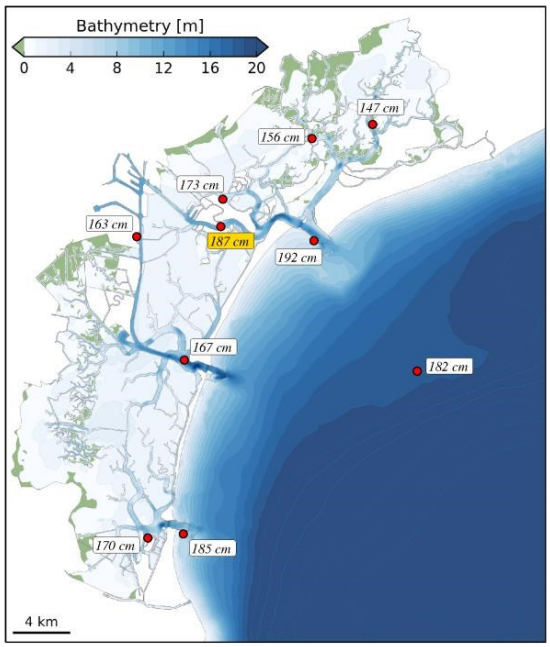

Figure 3.1: Maximum levels recorder on November 12, 2019 *(Ferrarin et al., 2019).*

Although the meteorological contribution induced by wind and pressure was lower than other events that occurred in the past, for example the exceptional tide on November 4, 1966, and the storm Vaia (October 28, 2018), the damage for the city was considerable. This has once again made evident the need to study these phenomena, to improve prevention, protection, and alarm systems as well as showed the necessity to study the undergoing climate changes, with its resulting sea level rise and the occurrence of increasingly intense storms.

3.1.1 Tidal levels

Tide is the slow oscillation of the sea level caused by the gravitational attraction of the Moon and the Sun acting on the water particles in the hydrosphere. In spite of the much larger mass of the Sun, due to the greater distance from the Earth, solar attraction plays a lower role (approximately 46% of lunar attraction). The biggest contribution is, therefore, given by the Moon. It is possible, however, to distinguish between the astronomical tide linked to the motion of heavenly bodies and the meteorological tide due to atmospheric conditions. In the absence of perturbations, the meteorological contribution is generally limited, vice versa in the presence of strong winds and low pressure this contribution can be significant.

The Adriatic Sea, in fact, is closed in the upper part and open in the lower one, and consequently a strong Sirocco wind, blowing from the south-east, can produce an accumulation of water towards the upper region. This phenomenon, favored by the long action area available for the wind, named as fetch, is then further accentuated by the presence of the shallow waters that characterize the northern Adriatic Sea. Furthermore, the atmospheric pressure alters the sea level with an inverse barometric effect, it means that a decrease in pressure corresponds to an increase in the sea level and vice versa.

During the phases of new moon and full moon, that is when the Sun-Earth-Moon are aligned, the effects add up, determining the maximum tidal fluctuations. This phenomenon is called spring tide. In the first and last quarter periods, however, the tide is less wide and regular in fact the Sun and the Moon attract the water in opposite directions. This phenomenon is called neap tide.

According to the method of harmonic analysis, the astronomical tide, in a specific place, can be calculated as a superposition of sinusoidal oscillations, each characterized by its own amplitude and phase. In Venice, for example, eight harmonic components are sufficient to describe the astronomical tide with a precision in the order of 1 cm (*Municipality of Venice*). These components are described individually in the following table.

Tidal type	Symbol	Description
Semidiurnal	M_2	Principal lunar tide
	S_2	Principal solar tide
	N_2	Monthly variation in lunar distance
	K_2	Changes in declination of Sun and Moon
Diurnal	K_1	Solar-Lunar constituent
	O_1	Principal lunar diurnal constituent
	P_1	Principal solar diurnal constituent
Longer	M_f	Moon’s fortnightly constituent

Table 3.1: Tidal components.

In the Nord Adriatic region, the tide is semidiurnal, with two high and two low tides occurring in 24 hours.

The levels area obtained starting from the data of four stations, all located near the Po Delta. In particular, as shown in Figure 3.2, from North to South:

- Chioggia - Diga Sud (Municipality of Venice): recording interval of 1 hour and time series between January 1, 1984, and October 11, 2020.
- Porto Caleri (ISPRA): recording interval of 10 minutes and time series between January 1, 2000, and December 1, 2019.
- Pila SIAP (AIPO): recording interval of 30 minutes and time series between January 1, 2000, and July 15, 2020.
- Porto Barricata (ARPAV): recording interval of 30 minutes until May 2020 then the system was implemented, and it was possible to obtain a data collection every 10 minutes. The time series is between May 15, 2013, and September 30, 2020. The station is located at 0 m s.l.m.

It is very important to observe how in the case of the first two stations (Chioggia and Porto Caleri) the altimetric reference is mZMPS (1897), i.e., the sea level measurement is carried out with reference to the zero-tide gauge of Punta della Salute. On the other hand, in the case of the station near Pila, the orthometric or geoid level is located at Z.I. = - 0.319 m, while in Porto Barricata it is not defined.

Figure 3.2: Location of level (a) and wind (b) measurement stations.

This system can provide the data about the water level, given by the sum of several contribution:

1. The astronomical tide: changes in water level, that occurs every time and easy to predict.
2. Sea level rise and subsidence: if the ground goes down, it looks like the water goes up, and this is randomly variable in the long term and mainly time dependent. The subsidence is in the order of a few millimeters per years if it is a natural subsidence.
3. Non tidal components: randomly variable caused by the surge and dynamic effects.

Generally, the measured water level is the sum between three components, the astronomical tide (η_A), the mean sea level (MSL) and finally other contributions given by the climate condition or storm surge (WL):

$$\eta(t) = WL(t) - MSL(t) - \eta_A(t) \qquad \text{Eq. 3.1}$$

To evaluate the MSL (Mean Sea Level) over time, it is possible to refer to historical time series such as the one provided by the Punta della Salute station in Venice, belonging to the Mareographic Network of the Venice Lagoon and the North Adriatic coastal arc (RMLV). This allows us to observe the annual average values starting from 1872 to 2020 as indicated in the following table:

Year and decade	**0**	**1**	**2**	**3**	**4**	**5**	**6**	**7**	**8**	**9**	**Mean**
	cm	**cm**	**cm**	**cm**	**cm**	**cm**	**cm**	**cm**	**cm**	**cm**	**cm**
1870	n.d.	n.d.	0,3	-1,5	-9,2	-9,0	-1,2	0,5	-0,4	4,5	***-2,0***
1880	-5,9	-1,5	-5,4	-4,3	-7,8	0,0	0,1	-3,6	-0,8	-0,4	**-3,0**
1890	-2,3	-2,2	3,2	-1,0	-3,2	7,2	-1,2	2,2	0,7	-2,7	**0,1**
1900	4,9	3,1	3,5	0,8	2,1	3,3	3,1	0,8	-2,5	6,3	**2,5**
1910	11,4	4,3	1,3	-0,6	8,1	15,5	13,9	5,6	4,1	9,5	**7,3**
1920	7,0	-3,5	3,3	6,8	3,7	4,4	7,9	7,6	5,6	0,8	**4,4**
1930	8,3	10,0	4,7	8,4	9,6	10,1	14,5	17,7	6,3	12,7	**10,2**
1940	13,7	15,7	10,9	6,2	11,4	11,0	12,9	15,3	10,7	5,0	**11,3**
1950	11,5	21,7	16,3	12,5	14,6	18,9	15,2	14,0	18,8	15,8	**15,9**
1960	25,1	21,2	20,3	22,9	14,5	21,5	24,9	19,5	21,9	26,8	**21,9**
1970	24,4	23,0	21,4	18,1	20,7	18,9	19,5	21,2	22,7	25,4	**21,5**
1980	22,7	22,9	21,7	20,3	24,4	21,9	23,1	25,8	22,1	16,5	**22,1**
1990	16,8	19,1	18,4	18,9	22,7	22,5	27,6	24,4	24,3	25,6	**22,0**
2000	25,8	28,2	27,7	23,8	27,6	25,4	25,7	24,1	27,8	33,4	**26,9**
2010	40,5	29,5	29,5	36,5	40,0	31,6	33,0	28,8	36,1	35,5	**33,9**
2020	32.37 (31.93)										***32,4***

Table 3.2: Average annual and decennial values of the mean sea level in Punta della Salute *(ISPRA)*.

In the year 2020 there are two different values due to the activation of the Electromechanical Experimental Module (MoSE). The first refers to the mean sea level recorded in Punta della Salute, including the values during the closing of the mobile barriers. The second, on the other hand, indicates the sea level in Punta della Salute integrated with the average daily sea level calculated at Platform Acqua Alta (8 nautical miles off the Venetian coast), on the days when the mobile barriers are closed. Between 1972 and 2020, the average sea level increased by an average of 2.53 mm per year with a non-uniform trend over the time and it is mainly linked to the phenomenon of subsidence (natural and artificial) and eustatism on a global scale.

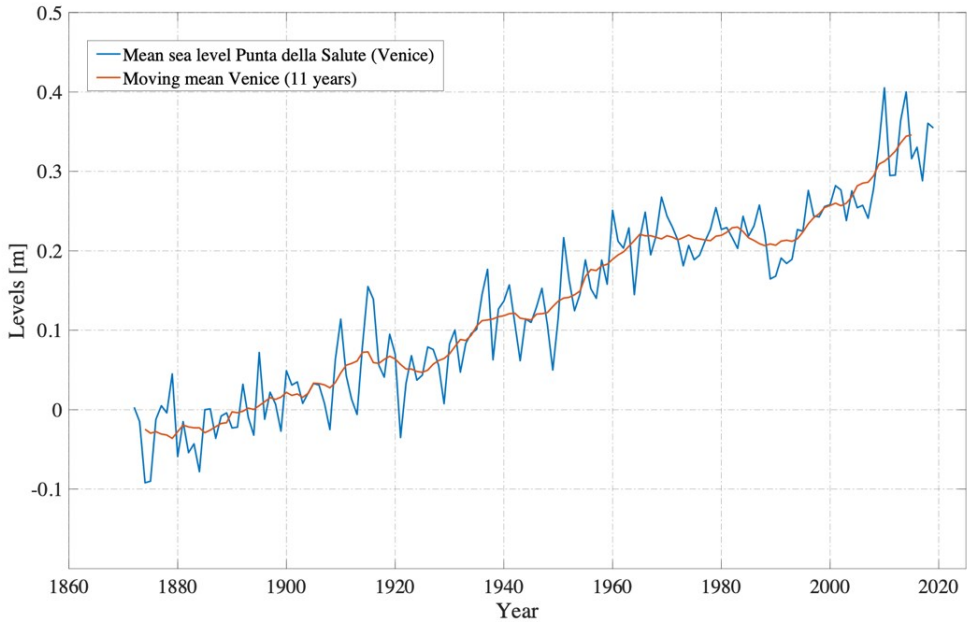

Figure 3.3: Annual trend of the mean sea level in Venice and moving mean (11 years).

As for the Scardovari Lagoon, the closest survey station is at Porto Barricata, however, due to the lack of data before May 15, 2013, it is possible to combine the data with the much longer numerical series relating to the Chioggia station, and then compare the results. In particular, it was chosen the time interval common to both, this means the period between May 15, 2013, and September 2020.

However, it is important to observe how unlike the Chioggia monitoring station where the elevation reference coincides with the Z.M.P.S. (1897), in the case of Porto Barricata station the reference is not defined. For this reason, comparison of the two series is needed. In the following picture (Figure 3.4) it is possible to observe the average daily hydrometric level obtained from station at Chioggia (Diga Sud), and the comparison with the station of Porto Barricata (n° 552 ARPAV).

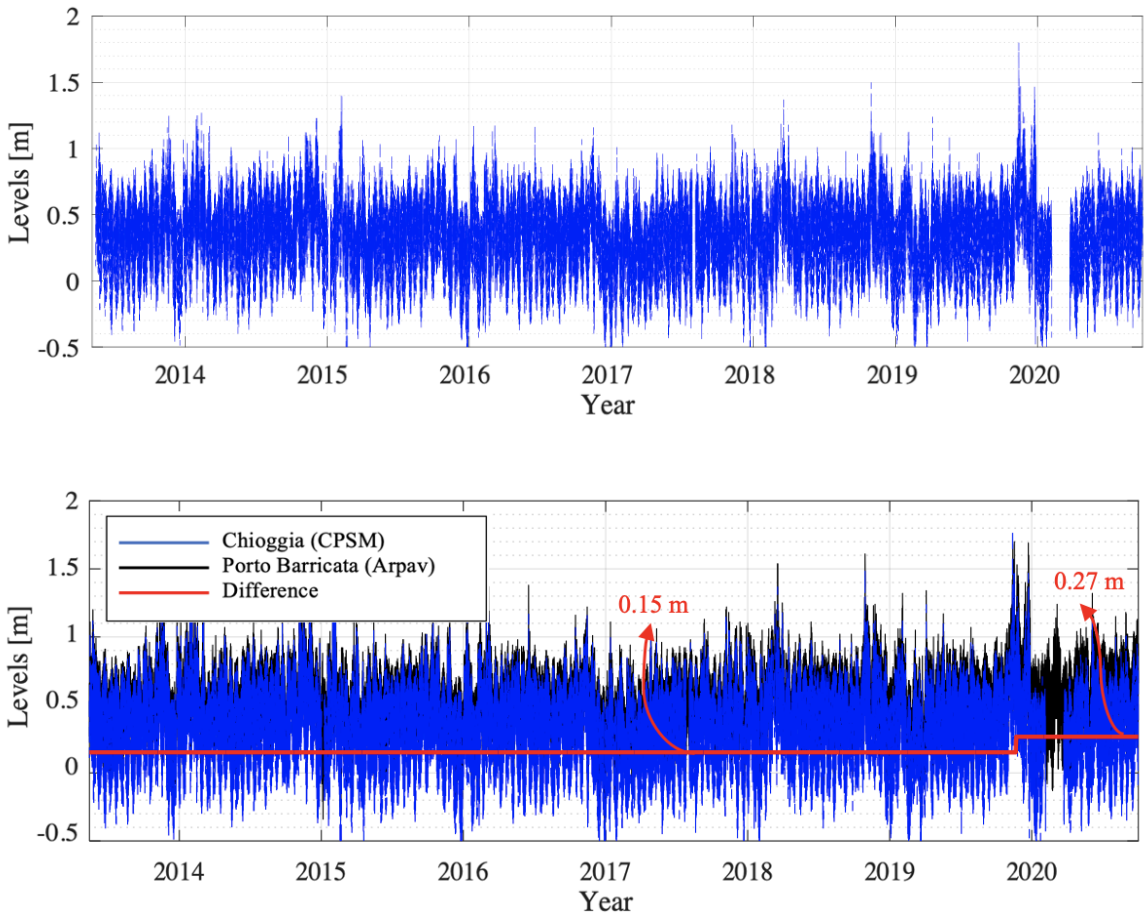

Figure 3.4: Levels recorded in Chioggia (Diga Sud) from May 2013 to December 2020 (upper graphic), comparison between Chioggia and Porto Barricata data (lower graphic).

By observing the previous figure, it is possible to identify some missing data in the series provided by the Chioggia monitoring station, especially from February 6 to March 23, 2020, probably due to malfunctions or maintenance of the system. On the other hand, the difference observed between the two measurements is very important. This is not always constant but remains equal to about 15 cm until December 2019 and then grows considerably to 27 cm.

It may also be interesting to observe the trend of the astronomical tide calculated through the harmonic analysis and compare it with the sum between the meteorological tide and the astronomical tide itself. It is also important to note, as well, that in Figure 3.5 a further contribution related to the average sea rise compared to the Z.M.P.S. of 1897 has been neglected. This last one is the level on which are based the measurements carried out both in Chioggia and throughout the Venetian lagoon, even if, nowadays, the average sea level is about 30 cm higher than this reference value.

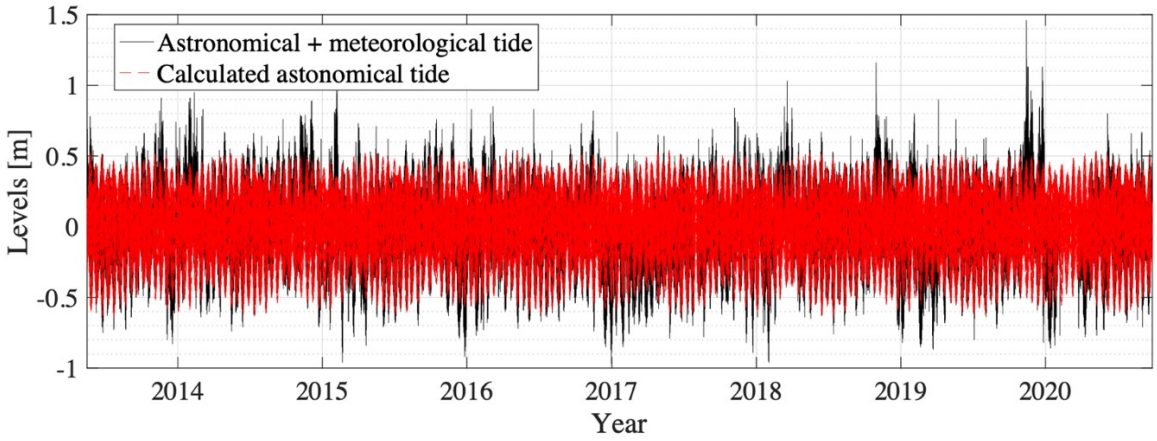

Figure 3.5: Comparison between calculated astronomical tide and the sum of astronomical plus meteorological tides.

In Figure 3.6, instead, it is possible to observe the behavior of all the contributions involved. In fact, the total level recorded by the Chioggia monitoring station corresponds to the sum between the calculated astronomical tide, the residual contribution given by the meteorological component and the seiche, and finally the mean sea level that is taken as a reference.

This means that one of the most important contributions is given by the seiche, the longitudinal and transverse oscillations due to the passage of perturbations and accentuated by the particular conformation of the Adriatic Sea. In fact, due to its shape, when the impulse induced by the perturbation ceases, a disturbed situation remains in the system. In the Venice Lagoon the longitudinal oscillation has a period of approximately 22 hours (*Municipality of Venice*).

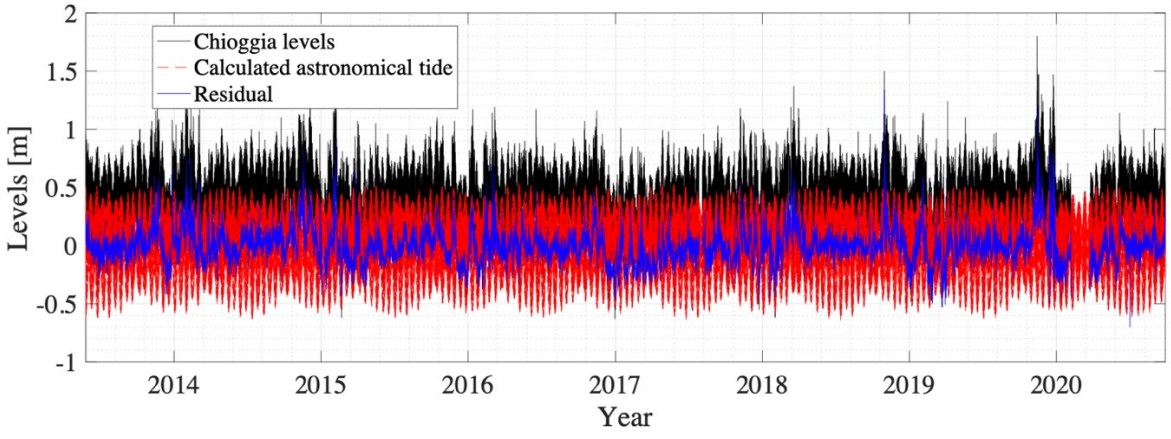

Figure 3.6: Calculated astronomical tide, residual contribution, and total level in Chioggia.

In the previous graph it is not easy to directly understand the single components involved. For this reason, it is appropriate to refer to a much shorter time series. In Figure 3.7 it is possible to observe the trend of the calculated astronomical tide, the residual contribution (meteorological component

plus seiche) and compare them with the value recorded in Chioggia during the exceptional tide of November 12, 2019.

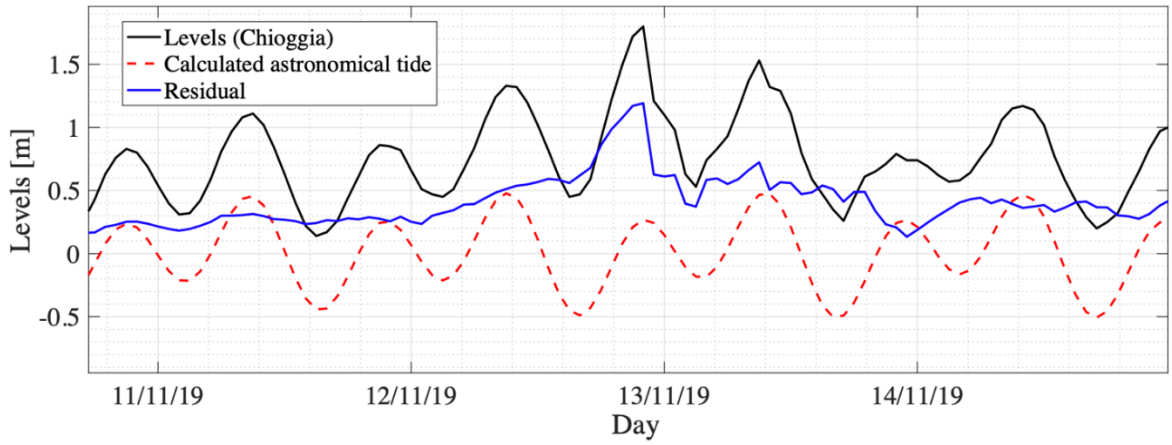

Figure 3.7: Calculated astronomical tide, residual contribution, and total level in Chioggia during an exceptional tide.

The theoretical tide, which depends exclusively on the astronomical conditions and the topography of the area, can be easily predicted through the equation:

$$y(t) = A_0 + \sum_{n=1}^{N} A_n \cos(\sigma_n t - k_n) \qquad \text{Eq. 3.2}$$

Where: A_0 is the reference mean sea level, A_n is the amplitude, σ_n is the pulsations of elementary waves and finally k_n is the phase.

To characterize the astronomical tides in the different stations, the 8 harmonic components (M_2, S_2, N_2, K_2, K_1, O_1, P_1, S_1) are defined. To compare the Chioggia monitoring station with that of Porto Barricata it is obviously necessary to consider the same period, this means the years from 2013 to 2020. The following tables summarize all the results:

Chioggia								
	M_2	S_2	N_2	K_2	K_1	O_1	P_1	S_1
A [cm]	23.0	13.5	3.9	4.1	17.1	5,5	5.4	1.5
k [°]	291.5	298.9	289.1	293.3	78.1	67.5	76.9	278.7
ω [°/h]	28.984	30.0	28.44	30.082	15.041	13.943	14.959	15.0

Table 3.3: Amplitude (A), phase difference (K) and angular velocity (ω) in Chioggia.

Porto Barricata								
	M_2	S_2	N_2	K_2	K_1	O_1	P_1	S_1
A [cm]	18.4	10.6	3.2	3.2	16.2	5.2	5.2	1.5
k [°]	297.4	305.1	294.5	300.6	81.5	71.4	78.7	297.1
ω [°/h]	28.984	30.0	28.44	30.082	15.041	13.943	14.959	15.0

Table 3.4: Amplitude (A), phase difference (K) and angular velocity (ω) in Porto Barricata.

A series of observations can be made starting from the previous data and graphs. In particular, the Porto Barricata time series, despite being characterized by a shorter time interval than the Chioggia series (every 30 minutes Porto Barricata and 1 hour Chioggia) is much shorter. The data are in fact available only for 7 years.

Then comparing each single element involved, it is possible to see how the astronomical tides that characterize the two series are similar to each other. Despite this, the series of data provided by the Porto Barricata station appears unreliable, especially as far as the trend of the meteorological tide is concerned. As shown in the graph of Figure 3.8, during the extreme event of November 12, 2019, an anomalous and rapid decrease in the level is recorded during the peak phase.

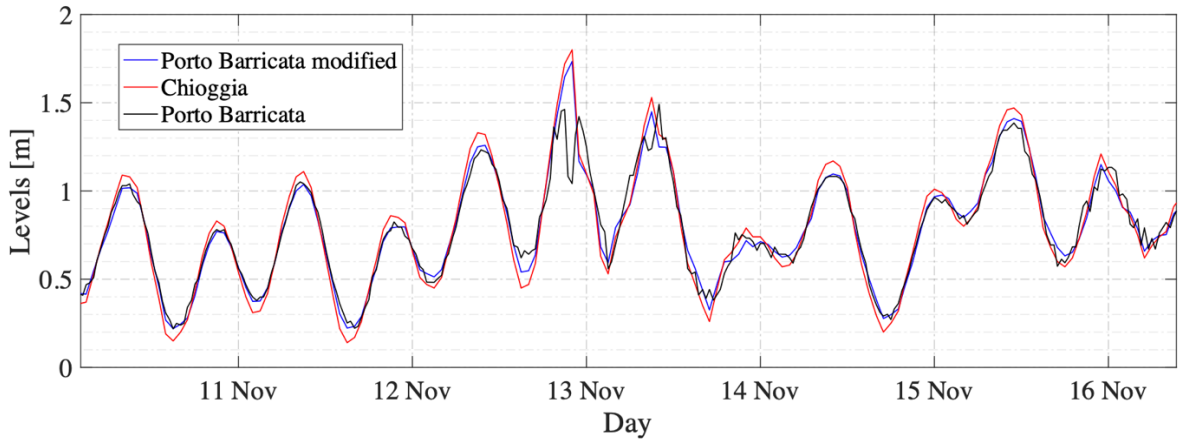

Figure 3.8: Comparison between Chioggia, Porto Barricata, and modified Porto Barricata data.

These are the reasons why the series of real data provided by the Porto Barricata station will not be used, but rather a modified or reconstructed series, starting from the meteorological component of Chioggia to which the astronomical component of Porto Barricata is added.

According to the "*Direttiva Alluvioni 2007/60/EC"* and the Flood Risk Management Plan for the Veneto Region, the return times chosen for the tidal level and wind forcing are:

- Tr = 30 years: low probability of floods or extreme event scenarios
- Tr = 100 years: average probability of floods
- Tr = years: high probability of floods

Once the return time has been defined, the statistical analysis of events can be conducted through the Peak Over Threshold (POT) method, which allows to consider all the events whose maximums exceed a certain threshold. The most used distribution to approximate the surpluses beyond the threshold is the generalized Pareto distribution (GPD). It expresses the cumulative distribution as a function of the threshold value μ.

$$F(y) = \begin{cases} 1 - \left(1 + k\frac{y}{\sigma}\right)^{-1/k} & k \neq 0 \\ 1 - exp\left(-\frac{y}{\sigma}\right) & k = 0 \end{cases} \quad \text{Eq. 3.3}$$

Where: F(y) is the cumulative probability function, σ is always positive and define the scale parameter while k is the shape parameter. This last one is the most important parameter as it defines the distribution trend. In particular, k > 0 implies a heavy-tailed distribution, k = 0 an exponential distribution and, finally, k < 0 a short-tailed distribution.

However, a very important problem in the application of the POT method is the choice of the threshold μ. This can be solved basing it on empirical techniques *(Coles et al., 2001),* such as the interpretation of the Mean Excess plot or the stability verification related to the shape and scale parameters of the GPD.

To estimate the final values characterized by the previously defined return times (30, 100 and 300 years) a reconstructed series, given by the sum between the meteorological component of Chioggia and the astronomical tide of Porto Barricata are used.

The following table shows the results of the GPD statistical analysis for the Chioggia series and the Porto Barricata series (reconstructed).

	Chioggia h (m s.l.m.m.)	Barricata h (m s.l.m.m.)
Threshold	70 cm	70 cm
Tr = 2 years	1.07	1.01
Tr = 10 years	1.26	1.2
Tr = 30 years	1.39	1.34
Tr = 50 years	1.45	1.41
Tr = 100 years	1.54	1.49
Tr = 300 years	1.68	1.64

Table 3.5: Level statistical analysis results.

From the table it is easy to see that the values of the Chioggia series are greater than those obtained with the reconstructed one related to Porto Barricata. The results obtained in the two series, in the period between 1984 and 2020, are visible in the following figures:

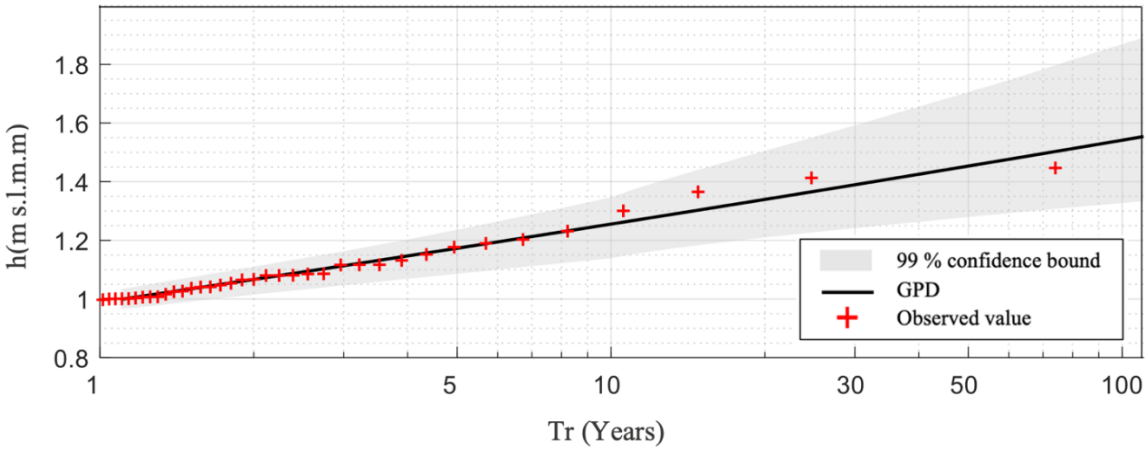

Figure 3.9: Statistical results of Chioggia levels.

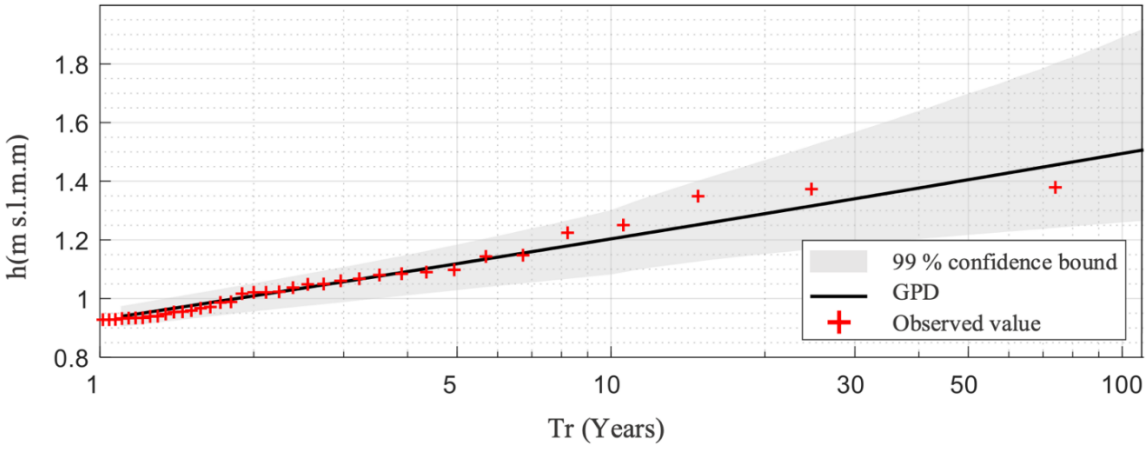

Figure 3.10: Statistical results of Porto Barricata (modified).

An interesting analysis can then be conducted on the Chioggia data series and in particular on the identification of the limit values recorded from 1984 (year of installation of the instruments by the Tide Forecast and Reporting Center) up to October 12, 2020 and, the average duration above a given value.

The maximum data found is + 1.8 mZ.M.P.S., recorded on November 12, 2019, at 22:00, coinciding with the second highest tide recorded also in the city of Venice (187cm). The minimum data instead is - 0.87 mZ.M.P.S., recorded on February 06, 1989, at 16:00.

After dividing the different tidal events, by identifying the peak in both maximum and minimum terms, it was possible instead to define the average duration above a given water level. In other words, in the following table it is possible to observe how many hours, on average, a level remains in the studied area:

Level [m]	Number of events	Mean duration [h]
Greater than 1,7 m	1	2
Greater than 1,6 m	2	2
Greater than 1,5 m	7	2,29
Greater than 1,4 m	15	2,6
Greater than 1,3 m	28	3,18
Greater than 1,2 m	74	2,91
Greater than 1,1 m	200	2,97
Greater than 1,0 m	438	2,94
Greater than 0,9 m	1051	3,03
Greater than 0,8 m	2475	3,11

Table 3.6: Average duration above a given value.

Although those previously calculated are the average values, it is important to note that:

- Between 31/10/2012 and 01/10/2012 the tide has exceeded the value of 1.2 mZMPS for 15 consecutive hours.
- Between 31/10/2012 and 01/10/2012 the tide has exceeded the value of 1.1 mZMPS for 16 consecutive hours.
- Between 05/02/2015 and 06/02/2015 the tide has exceeded the value of 1.0 mZMPS for 17 consecutive hours.

- Between 29/10/2018 and 30/10/2018 the tide has exceeded the value of 1.0 mZMPS for 16 consecutive hours.

The following plot resume the average duration above a given water level, for the analyzed cases:

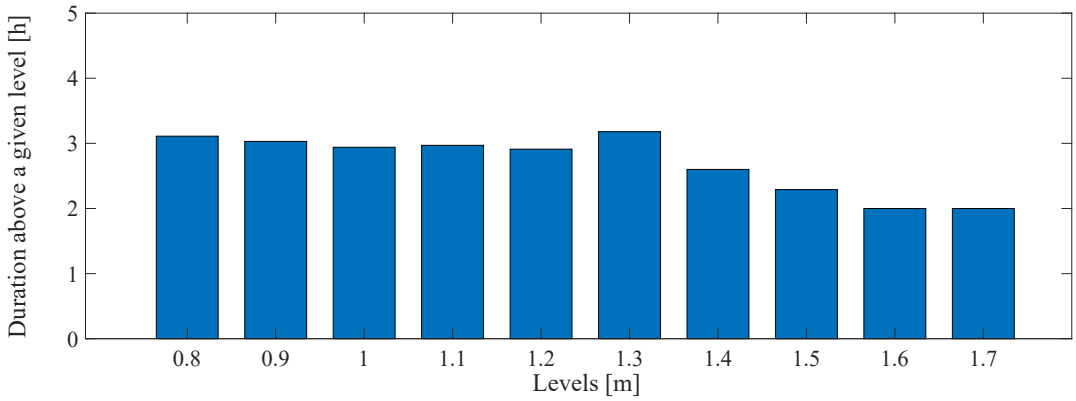

Figure 3.11: Consecutive hours during which the level was greater than a given threshold.

3.1.2 Wind

The northern Adriatic Sea is characterized by two main wind regimes, namely Scirocco which blows from the South-East and the Bora which blows from the North-East. When the intensity of the wind is high, waves and level rises can form, causing erosion and flooding in the coastal area.

Wind waves are gravity waves generated by the wind itself, which propagate at the interface between water and air. Depending on the wave period and the energy density, it is possible to distinguish different types of waves, as shown in Figure 3.12, where the energy sources associated with each type of wave are also indicated.

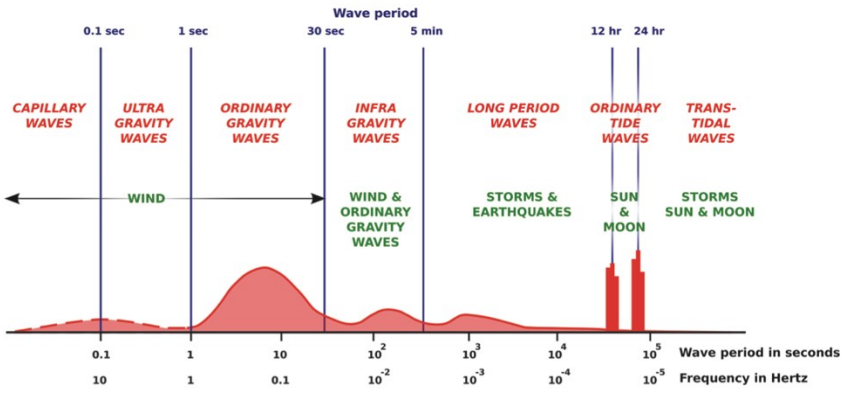

Figure 3.12: Wave classification according to the wave period.

It is easy to see that the waves with the highest energy content are ordinary gravity waves. These are mainly generated by the action of the wind, although however it is also necessary to consider other factors such as the pressure and temperatures of both water and air. The wave formation mechanism is complex and is based on the ability of the wind to transfer part of its energy to the surface of the sea. The waves are formed in an area called "generation area" where the wind begins to blow. The air that interacts with the water surface generates waves, which interacting with each other exchange energy and thus forming new waves. This process, however, is limited. In fact, it continues until the energy transferred to the sea is equal to the energy dissipated by the breaking of the waves.

To study the wind wave mechanisms, it is necessary to consider some key parameters, such as the wind speed, the wind direction and duration and finally, the fetch. This last one is defined as the land of the sea where the wind blows, and it is a geometrical consideration.

In order to assess the wind conditions in the area of interest, it is possible to rely on the data provided by the monitoring stations located in Chioggia, Pradon Porto Tolle and at the Po mouth. With reference to the Figure 3.2, from North to South:

- Chioggia - Diga Sud (Municipality of Venice): recording interval of 15 minutes and time series between January 1, 2000, and December 31, 2019.
- Foce Po (ISPRA): recording interval of 10-15 minutes and time series between April 4, 2002, and December 31, 2019.
- Pradon Porto Tolle (ARPAV): recording interval of 1 hour and time series between April 19, 1989, and August 1, 2020.

However, having to carry out an analysis on the trend of the winds along the coast, the only two stations that can be used are that of Chioggia and the one called Foce Po. The Pradon Porto Tolle station is in fact located in the hinterland. Figure 3.13 shows the wind intensity and direction in the two stations.

Therefore, the prevailing direction for the Chioggia station, located in the northern part of the area of interest, the Po Delta Region, is represented by the Bora sector (30 - 60 °N) while the prevailing direction for the *Foce Po* station is represented by the Scirocco sector (120 - 150 °N) although the presence of the Bora wind may also be of considerable importance in this case. The *Foce Po* station can be considered representative of the southern region of the Po Delta.

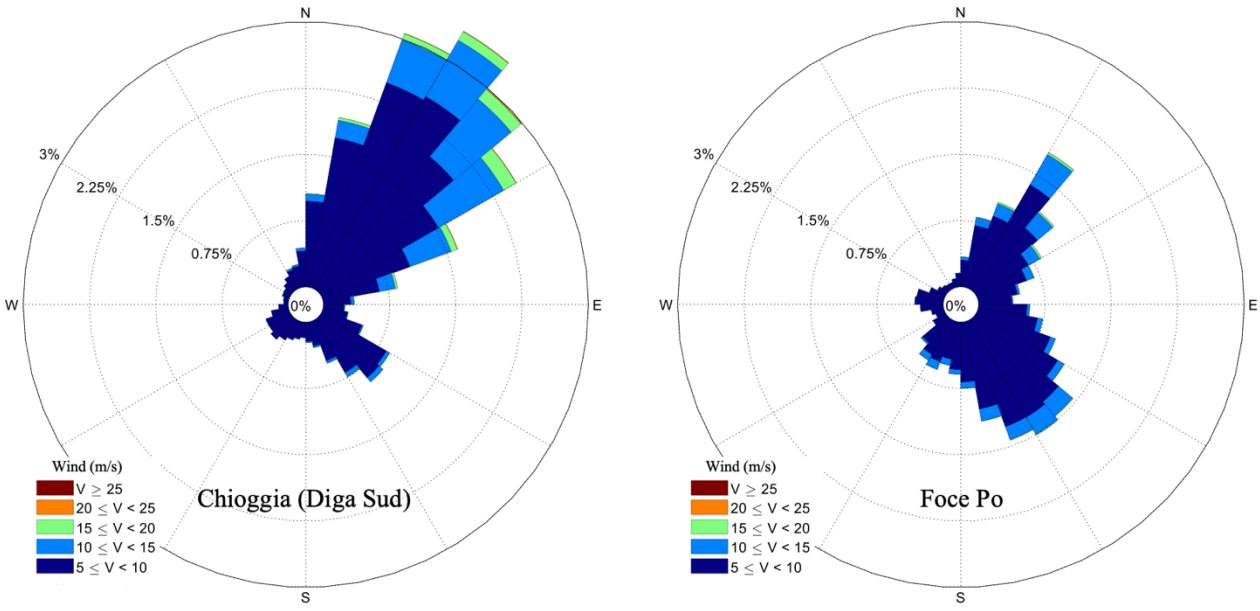

Figure 3.13: Wind intensity and direction in Chioggia and Foce Po.

As in the case of the levels, a GPD statistical analysis was also conducted for the wind, setting a threshold of 15 m/s for both Chioggia and *Foce Po*.

	v (m/s) Chioggia	v (m/s) Foce Po
Threshold	15 m/s	15 m/s
Tr = 2 years	21.7	19.2
Tr = 10 years	23.5	21.4
Tr = 30 years	24.4	22.7
Tr = 50 years	24.7	23.3
Tr = 100 years	25.1	24.0
Tr = 300 years	25.7	25.0

Table 3.7: Wind statistical analysis results.

From the table it is easy to see that the values of the Chioggia series are greater than those obtained with *Foce Po* station. The results are then plotted in Figure 3.14 and 3.15.

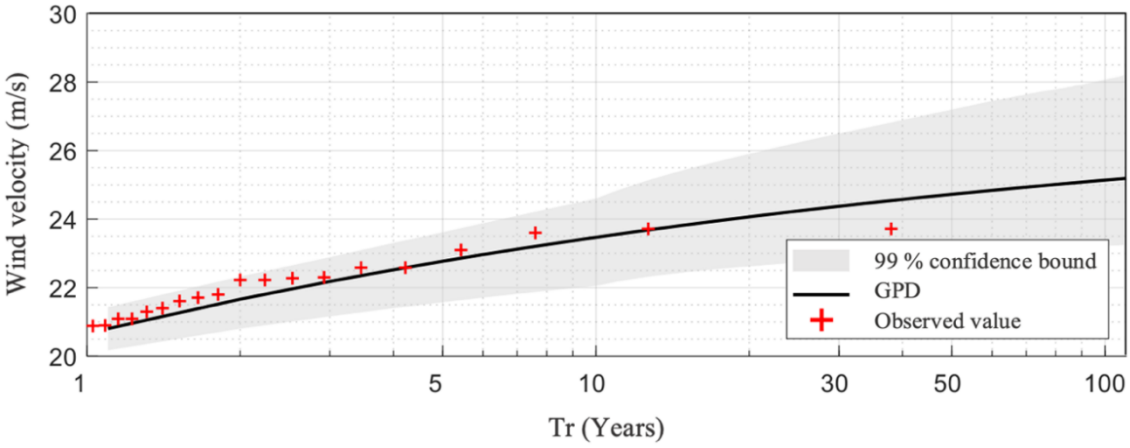

Figure 3.14: Statistical results of Chioggia wind velocity.

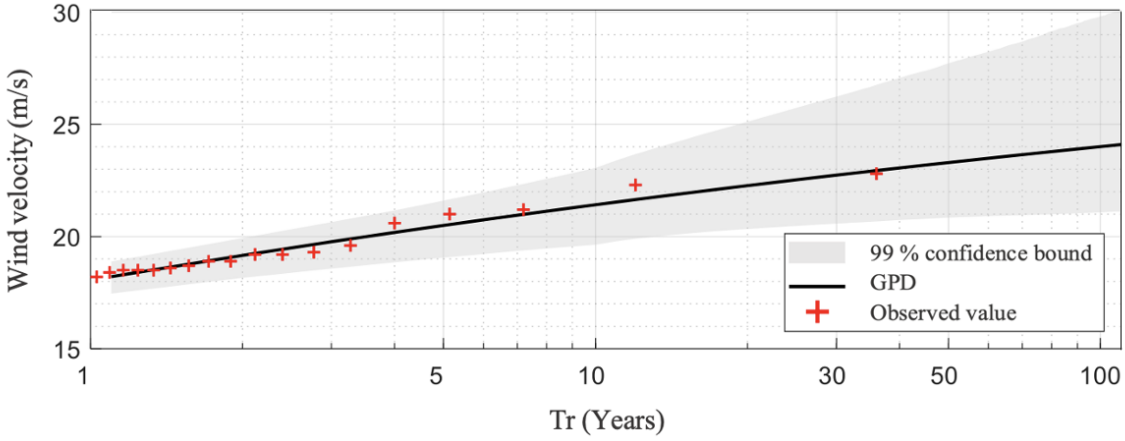

Figure 3.15: Statistical results of Foce Po wind velocity.

3.2 Forecasts of sea level rise due to climate change according to the IPCC data

Populations in contact with coastal environments are highly exposed to changes in the oceans and cryosphere, that is, the set of frozen components of the earth both on and below its surface. The role of the sea is not only fundamental from a climatic point of view, for the absorption of carbon dioxide, but also for the economy (trade and tourism), the energy and as a source of food. The main studies concerning Global Mean Sea Level rise (GMSL) and Extreme Sea Levels (ESL) have been conducted by the IPCC (Intergovernmental Panel on Climate Change) since 1991. The last report provided, containing the latest updates regarding sea level rise forecasts, takes the name of "Special Report on the Ocean and Cryosphere in a Changing Climate (SROCC, 2019)".

Global Mean Sea Level (GMSL) is rising and accelerating due to several factors, the most important is the melting of the Greenland and Antarctic ice sheets, the progressing loss of mass from glaciers and ocean thermal expansion. Nowadays, the melting of ice is the main cause linked to the increase in GMSL; in fact, the ice sheets of Greenland and Antarctica contain most of the fresh water on Earth and the change in sea level can be accentuated by the loss or increase of ice from the ice sheets themselves. In recent years, the Greenland Ice Sheet (GIS) has lost mass at about twice the rate of the Antarctic Ice Sheet (AIS). Between 2006 and 2015, the Greenland ice sheet, mainly due to surface melting, lost mass at an average rate of 278 ± 11 Gt/year. Considering that 360 Gt of ice correspond to 1 mm of mean global sea level rise (*IPCC*) this implies that it is equivalent to 0.77 ± 0.03 mm/year of global sea level rise. In the same period, however, the Antarctic ice sheet lost mass at an average rate of 155 ± 19 Gt/year (0.43 ± 0.05 mm/year).

Another key aspect is related to thermal expansion. In particular the increase in temperature leads to an increase in density and consequently to an increase in volume per unit of mass, so it means that even in the absence of mass variation, due to heating the sea level tends to rise.

However, it is also very important to consider anthropogenic factors such as the subsidence as a result of the extraction of water and gas from the subsoil, the reclamation, the water storage in mountain basins and the uses from a domestic, agricultural, industrial and energetic point of view. Figure 3.16 schematizes the main climatic and anthropogenic processes that can influence the mean sea level both on a regional and global scale.

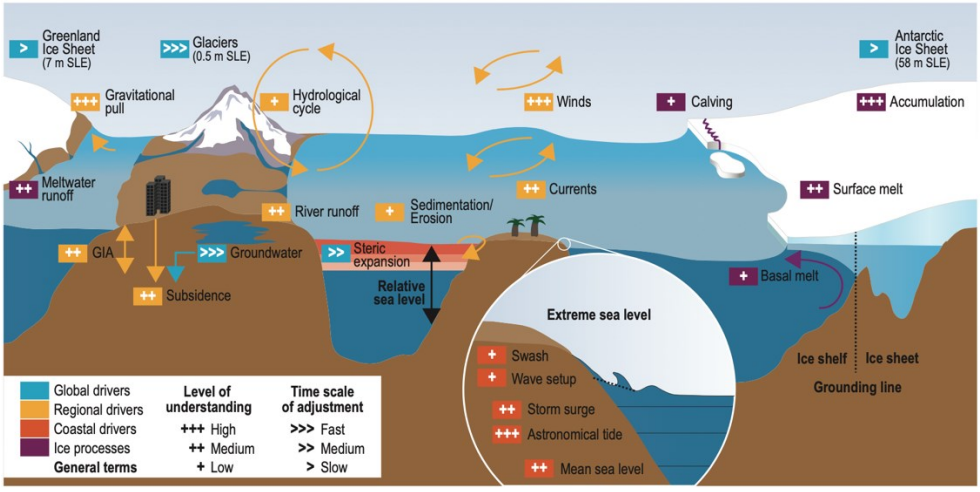

Figure 3.16: Climatic and non-climatic processes that can influence the sea level distinguishing between global drivers (blue), regional drivers (yellow), coastal drivers (red) and ice processes (purple). Focus on the Extreme Sea Level *(IPCC, SROCC, 2019).*

The previous figure also takes into account the phenomena that can overlap the RSL, in particular, the tides, storm surges, and the action of the waves. However, the study of them is based on the knowledge of localized phenomena such as coastal erosion, the transport of sediments in the delta areas of rivers, the impact of the wind and the behavior of the seabed. In the presence of favorable situations, these phenomena can significantly worsen the exposure of the coastal area.

According to data provided by the IPCC, from 1900 to 2015 the global mean sea level (GMSL) increased significantly, in particular the increase was 1.4 mm per year in the period 1901-1990, of 2.1 mm per year in the period 1970–2015, 3.2 mm per year in the period 1993–2015 and finally by 3.6 mm per year in the period 2006–2015. Obviously, the globally rise is not uniform but varies from one region to another.

In the future, the increase of GSML will instead depend on the emission scenario given by the Representative Concentration Pathway (RCP). The IPCC has in fact identified four main emission scenarios, called RCP 2.6, RCP 4.5, RCP 6.0 and RCP 8.5, all possible but different in terms of the volume of greenhouse gases emitted in the future. In particular:

- RCP 2.6: Pathway where radiative forcing peaks at 2.6 W m^{-2} before 2100 and then decreases. In this way important political measures are taken in favor of climate protection, and it is possible to achieve the objectives of Paris climate agreement (2016).
- RCP 4.5 and RCP 6.0: Intermediate pathways where radiative forcing peaks respectively at 4.5 W m^{-2} and 6.0 W m^{-2} after 2100. The emission of greenhouse gases is contained, but their concentrations in the atmosphere will increase further over the next 50 years.
- RCP 8.5: High pathway for which radiative forcing reaches more than 8.5 W m^{-2} by 2100 and then continues to rise. In this case no measures are taken in favor of climate protection.

	Near term [2031-2050]		End of century [2081-2100]	
Scenario	Mean [°C]	Likely range [°C]	Mean [°C]	Likely range [°C]
RCP 2.6	1,6	1,1 to 2,0	1,6	0,9 to 2,4
RCP 4.5	1,7	1,3 to 2,2	2,5	1,7 to 3,3
RCP 6.0	1,6	1,2 to 2,0	2,9	2,0 to 3,8
RCP 8.5	2,0	1,5 to 2,4	4,3	3,2 to 5,4

Table 3.8: Global mean surface temperature change with different scenarios (*IPCC, SROCC 2019*).

According to the forecasts provided by the IPCC, the global mean sea level will increase by 2100 of 0.43 m in the very high emission reduction scenario (RCP2.6) and approximately of 0.84 m in the high emission scenario (RCP8.5), compared to the period 1986-2005. In addition, the rate of growth will be ever faster and will continue for centuries due to the melting of the Greenland and Antarctic ice sheets as well as the continuous absorption of heat by the sea. This means that without adaptation measures and with the increasingly frequent occurrence of extreme sea levels induced by tides, storm surges and waves, the damage to the coastal environment could become enormous.

It is important to note, however, that the determination of the impacts due to the increase in the average sea level are very complex to obtain. Above all because they vary from area to area, depending on anthropogenic activity and on the ability of nature to respond to changes (development of sand dunes, salt marshes and mangroves). However, uncertainty about future sea level (2050) caused by climate change is small and so it provides a basis for short-term adaptation planning. Beyond 2050, however, uncertainty increases mainly because of the difficulty of predicting future emission scenarios and associated climate changes.

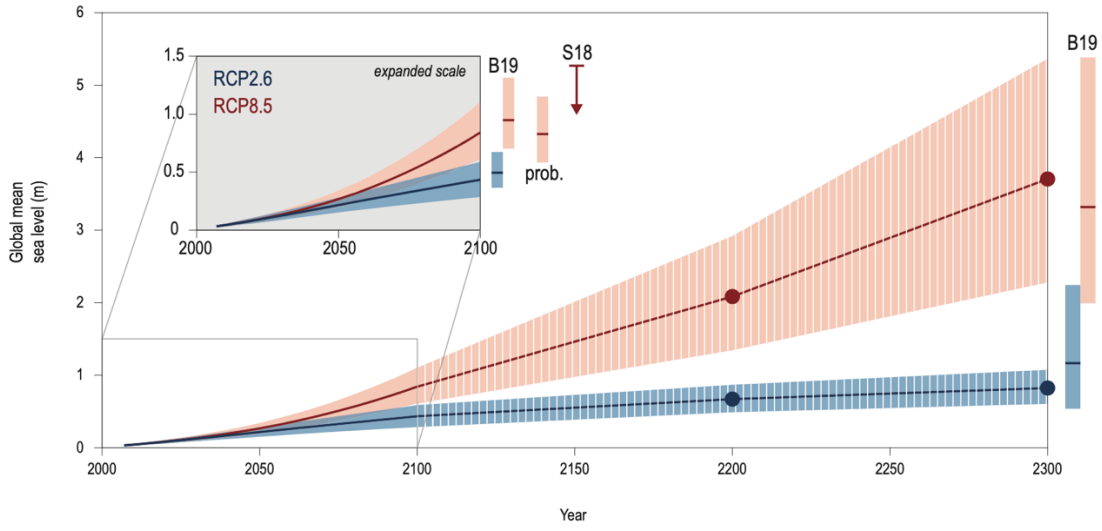

Figure 3.17: Sea level rise until 2300, for RCP2.6 and RCP8.5 (*IPCC, SROCC, 2019*).

The previous graph (Figure 3.17) shows the expected sea level rise to 2300, with a particular focus up to 2100, for RCP2.6 and RCP8.5. It is important to note that projections for longer time scales are very uncertain compared to shorter ones.

However, considering the area of interest, that is North Adriatic, the average sea level rise, as shown in table 3.9, is lower than the global average trend in both 2050 and 2100.

Scenario	SLR 2050		SRL 2100	
	Value [m]	Confidence interval	Value [m]	Confidence interval
RCP 2.6	0,161	0,122-0,204	0,306	0,209-0,418
RCP 4.5	0,170	0,106-0,237	0,402	0,291-0,531
RCP 8.5	0,207	0,148-0,274	0,639	0,465-0,849

Table 3.9: Sea level rise forecasts in the North Adriatic Sea (*IPCC, SROCC, 2019*).

Thanks to the data collected by the Mareographic Network stations of the Venice Lagoon and the North Adriatic (RMLV), it is possible to obtain an indicative trend of the average sea rise in this region over the last 145 years and then compare it with possible future scenarios. In fact, the reference station, namely Punta della Salute in Venice, collected data starting from 1872 to 2016, highlighting an increase of the sea level. This growth, however, was not constant but in some cases very sustained (for example also following the extraction of water from the subsoil for use in Porto Marghera) and in others it was reduced. Overall, in the entire period analyzed, the growth rate was 2.5 mm/year (*ISPRA, 2017*).

Graph 3.18 shows the average sea level trend recorded in Venice from 1872 to 2016 and possible future scenarios depending on the emissions. It is important to note that, unlike the RCP 2.6 scenario where the increase is in line with the past, in the case of the RCP 8.5 scenario the increase is very marked and can lead to serious dangers and risks for the Northern Adriatic area.

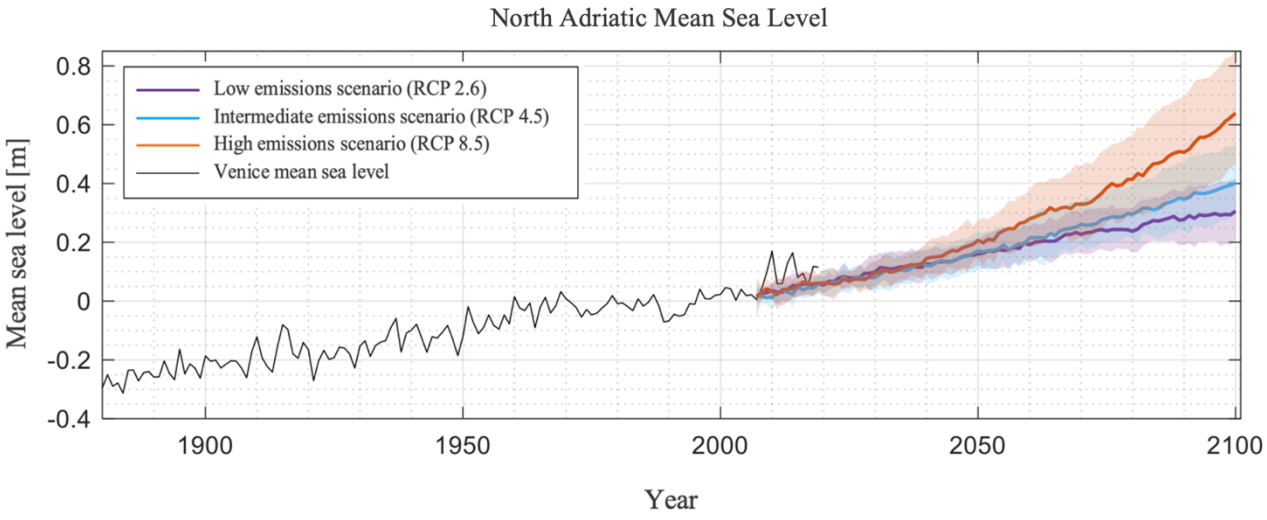

Figure 3.18: Sea level rise in the North Adriatic Sea from 1872 and 2016 (*ISPRA, 2017*) and future forecasts according to IPCC.

3.3 Wave and water level modeling

To simulate the flow within coastal lagoons such as those of the Po Delta, it is necessary to consider the implementation of two-dimensional or three-dimensional models of shallow waters. The final results depend not only on the resolution required but also on the specific characteristics of the studied area. An adequate solution requires the ability to model physical phenomena that are often neglected through the numerical solution, in fact, for the study of these regions it is not always sufficient to adopt computational grids and well-structured numerical schemes. The solution is the formation of sub-grid patterns. For the study of water level increases and wave fields, the 2DEF hydrodynamic model and the SWAN wave model are introduced. In fact, a series of numerical simulations are available which made it possible to obtain the initial conditions in terms of sea level. These were then used for the geotechnical analysis.

3.3.1 2DEF hydrodynamic model

The 2DEF hydrodynamic model is a coupled 1D-2D model that exploits a finite element scheme and that solves the differential equations governing the two-dimensional motion of a free surface current on shallow water. These last ones have been modified in such a way as to describe also dry, partially dry or flooded areas depending on the studied region. The domain is then discretized through a grid of two-dimensional triangular elements, combined with one-dimensional elements. The latter are essential to consider the presence of the small canals that characterize the area.

Among the main studies conducted, the one given by *D'Alpaos & Defina (2007)* is certainly one of the most significant. They proposed to consider the large canals by means of two-dimensional elements and the smaller canals as topographical irregularities. The problem, however, arises in the presence of intermediate channels where both simplifications previously described are gross. The solution can be obtained by observing that the flow in the shallow and narrow channels has a one-dimensional character, thus suggesting the use of one-dimensional elements to represent them in the model *(Defina et al., 1994, D'Alpaos and Defina, 2007).* Overall, a model was created capable of coupling the 1D model to describe the flow in the channel and a 2D model for the hydrodynamics of shallow water.

3.3.2 SWAN model

SWAN (Simulating WAves Nearshore), developed at Delft University of Technology, is a third-generation wave model for obtaining realistic estimates of wave parameters in coastal areas, lakes and estuaries from specific wind, current and seabed conditions. As in the case of the wave motion that propagates towards the shore, the model simulates the development of wave spectra traveling from deep water to shallow water.

SWAN is based on the balance equation of the wave action in discrete form, it is also a spectral model both in the field of directions and in that of frequencies. This means that waves that propagate at the same time but from different directions can also be adequately described. The reference equation is:

$$\frac{\delta}{\delta t}N(\sigma,\theta) + \nabla_{x,y}\cdot\left[c_{x,y}N(\sigma,\theta)\right] + \frac{\delta}{\delta\sigma}\left[c_{\sigma}N(\sigma,\theta)\right] + \frac{\delta}{\delta\theta}\left[c_{\theta}N(\sigma,\theta)\right] = \frac{S(\sigma,\theta)}{\sigma} \qquad \text{Eq. 3.4}$$

Where: σ = relative frequency

θ = wave direction of propagation

E (σ,θ) = energy density

$N(\sigma,\theta) = \frac{E(\sigma,\theta)}{\sigma}$ = action density

In a simplified way it is possible to remove the time, i.e., d/dt = 0 in order to reduce the simulation time. This simplification is generally accepted as the residence time of the waves is much shorter than the time scale of changes in the boundary conditions of the waves, ambient current, wind or tide *(Booij et al. 1996).* If, on the other hand, the time scale is important, it is possible to repeat the calculations for established intervals and through a quasi-stationary approach.

It is then possible to directly combine the SWAN model with the 2DEF hydrodynamic model, considering two distinct grids. In particular a structured rectangular mesh grid for the SWAN model and an unstructured one with triangular-shaped finite elements for the 2DEF model. The combination, for all lagoons, consists in the morphological representation of the lagoon bottoms and the sea through the grid of the 2DEF model to which is subsequently superimposed the grid of the SWAN model. This last one must be characterized by such small cells as to be contained within the triangular cells of the hydrodynamic model. The model configured in this way is able to produce, as an output, both wave fields and the hydrodynamic field.

3.4 Final results

For each lagoon one simulation results, both in terms of the wave height and final levels, are presented.

As regards the Sacca degli Scardovari, the simulation shown in Figure 3.19 is obtained considering Scirocco wind (direction 150°), with a speed of 25 m/s, an initial level of 1.4 m and a wave height of 2 m offshore.

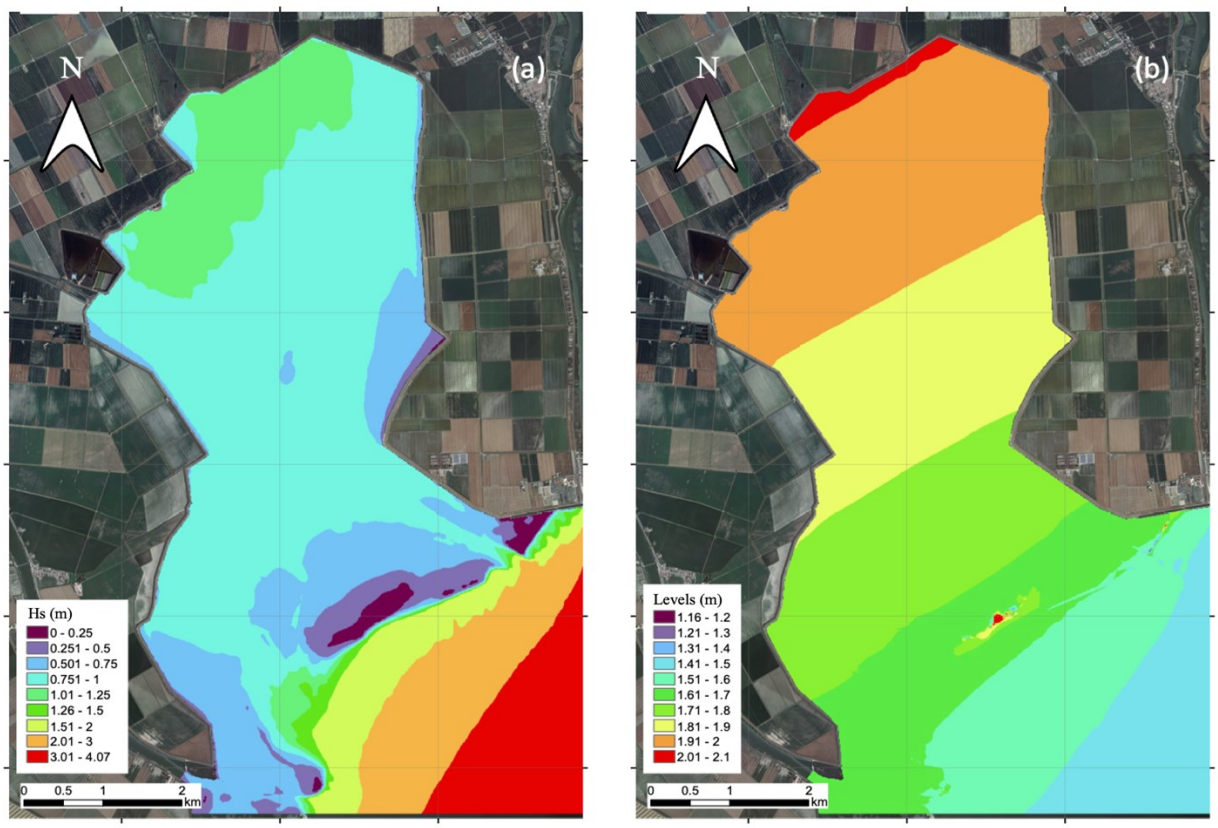

Figure 3.19: Simulation of wave height (a) and final levels (b) in Sacca degli Scardovari. (Dipartimento ICEA, Università degli studi di Padova, *'Studio sui possibili interventi di ripristino e protezione degli argini di difesa a mare della Sacca degli Scardovari'*, 2022).

It is possible to observe how the height of the wave is greater offshore and tends to decrease as it penetrates inside the lagoon. The wave height is then lower near the sandbar (*Scanno del Palo)* which therefore acts as a protection for the area behind it. Then due to the direction of the wind and the wave itself, the height of this last one is greater on the north and west side than on the east side. Instead, by analyzing the levels, they increase near the innermost area of the lagoon.

Instead, for the Caleri Lagoon in Figure 3.20 is shown the simulation obatained with Bora wind (direction 60°), with a speed of 15 m/s, an initial level of 2.1 m and a wave height of 2 m offshore.

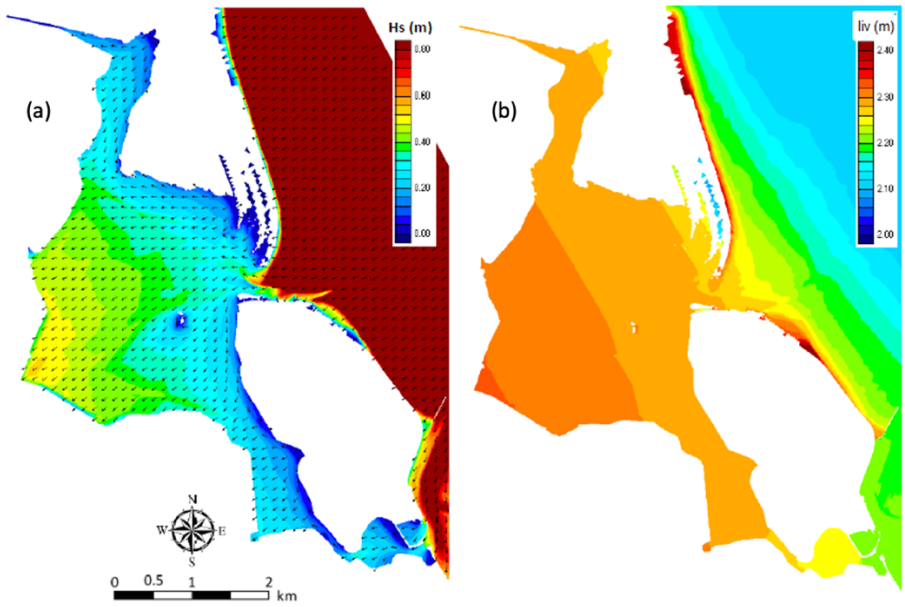

Figure 3.20: Simulation of wave height (a) and final levels (b) in Caleri Lagoon. (Dipartimento ICEA, Università degli studi di Padova, 'Studio sui possibili interventi di ripristino e protezione degli argini di difesa a mare della Sacca degli Scardovari', 2022).

Figure 3.21 shows the simulation for the Vallona Lagoon. This is given assuming Bora wind, coming from 45°N and with an intensity of 15 m/s, an initial water level of 2.1 m and a significant wave height of 2 m offshore.

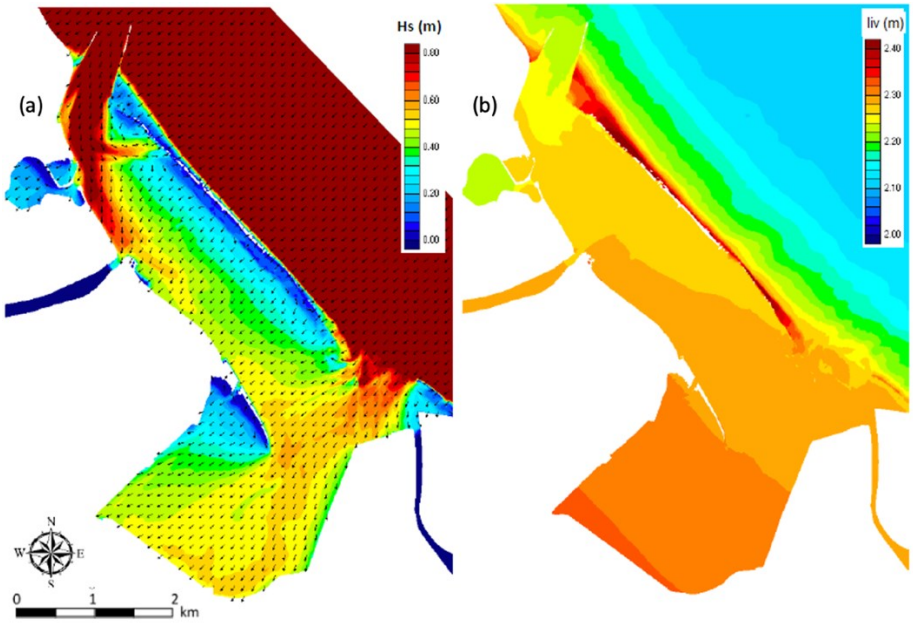

Figure 3.21: Simulation of wave height (a) and final levels (b) in Vallona Lagoon. (Dipartimento ICEA, Università degli studi di Padova, 'Studio sui possibili interventi di ripristino e protezione degli argini di difesa a mare della Sacca degli Scardovari', 2022).

In Barbamarco Lagoon, the simulation conducted considers with a Bora wind (with a direction of 45°N) and a speed of 15 m/s, an initial water level of 2.1 m and a significant wave height of 2 m offshore.

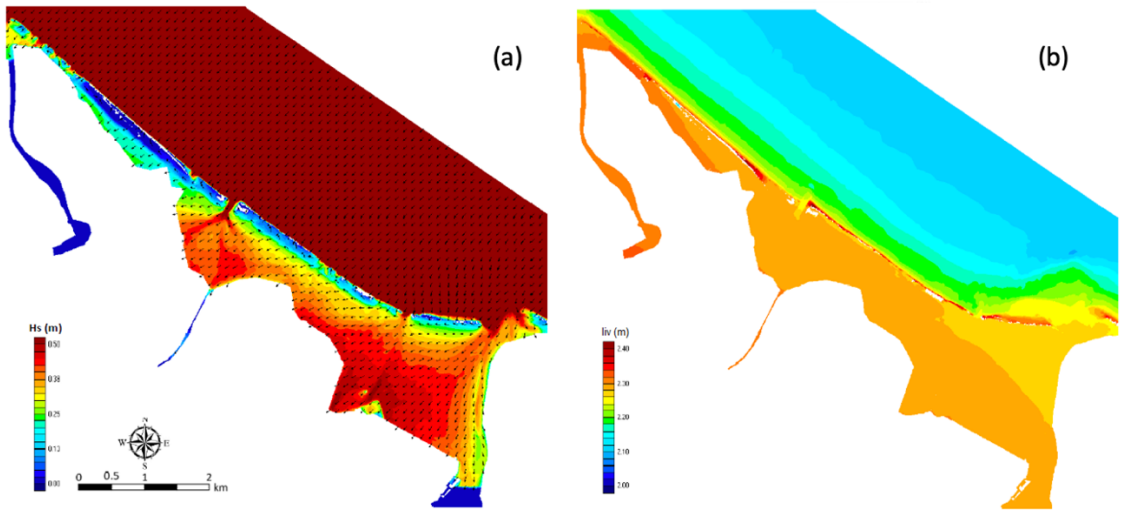

Figure 3.22: Simulation of wave height (a) and final levels (b) in Barbamarco Lagoon**.** (Dipartimento ICEA, Università degli studi di Padova, 'Studio sui possibili interventi di ripristino e protezione degli argini di difesa a mare della Sacca degli Scardovari', 2022).

Due to its conformation, it is important to observe how, unlike the other lagoons, that of Barbarco is characterized by a very high wave height inside and not only near the inlets. Finally, for the Canarin Lagoon the level conditions are always the same (initial water level of 2.1 m and a significant wave height of 2 m offshore), but the wind comes from 120°N (Scirocco) with a velocity of 15 m/s.

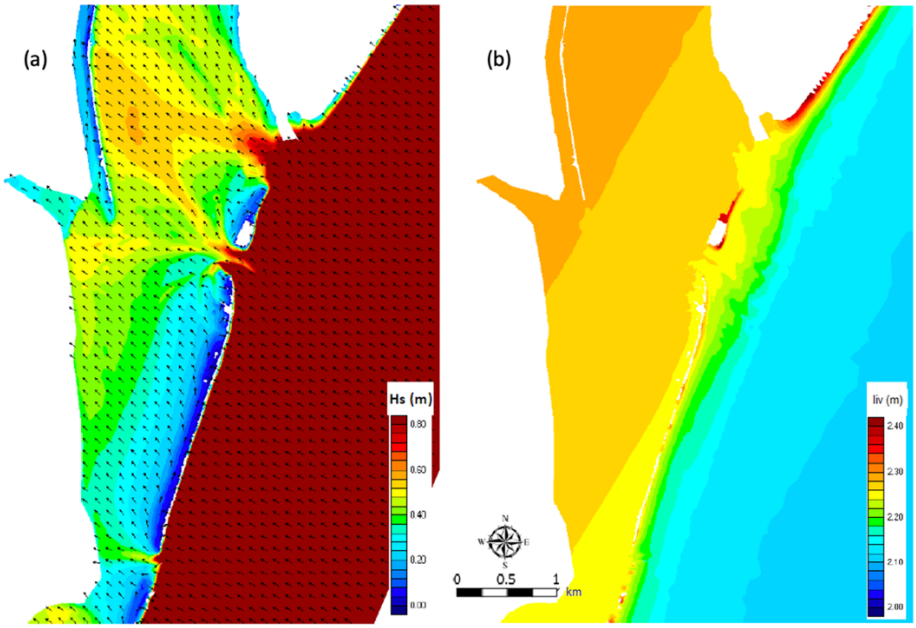

Figure 3.23: Simulation of wave height (a) and final levels (b) in Canarin Lagoon**.** (Dipartimento ICEA, Università degli studi di Padova, 'Studio sui possibili interventi di ripristino e protezione degli argini di difesa a mare della Sacca degli Scardovari', 2022).

4. GEOTECHNICAL DATA COLLECTION AND ANALYSIS

To study the stability and the filtration phenomena that occur both inside and below a coastal dike, a geotechnical characterization is required. This last one must consider not only the materials used to create the embankment but also the foundation soil. Starting from 2021, the AIPO (Interregional Agency for the Po River) has carried out several in situ geotechnical boreholes along the dikes of Sacca degli Scardovari. In addition to these, it was also possible to perform different geotechnical laboratory tests. This large availability of data made it possible to have important information useful for geotechnical modeling. However, they are not available for the other Po Delta lagoons such as Caleri, Vallona, Barbamarco and Canarin. Carrying out such evaluations also in these areas would allow to have a better geotechnical characterization and to obtain more accurate results.

4.1 Sections subdivision

For the analysis, Sacca degli Scardovari was divided into 25 sections, in agreement with the AIPO surveys (2020-21). However, the tests conducted in situ provided only 14 different surveys areas, 1 km far from each other.

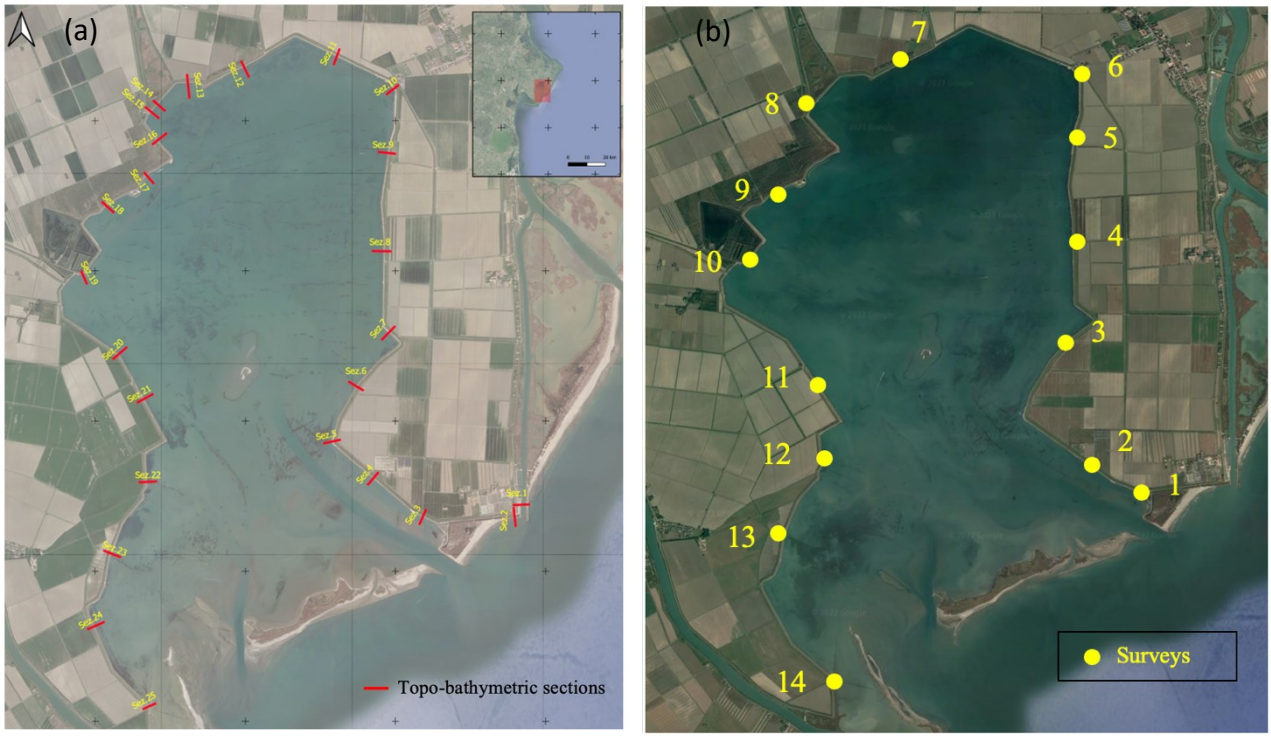

Figure 4.1: Sections surveyed by AIPO in 2020-21 (a), location of surveys and CPTU tests (b).

4.2 Geotechnical surveys

Geotechnical surveys are essential for acquiring information on the soil characteristics, useful for the design of engineering works such as, for example, the construction or modification of embankments. A geotechnical examination includes both surface and subsoil analysis, by sampling of this last one and laboratory analysis. Geotechnical investigations have acquired considerable importance especially in the prevention of instability phenomena, subsidence, failure conditions both related to human and natural activity such as earthquakes, floods, and storm surges.

The geotechnical characterization of the site consists in the study of the lithological, geomorphological, and hydrogeological characteristics of the survey area. The amount of information to build an adequate geotechnical model, that is a representative scheme of the stratigraphic, mechanical and physical conditions of the analyzed sample, depend on the type of work and the complexity not only of the system itself but also of the soil on which this will be built. The analyzed volume must be representative of the area directly and indirectly influenced by the construction of the work, once again it depends on the type of work, its dimensions, the characteristics of the soil foundation and the applied loads.

To obtain the data and information, it is possible to use both in situ and laboratory tests. It is important to observe how these two methodologies are complementary to each other thus allowing to significantly reduce the uncertainties on the measurements. In fact, each of them has specific advantages, in particular the in-situ tests allow to study a much greater portion of soil than that transportable in laboratory, moreover with them it is possible to continuously study the trend of the geotechnical characteristics as the depth varies. They are faster and less expensive. On the other hand, the laboratory tests allow to consider known and constant conditions, moreover not all tests can be carried out in situ, this due to the special techniques and instruments used.

There are different methods of boring the soil, the most common are the rotary drilling, percussion drilling, vibration, or a combination of this techniques. Depending on the investigations to be conducted, it may be necessary to have an undisturbed or altered sample. The first term refers to a sample that maintains the same structure and water content of the natural soil, vice versa a sample is defined as remolded if these characteristics are not preserved. To define the physical and mechanical properties it is necessary to study an undisturbed sample while the remolded samples can be useful for obtaining information on the soil stratigraphy.

4.3 In situ tests

The purpose of the site investigation is to provide information on the geotechnical and engineering properties of the land to design and then build a work such as an embankment. As regards this last one, it is necessary to investigate the resistance, the permeability of the foundations and the body of structure, the compressibility, as well as the quality and quantity of the materials that can be used. The site must be thoroughly examined so that the analyzes and design procedures are adequate and representative. The information required will obviously depend on the work to be built, but in general it is necessary to investigate the failures, the possible measures of enlargement or modification. These can be obtained starting from a general knowledge of the location soils where the work will be built, from geological survey maps, and above all from personal onsite investigations. The site exploration is always essential, as a poor representation of the subsoil conditions and an incorrect determination of the geotechnical parameters can lead to the instability of the work and a consequent final increase in term of costs aimed at redesigning or restored the system. The site investigation can then be divided into three phases:

- Preliminary: has the purpose of assessing the suitability of the selected site or identifying an alternative one. It is necessary to establish the general characteristics of the site and the geological information that allow an initial assessment and planning of subsequent investigations such as the boreholes' location and the equipment to be used.
- General exploration: the areas of greatest interest are selected, and soil surveys are conducted in a fixed place, to obtain the required samples and perform the most appropriate tests. Much more information is needed for this step than the previous one.
- Detailed exploration: it is used principally in the case in which the works are large and important, the cost is usually high since it requires the use of special techniques.

The number and the position of the boreholes depend on the project type and size, the budget for the site investigation and the soil variability. The number must be enough to well define the soil properties but not too much to avoid excessive costs. The boreholes, instead, are generally located where the loads are expected. The boring should be extended at a minimum depth equal to twice the embankment height unless a hard stratum is encountered above this level.

Considering the Po Delta lagoons, it is necessary to make a distinction between the Sacca degli Scardovari and the others. In fact, in this region, under the AIPO directive, geotechnical surveys were carried out in 2021, to characterize the embankment areas.

In particular, the main in situ tests were:

- Geotechnical boreholes: 14 continuous core drilling tests up to -20 m. However, it is important to note that this measure refers to the test starting point, meaning that in some cases the results refer to the coastal dike crown while in others the lateral bank (landside). Thanks to these measurements, it is possible to study the horizontal pattern of the different layers that characterizes the soil stratigraphy below the embankment.

- CPTU tests: 14 Static Penetrometric Test with Piezocone. As in the case of the geotechnical boreholes, the portion of land analyzed goes from the reference height, that is the top of the embankment or the lateral bank, up to a depth of -20 m.

- Dissipation tests: they are 26, carried out during the penetration with the piezocone and which allow to evaluate the consolidation properties of the clayey soils.

- Lefranc tests: 27 permeability tests were conducted to determine the average permeability coefficient (k) of the investigated sandy and silty soils inside the borehole. The order of magnitude of this last one is between 10^{-6} and 10^{-5} m/s.

- Seismic tests: divided into 8 MASW (Multichannel Analysis of Surface Waves) tests and 4 seismic refraction tomographies. The first one allows to characterize the soils from a seismic point of view, while the second ones to estimate the homogeneity of the soil layers. The MASW method is a survey technique that does not require the execution of drilling, thus allowing to limit costs. It is able to identify the velocity profile of the vertical shear waves, starting from the measurement of the surface waves made in correspondence of different sensors, placed on the ground.

Finally, undisturbed samples were taken for each borehole, to perform geotechnical tests in the laboratory, such as oedometric consolidation and compressibility.

These tests conducted exclusively for the Sacca degli Scardovari should also be developed in the other lagoons that characterize the Po Delta. This in order to obtain important geotechnical information and identify possible risk factors such as slope instability, failure mechanisms and filtration processes below the embankment. The test and the results obtained in the Sacca degli Scardovari are described in the following paragraphs.

4.3.1 In situ determination of the permeability coefficient

To define the permeability of an area, different types of permeability tests can be performed. One of the most important is the Lefranc test. Determining the permeability coefficient is very complex due to the presence of heterogeneous and anisotropic soils but also for the uncertainty regarding the boundary conditions. However, there are many different methods, and the appropriate choice must consider the characteristics of the soil and the required accuracy. In any case, the reference standard is the AGI (1977) "Recommendations on the planning and execution of geotechnical investigations".

As regards the tests in superficial wells, these allow to define the permeability of the superficial soils above the groundwater level. They can be performed on circular or square base wells and are divided into:

1. Constant load tests: if once the well has been filled with water, the flow rate necessary to keep the level constant is measured.
2. Variable load tests: if the rate of lowering of the level over time is measured.

As shown in Figure 4.2 the measurements are standardized, the well diameter must be greater than about 10-15 times the maximum diameter presents in the size particle, furthermore during the test the distance between the bottom of the well and the water table must be equal to at least 7 times the height of the water in the well itself.

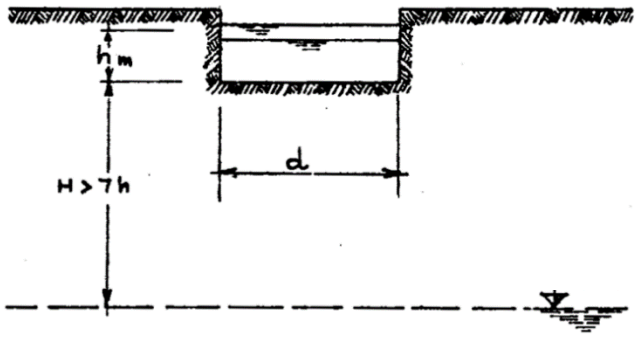

Figure 4.2: Permeability test in a superficial well, AGI (1977) *"Recommendations on the planning and execution of geotechnical investigations".*

The permeability coefficient k [m/s] is calculated from empirical formulas, and by the knowledge of h_m that is the average height inside the well, d the diameter, b the base side of the rectangular well, q the flow rate and t the time.

Constant load tests

Circular well $\longrightarrow$ $k = \frac{q}{dh_m}\frac{1}{\pi}$ Eq. 4.1

Rectangular base well $\longrightarrow$ $k = \frac{q}{b^2}\frac{1}{27\frac{h}{b}+3}$ Eq. 4.2

Variable load test

Circular well $\longrightarrow$ $k = \frac{d}{32}\frac{h_2-h_1}{t_2-t_1}\frac{1}{h_m}$ Eq. 4.3

Rectangular base well $\longrightarrow$ $k = \frac{q}{b^2}\frac{1}{27\frac{h}{b}+3}$ Eq. 4.4

Although it is a very simple method in terms of execution, it can only be used to a limited extent, in particular on the most superficial soil layers. Furthermore, the previous equations are based on very strong hypotheses such as the presence of an isotropic, homogeneous soil and with permeability greater than 10^{-6} m/s.

When it is necessary to investigate at greater depths, borehole tests or Lefranc tests are used. They allow to determine the permeability above or below the groundwater level. Also, in this case they can be carried out with constant or variable load. Furthermore, the variable load tests below the groundwater level can be divided into ascent tests *(prove di risalita),* if the ascent rate of the level is measured after that this last one has been decreased by a known quantity, or lowering tests (*prove di abbassamento*), if it is measured the lowering speed after filling the hole with a known quantity of water.

As shown in Figure 4.3, the wells are suitably lined with pipes, up to the depth at which the measurement is carried out. Then defined as A the base area of the hole, h the height of the water levels with respect to the level of the undisturbed aquifer, t the time, and C_L the shape coefficient, it is possible to calculate the coefficient of permeability with variable load, as follow:

$$k = \frac{A}{C_L(t_2 - t_1)} \cdot ln\ \frac{h_1}{h_2} \qquad [m/s] \qquad \text{Eq. 4.5}$$

On the other hand, for tests at constant load the permeability coefficient is calculated as:

$$k = \frac{q}{C_F \cdot h \cdot d} \qquad [m/s] \qquad \text{Eq. 4.6}$$

Where: q is the flow rate entered the system, h the water level inside the hole, d the hole diameter and C_F the shape coefficient.

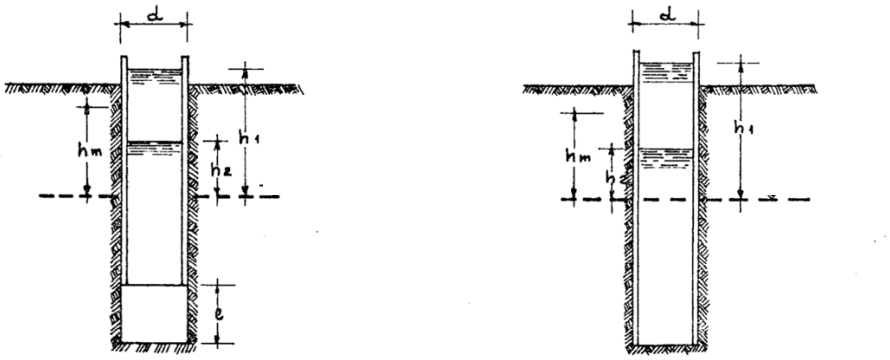

Figure 4.3: Borehole tests schemes AGI (1977) *"Recommendations on the planning and execution of geotechnical investigations".*

Table 4.1 summarizes all 27 Lefranc tests, conducted at the Sacca degli Scardovari, two per borehole with the exception of n° 2 where only one was carried out. For each of them, the depth value with respect to the ground level, the final value of the permeability coefficient, calculated by the eq. 4.5, and the soil type, are reported. This last information is obtained starting from the stratigraphic reconstruction. The shape coefficient is 0.5 for all the tests, like also the diameter of the test section that is equal to 0.127 m.

SURVAY	LEFRANC TEST			
	N° test	Depth [m]	Permeability coefficient k [m/s]	Soil type
1	1	2,5 – 3,0	4,95 E-06	Silty sand
	2	7,5 – 8,0	1,28 E-05	Fine and silty sand
2	1	3,0 – 3,5	3,20 E-06	Medium-fine sand
3	1	2,0 – 2,5	7,66 E-06	Slightly silty fine sand
	2	7,0 – 7,5	1,37 E-05	Silty sand
4	1	3,0 – 3,5	7,35 E-06	Silty sand
	2	6,0 – 6,5	7,35 E-06	Silty sand
5	1	3,0 – 3,5	5,49 E-06	Silty sand
	2	10,0 – 10,5	1,85 E-05	Medium-fine sand
6	1	3,0 – 3,5	5,08 E-06	Fine sand

	2	5,0 – 5,5	3,06 E-06	Silty sand
7	1	3,0 – 3,5	5,64 E-06	Fine sand
	2	10,0 – 10,5	1,26 E-05	Very fine sand
8	1	7,0 – 7,5	2,20 E-05	Silty clay
	2	9,0 – 9,5	4,74 E-06	Medium-fine silty sand
9	1	4,0 – 4,5	4,43 E-06	Fine silty sand
	2	7,0 – 7,5	8,99 E-06	Slightly silty sand
10	1	5,0 – 5,5	3,41 E-06	Medium-fine silty sand
	2	6,0 – 6,5	8,03 E-06	Medium-fine silty sand
11	1	5,5 – 6,0	4,40 E-06	Silty clay
	2	7,0 – 7,5	5,86 E-06	Silt - Sandy silt
12	1	3,25 – 3,75	8,28 E-06	Clayey and silty sand
	2	5,0 – 5,5	4,09 E-05	Fine sand
13	1	3,25 – 3,75	6,28 E-06	Silty clay and sand
	2	5,0 – 5,5	2,46 E-05	Very fine sand
14	1	2,5 – 3,0	6,35 E-06	Sandy silt
	2	9,0 – 9,5	4,66 E-06	Medium-fine sand

Table 4.1: Lefranc tests performed for all the 14 surveys.

From the previous table it is possible to observe how the permeability coefficient k, whose value depends both on the properties of the fluid such as density and viscosity, and on the characteristics of the porous medium, assumes values with an order of magnitude between 10^{-6} and 10^{-5} m/s. This can lead to hypothesize the presence of silty soils. However other in situ and laboratory tests are needed to characterize the soil.

4.3.2 Penetration tests

The static cone penetrometer (CPTm, CPTe) and the piezocone (CPTu and SCPTu) are among the most important tools to characterize soils, especially because they are fast and simple to use, cheap and allow to repeat the same operation several times. A CPT system is made by an electrical or mechanical penetrometer, a pusher system, a cable or a transmission device, a depth recorder and finally a data acquisition unit.

The mechanical cone penetration test consists in pushing a cone penetrometer into the ground, at a constant speed, equal to 20 mm/s, with a series of rods. During penetration, thanks to the presence of

sensors placed at ground level, the resistance to penetration of the cone or tip (q_c), the resistance to total penetration and the friction of the sleeve (f_s) can be recorded.

As can be seen in Figure 4.4, the front end is characterized by a 60° conical tip, and two standard versions are generally available. The first with a diameter of 35.7 mm and with a corresponding cross-sectional area (A_c) equal to 10 cm^2, and a second one with a diameter of 44 mm and A_c = 15 cm^2. Furthermore, according to the characteristics, three sub-categories of the cone penetration test are considered:

- Electrical cone penetration test (CPTe) where the cone resistance and the sleeve friction are measured every 2 cm of penetration.
- Piezocone test (CPTu) that is a cone penetration test with the possibility of measuring pore pressure as well. Depending on the kind of soil, the CPTu can be equipped with a porous filter, that can be located just behind the cone tip or at the midface. The measured pore pressure is influenced by soil type and the filter location on the cone penetrometer. This is the sum of two components, the original in situ pore water pressure and the additional pore pressure due to the penetration of the cone into the ground.
- Seismic piezocone test (SCPTu) which is a piezocone with the possibility of measuring the propagation speeds of shear waves.

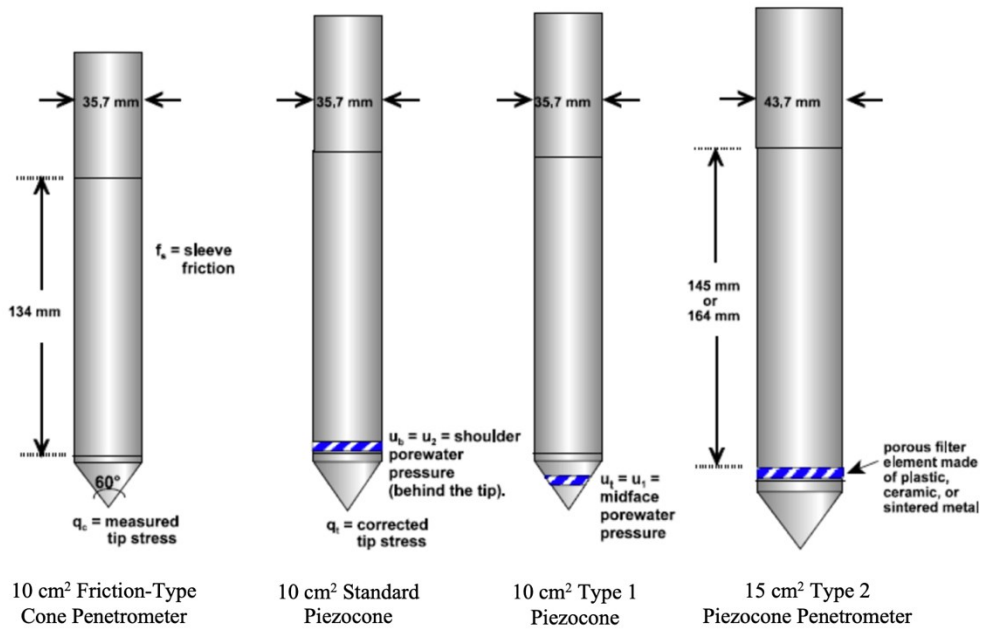

Figure 4.4: Cone penetration test devices.

All the indications in terms of dimensions and tolerances, regardless the kind of device, are collected in the International Reference Test Procedure, ASTM D 5778, 2000 and the ISO 22476-12.

As regards the measures involved, the cone resistance (q_c) is defined as the ration between the measured force on the cone (Q_c) and the area (A_c).

$$q_c = \frac{Q_c}{A_c} \qquad \text{Eq. 4.7}$$

The corrected tip stress is instead defined as q_t. It requires the knowledge of the cone resistance (q_c) the net area ratio (a_n) from a triaxial calibration and the field porewater pressures (u_b).

$$q_t = q_c + (1 - a_n) \cdot u_b \qquad \text{Eq. 4.8}$$

The value of the tip resistance is low for the clay soil and high for the sand one. Unlike clays and silts where the cone resistance value must be modified due to neutral pressures, in sandy soils can be assumed $q_t = q_c$. The sleeve friction (f_s), instead, is measured as the axial force over the sleeve (F_s) and its area (A_s).

$$f_s = \frac{F_s}{A_s} \qquad \text{Eq. 4.9}$$

The unit of measures generally used are kPa or MPa for the corrected cone resistance and kPa for the sleeve resistance and pore water pressures. Instead, the friction ratio is defined by the knowledge of the sleeve friction and the cone tip resistance:

$$R_f = \frac{f_s}{q_t} \cdot 100 \quad [\%] \qquad \text{Eq. 4.10}$$

The friction ratio value is low in granular impermeable soil, and high in a clay soil.

Finally, the pore water pressure is defined as $u = \Delta u + u_0$ where Δu are the excess porewater pressures induced by the cone penetrometer.

When the device is driving through permeable soil, the value of the pore water pressure (u) is very similar or less then the hydrostatic one, while when the device is driving a clay soil, the value of u is much bigger than the hydrostatic level.

Overall, therefore, the CPT and CPTu tests make it possible to define the stratigraphy of the subsoil and estimate geotechnical parameters, thus providing essential results for the design and the numerical modeling. The soil classification can then be facilitated thanks to a series of charts, among which the Robertson graphs (1986 and 1990).

In 1986 Robertson & Campanella defined two classification graphs always using the cone resistance corrected depending on the u value (q_t) for the y-axis, but two different parameters for the x-axis, that are the friction ratio (R_f) and the pore pressure ratio (B_q) This last one is calculated as:

$$B_q = \frac{u_2 - u_0}{q_t - \sigma_{v0}} \qquad \text{Eq. 4.11}$$

Where u_0 is the hydrostatic pore pressure, u_2 is the pore pressure measured with a porous filter placed immediately after the base of the cone and σ_{v0} is the total vertical geostatic stress.

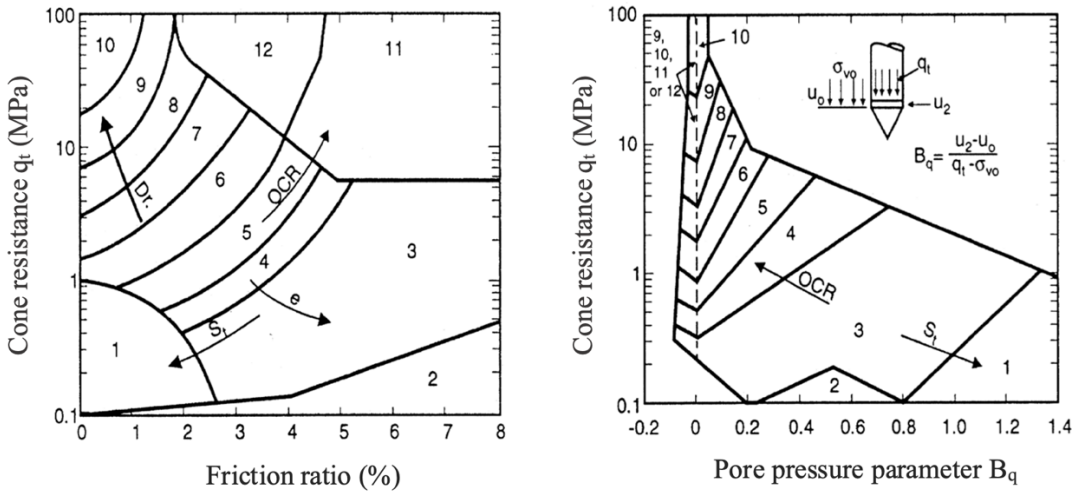

Figure 4.5: Soil Behavior Type chart (Robertson et al., 1986). 1) Sensitive fine grained, 2) Organic material, 3) Clay, 4) Silty clay to clay, 5) Clayey silt to silty clay, 6) Sandy silt to silty sand, 7) Silty sand to sandy silt, 8) Sand to silty sand, 9) Sand, 10) Gravelly sand to sand, 11) Very stiff fine grained, 12) Sand to clayey sand.

The authors suggest using both graphs, however this can lead to several indications. Consequently, if this happens it is necessary to refer to the competence and experience of the operator.
In the 1990 to consider the influence that the lithostatic pressure may exert at great depths, Robertson introduced a new chart with the normalized friction ratio and the normalized cone resistance (Q_{tn}).

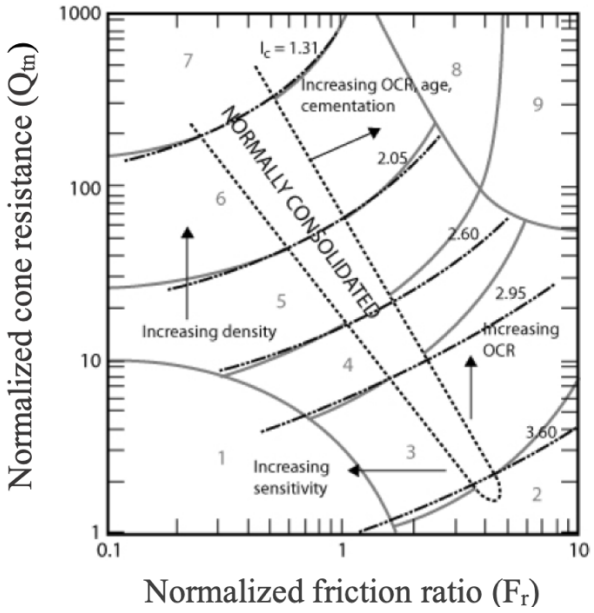

Figure 4.6: Soil Behavior Type chart (Robertson et al., 1990). 1) Sensitive, fine grained, 2) Organic soils, clay, 3) Clays, silty clay to clay, 4) Silt mixtures, clayey silt to silty clay, 5) Sand mixture, silty sand to silty silt, 6) Sands, clean sand to dense sand, 7) Gravelly sand to dense sand, 8) Very stiff sand to clayey sand, 9) Very stiff, fine grained.

The use of CPT and CPTu can be affected by different problems related to the presence of partially saturated soils, mixed soils, and the repeatability of the tests in different climatic conditions. In fact, the measured force on the cone and the sleeve friction depends on the in-situ conditions, which are related to the climatic conditions of the period when the tests are carried out.

In Sacca degli Scardovari, 14 CPTU static penetration tests were carried out with piezocone up to a depth of about - 20 m from the ground level. In addition, 26 dissipation tests were conducted, two per survey, except for n°12 and n°14 where the tests are instead only one.

The results obtained for survey n° 6 will then be presented. This was chosen because all tests, both in situ and in the laboratory were carried out on it, allowing a broad description of the system. Instead, the results of the other surveys subdivided in different areas according to the location (East, North and West) are reported in Figure 4.9.

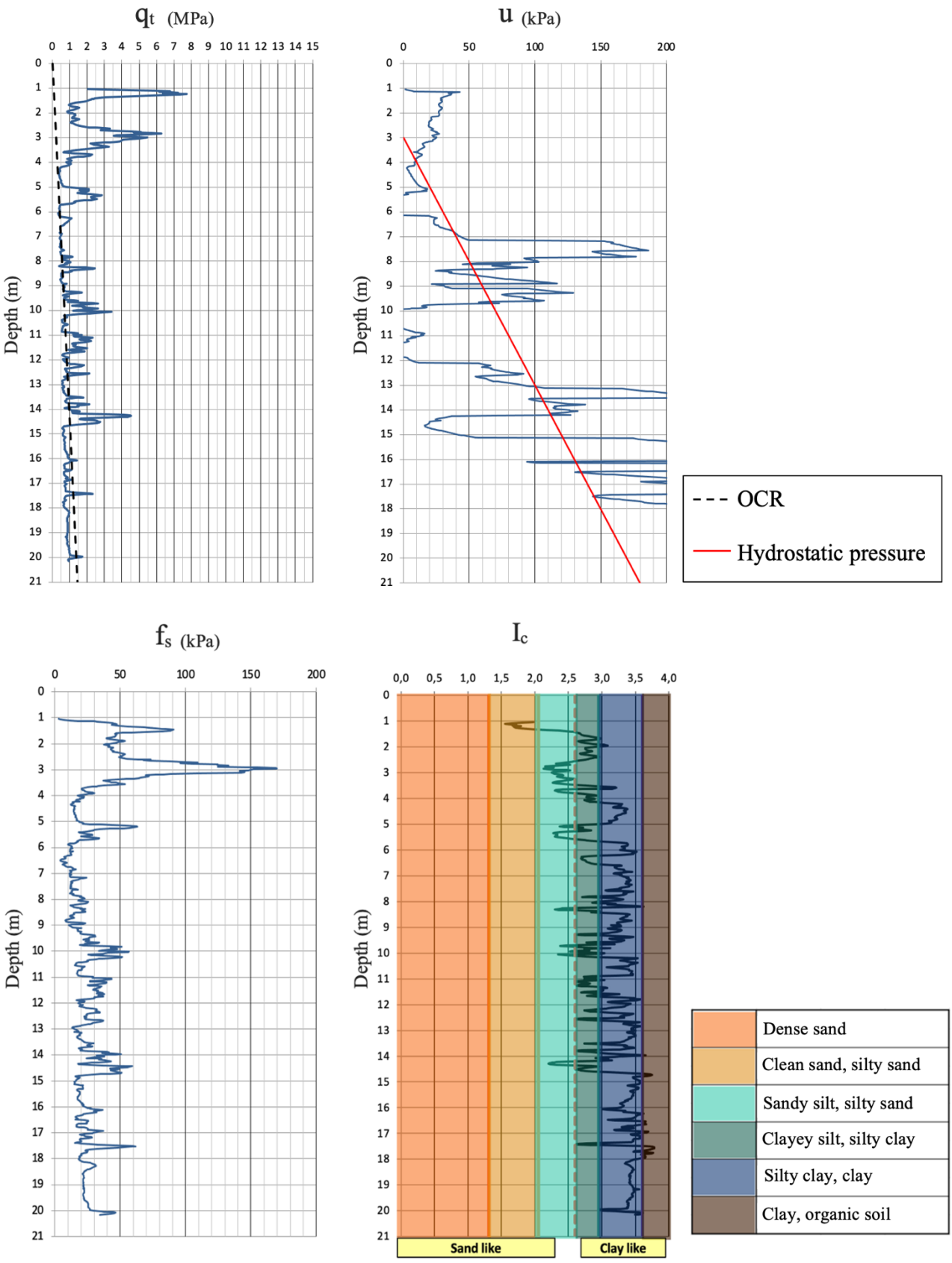

Figure 4.7: Tip resistance (t_p), porewater pressure (u), sleeve friction (f_s) and the SBTn index (I_c), in survey n°6 (Sacca degli Scardovari).

In the previous graphs it is also possible to observe the presence of the classification index I_c, that is defined as:

$$I_C = ((3{,}47 - logQ_t)^2 + (\log F_r + 1{,}22)^2)^{0{,}5} \qquad \text{Eq. 4.12}$$

Where Q_t is the normalized cone resistance, while F_r is the normalized friction ratio. According to the indications provided by *Robertson et al. (1990),* the non-normalized SBT index (I_{SBT}) is like the normalized SBTn index (I_c) but uses only the basic CPT measurements. Generally, normalized I_c provides more reliable identification of SBT than non-normalized I_{SBT}. However, little difference can be observed when the actual vertical stress in situ is between 50 kPa and 150 kPa.

Another significant element is the undrained shear strength (c_u) which can be obtained by the equation:

$$c_u = \frac{q_t - \sigma_{v0}}{10.5 + 7 \log (F_r)} \qquad \text{Eq. 4.13}$$

The following graph shows the results obtained in survey n° 6 at the Sacca degli Scardovari.

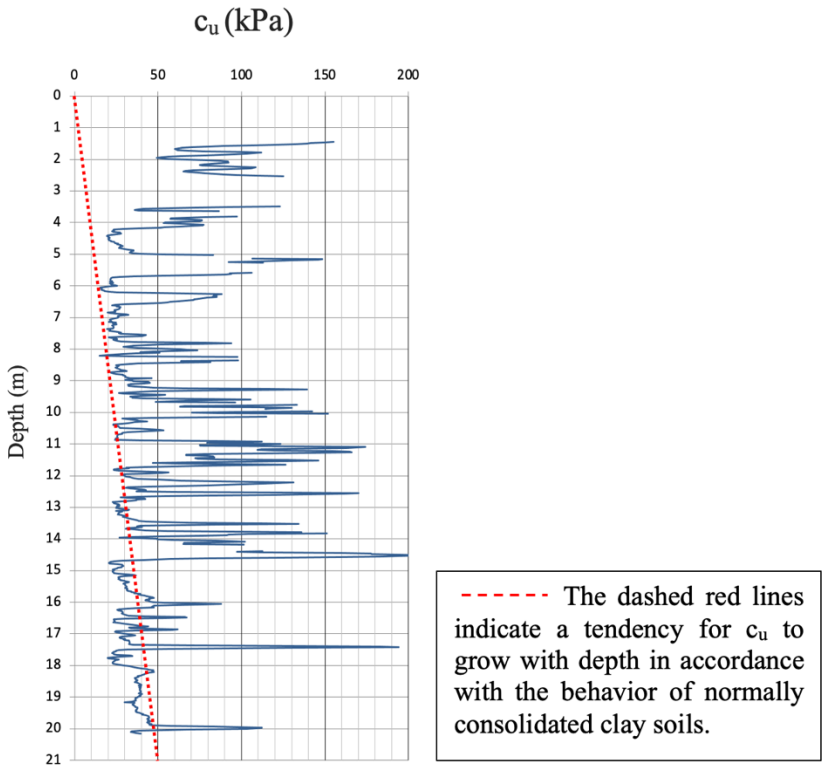

Figure 4.8: Undrained shear strength (c_u) in survey n° 6.

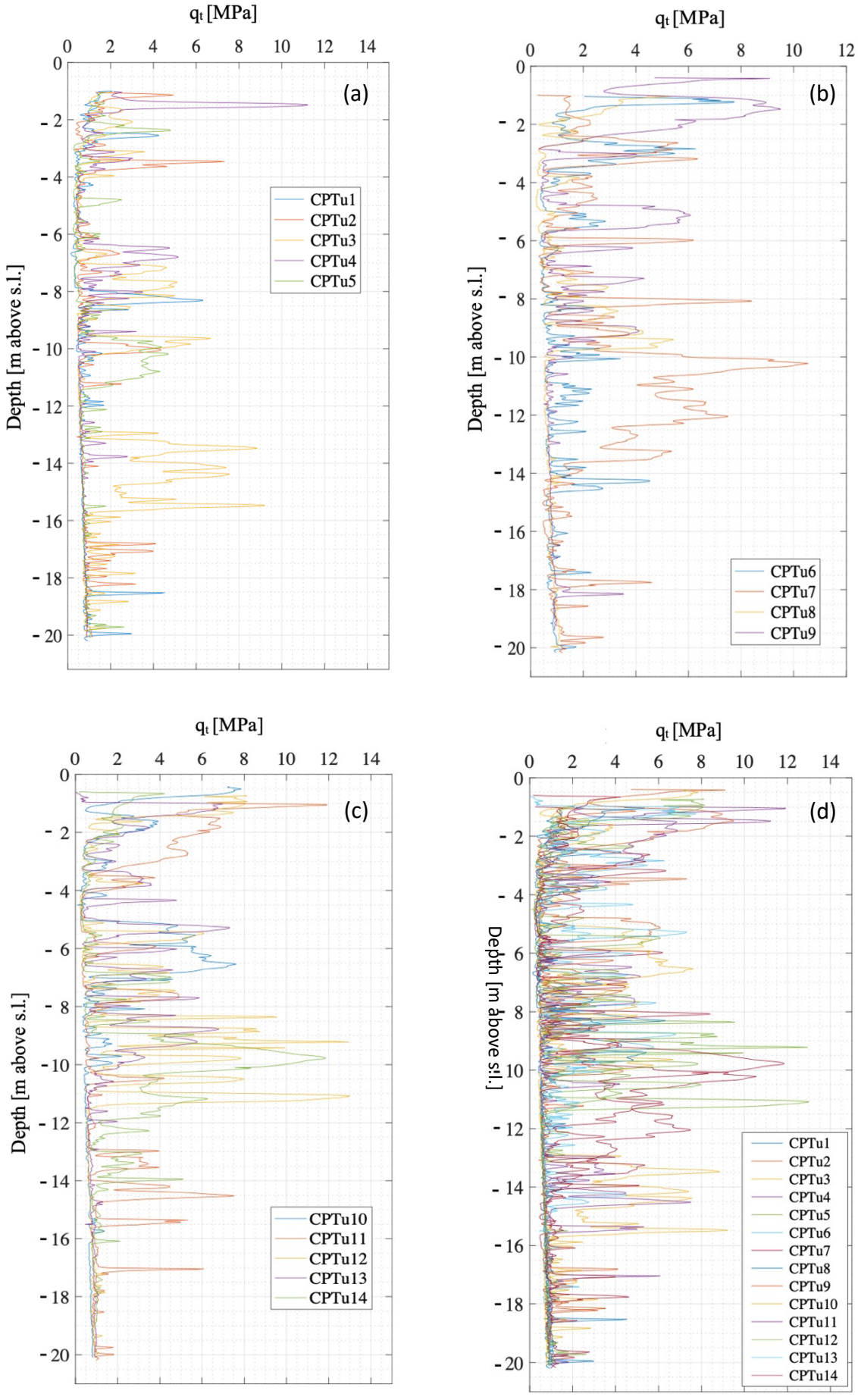

Figure 4.9: Profiles comparison derived from the 14 CPTU tests, subdivided in East area (a), North (b), West (c) and total (d).

4.4 Laboratory tests

Laboratory tests allow to obtain important information on the nature of the soils, compressibility, and permeability. Among these, some are tests aimed at identifying physical and mechanical properties such as shear stresses and oedometric consolidation, while others are permeability tests at both constant and variable loads. The samples studied in the laboratory are collected on site, using standardized equipment and procedures that differ from one case to another. The analysis is then conducted in accordance with both national and international standards such as, for example, UNI (Italian National Unification Association), ASTM (American Society to Testing and Materials) and AASHTO (American Association of State Highway and Transportation Officials).

4.4.1 Granulometric analysis

The granulometric analysis is a laboratory test that allows to define the weight distribution (percentage) of the soil grains with different diameters. In fact, it lets to identify the percentage of clay, silt, sand, gravel, and pebbles in the ground. The procedure is based on two separate tests: the sieve analysis and the sedimentation. The first one is carried out using sieves with meshes characterized by different openings to weigh the quantity of material gradually retained by each sieve. In this way it is possible to identify components such as gravel and sand. Vice versa, for silt and clay, and in general for diameters smaller than 0.075 mm, it is necessary to proceed through the particle size analysis by sedimentation. The final results are then represented in a semilogarithmic plot, called "granulometric curve". Figure 4.10 shows an example of this, obtained from the S6 survey, at the Sacca degli Scardovari.

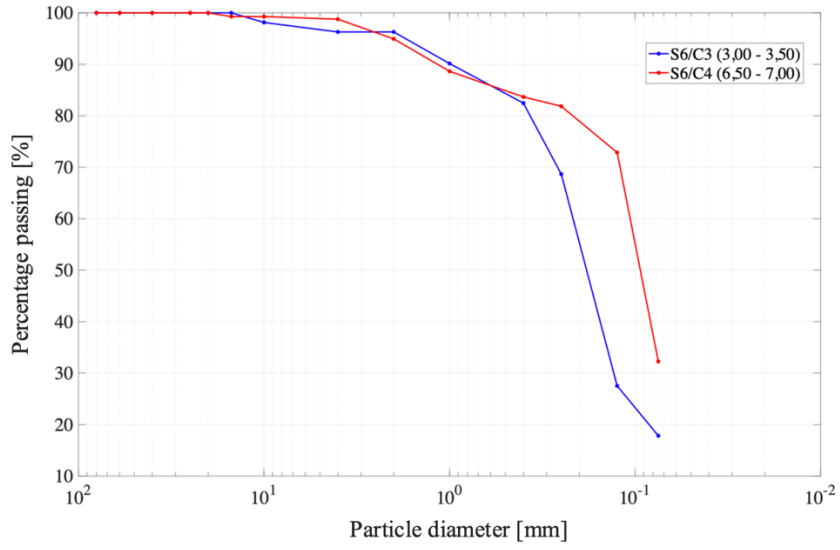

Figure 4.10: Granulometric curve, survey S6 (samples C3 and C4), Sacca degli Scardovari.

The figures from 4.11 to 4.14 show the full results obtained from the boreholes, at Sacca degli Scardovari.

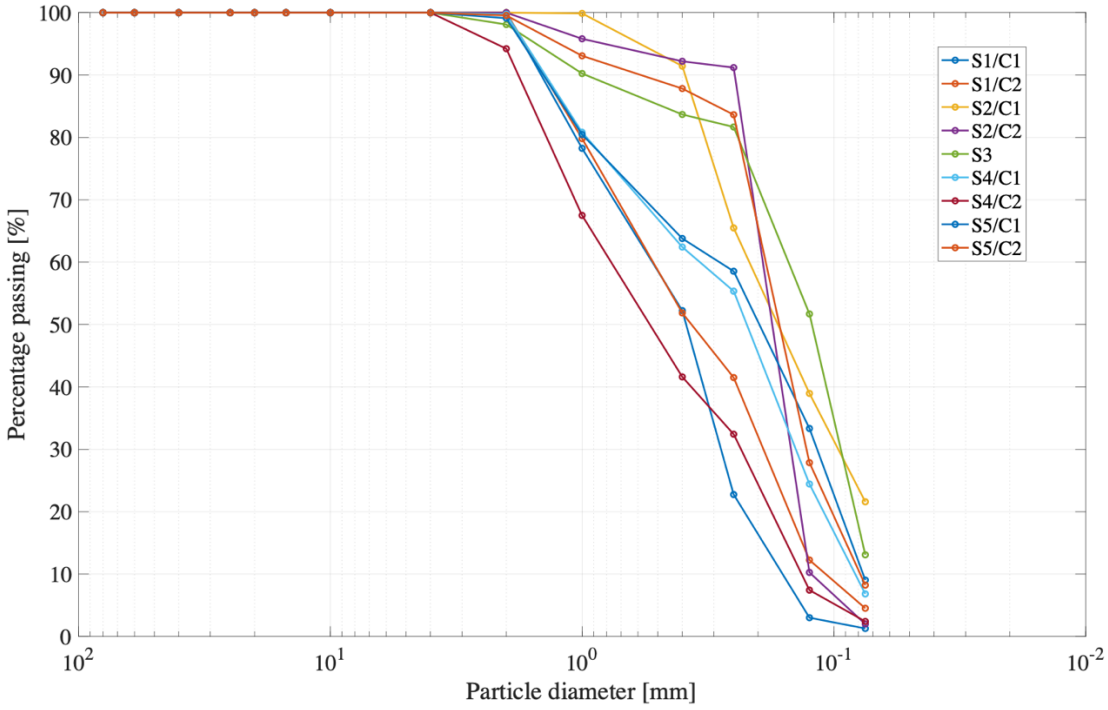

Figure 4.11: Granulometric curve, for boreholes in the East area of Sacca degli Scardovari.

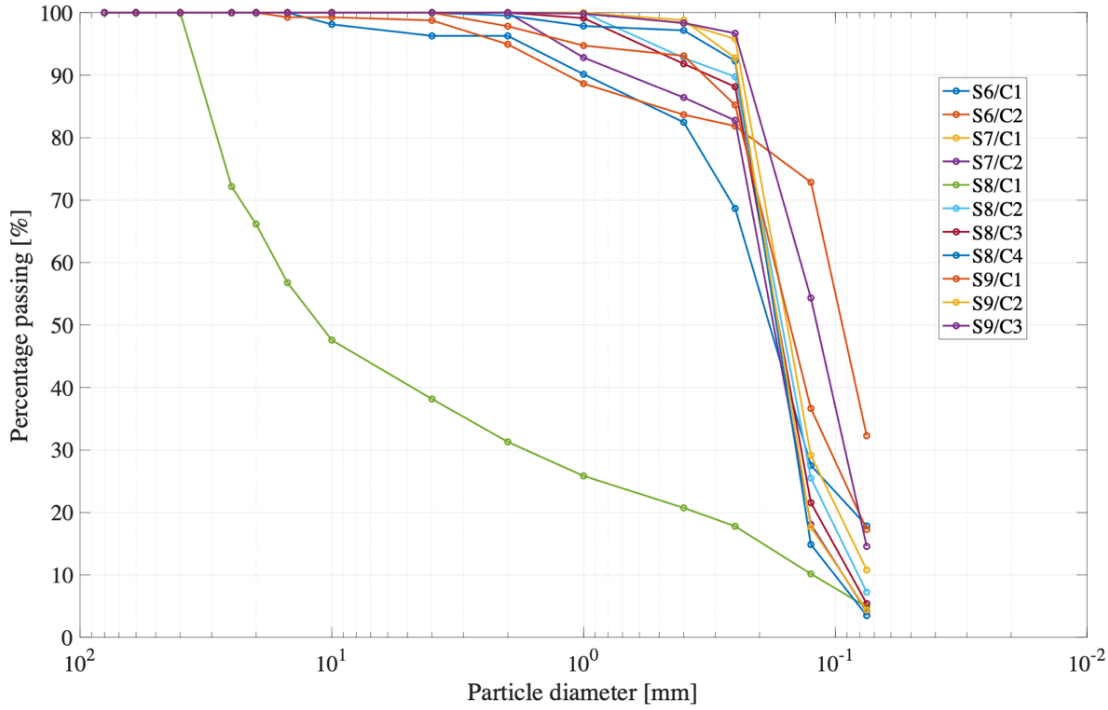

Figure 4.12: Granulometric curve, for boreholes in the North area of Sacca degli Scardovari.

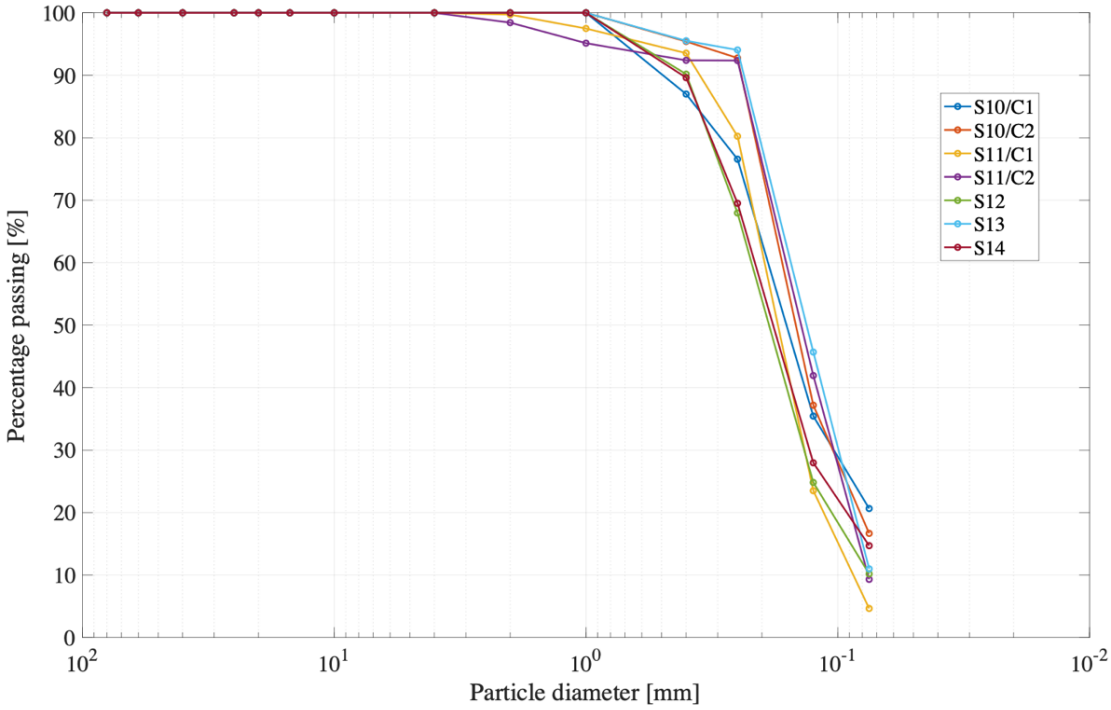

Figure 4.13: Granulometric curve, for boreholes in the West area of Sacca degli Scardovari.

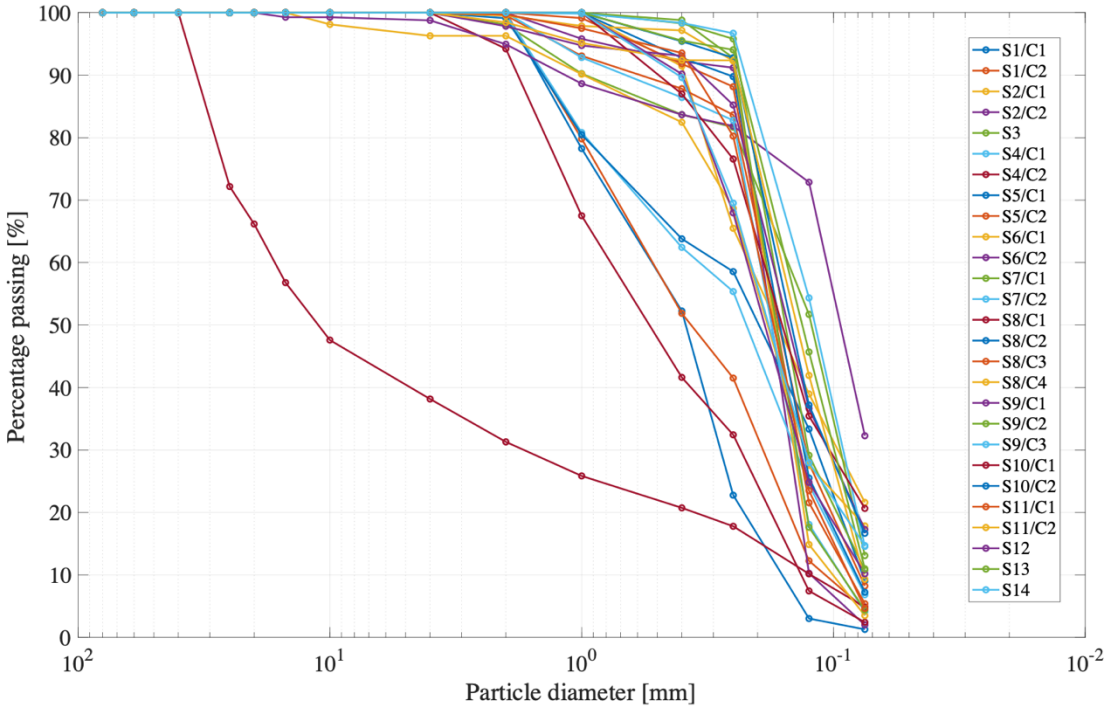

Figure 4.14: Granulometric curve, for boreholes in Sacca degli Scardovari.

4.4.2 Atterberg limits

The Atterberg limits are geotechnical parameters that are obtained in the laboratory using standard procedures and following specific standards such as UNI or ASTM. They have the purpose of understanding the behavior of a soil as the water content varies. These limits depend on the water content. It is possible to distinguish between solid, semi-solid, plastic, and liquid state. The transition from one state to another can be described through the Atterberg limits, as shown in Figure 4.15.

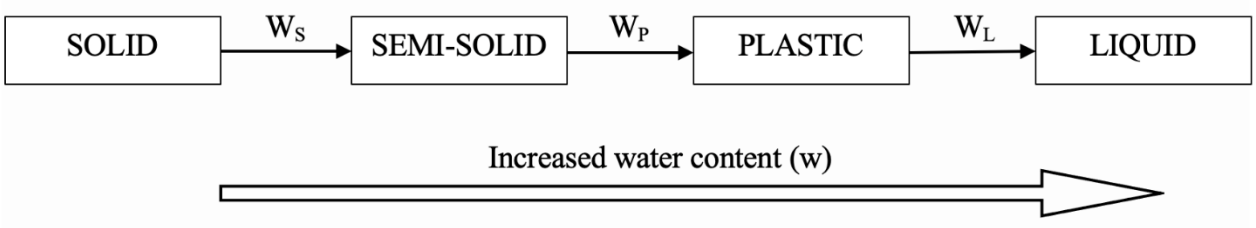

Figure 4.15: Atterberg limits and solid, semisolid, plastic, and liquid states.

It is therefore possible to distinguish three different limits, namely:

- Shrinkage limit W_S
- Plastic limit W_P
- Liquid limit W_L

The shrinkage limit is the water content that corresponds to the transition between the solid and semi-solid states. Below this value the soil, if dried, it no longer undergoes a reduction in volume. In fact, the volume of a soil decreases as the soil moisture is reduced, however below a given water content the volume remains constant. To define it, is necessary to gradually dry an undisturbed sample, then measuring the volume and the water content. The soil, placed in bowls with a known volume, is weighed in such a way as to obtain the wet weight. After drying it, by placing the sample into an oven at 105 °C for 24 hours, it is possible to calculate the dry weight. At this point, the soil is put inside a measuring cup together with mercury. Finally, the volume of the sample is obtained through the difference between the measured volume and that of the mercury, while the shrinkage limit is given by:

$$w_S = \frac{(P_i - P_f) - (V_i - V_f)}{P_f} \cdot 100 \qquad \text{Eq. 4.14}$$

With P_i initial weight of the sample, P_f weight of the sample after drying, V_i initial volume and V_f final volume.

The plastic limit corresponds to the transition between the semi-solid and the plastic state. It is also defined as the minimum water content with which it is possible to model cylindrical-sized soil mass of about 3 mm in diameter. These are rolled on a glass surface to gradually reduce the water, until the sample breaks. The test is conducted by attempts, starting from a sufficiently humid soil. This water content is then gradually reduced. The final result is given by the average of several measurements, where the water content equal to the plastic limit corresponds to the conditions in which the cylinder of soil (3 mm) breaks. Silt and sand are called non-plastic soils as it is not possible to shape the sample to form cylinders and consequently the plastic limit cannot be determined. Furthermore, as the particle size decreases, both the plastic and liquid limits increase.

The liquid limit is the water content that corresponds to the transition between the plastic and liquid state. It can be obtained through two standard tests: Casagrande cup and cone penetrometer. In the first case, a soil sample is used taken from the portion passing through sieve N° 40 and mixed with distilled water, so that the water content is greater than the liquid limit. After having properly positioned and leveled the sample inside the Casagrande Cup, a groove is made in the center. At this point, the number of blows needed to close the groove are counted.

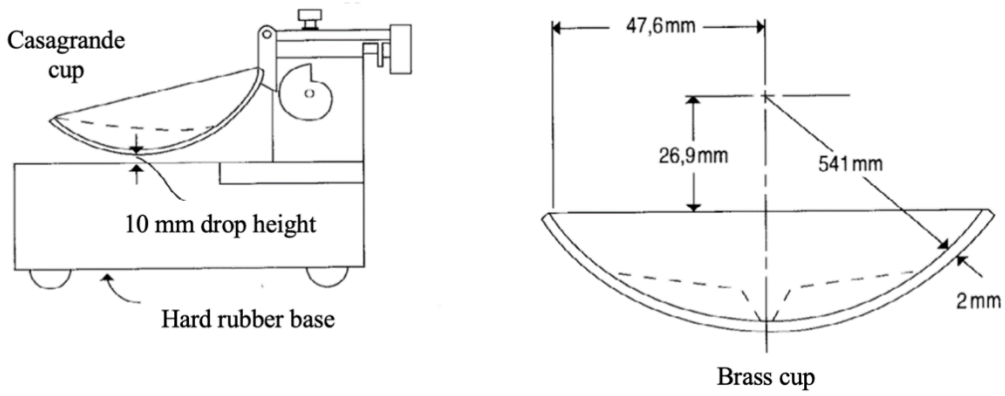

Figure 4.16: Casagrande cup.

The test is repeated at least three times, varying the moisture content. In this way it is possible to build a semi-log graph, placing the soil moisture (%) along the vertical axis and the number of blows in the x-axis. Conventionally, the liquidity limit is the water content related to the intersection with the abscissa of the 25 blows. In fact, the water limit is defined as the water content for which the groove closes (by 10 mm) with 25 blows. Figure 4.17 shows the results of the survey n°6 at the Sacca degli Scardovari, obtained in laboratory.

Sample	N° blows	Moisture content (%)
1	36	24,31
2	26	25,29
3	20	25,28
4	15	25,00
W_L	25	25,00

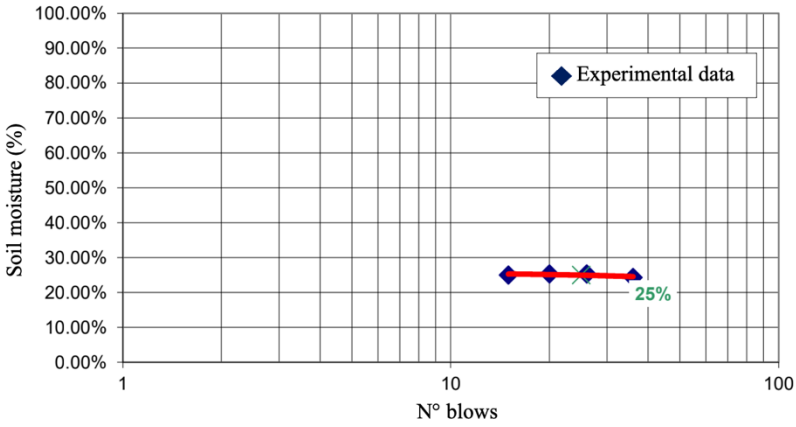

Figure 4.17: Surveys n°6 Sacca degli Scardovari, liquid limit (W_L).

Once the values of the liquid and plastic limits have been obtained, it is also possible to calculate the plasticity index (I_P):

$$I_P = W_L - W_P \qquad \text{Eq. 4.15}$$

It represents the water content range on which the soil retains its plastic state. In particular:

Soil	I_P
Non-plastic	0 – 5
Low plasticity	5 – 15
Plastic	15 – 40
High plasticity	> 40

Consistency	I_c
Liquid	< 0
Liquid – Plastic	0 – 0.25
Soft – Plastic	0.25 – 0.50
Plastic	0.50 – 0.75
Solid – Plastic	0.75 – 1
Semi-solid or solid	> 1

Table 4.2 and 4.3: Tables with different values of plasticity index I_P and consistency index I_C.

The consistency of a soil, on the other hand, is defined through the consistency index (I_C). This last one is calculated starting from the water content in the liquid limit (W_L), the natural water content of the sample (W_n), and the plasticity index:

$$I_C = \frac{w_L - w_N}{I_P} \qquad \text{Eq. 4.16}$$

These indices can be very useful for studying the slope stability. In fact, lower is the plasticity index and greater is the stability, vice versa lower is the consistency index and lower is also the slope stability.

Soils made mainly of silt and clay can be classified using the Casagrande's plasticity chart. This system is based on the Atterberg limits. The graph is built placing the liquid limit on the abscissa and the plasticity index on the y-axis. This plot is then divided into six areas which correspond to different characteristics of the terrain. The subdivision is obtained by vertical lines in correspondence of W_L = 50 and two straight lines with equation:

$$A - \text{line} \quad PI = 0.73\ (w_L - 20) \qquad \text{Eq. 4.17}$$

$$U - \text{line} \quad PI = 0.9\ (w_L - 8) \qquad \text{Eq. 4.18}$$

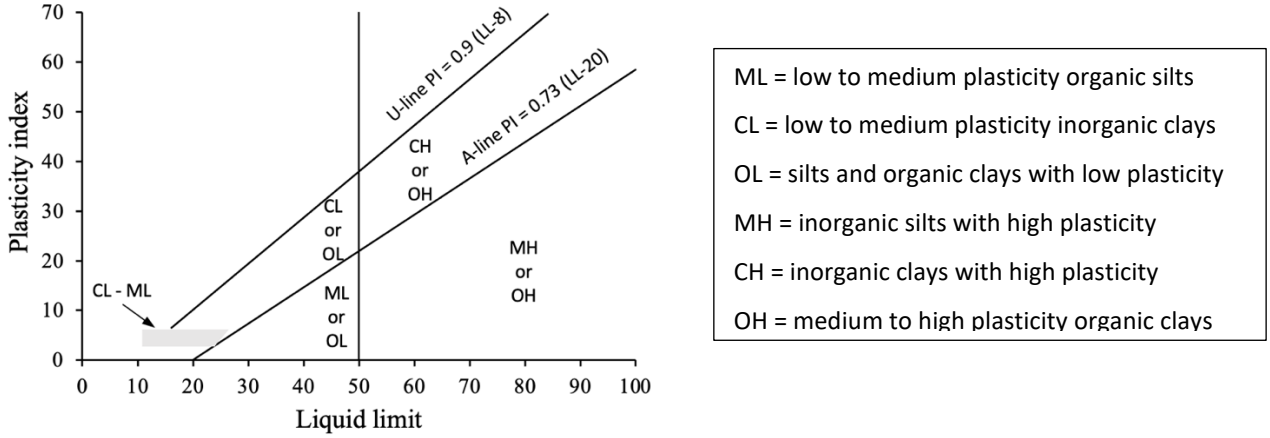

Figure 4.18: Casagrande's plasticity chart.

Referring to the surveys in Figure 4.1, at the Sacca degli Scardovari, the laboratory analyzes were conducted for the Atterberg limits except for S3 – S7 – S11 – S12 – S13. Through the results obtained it was possible to identify mainly the category CL so the low to medium plasticity inorganic clays (Surveys: S2 – S4 – S5 - S6 – S8 – S10 – S14). However, other surveys have led to different results, like the identification of silt and organic clays and inorganic silts, with low plasticity (ML - OL), or inorganic clays and inorganic silts, always with low plasticity (Cl-ML).

In the following graphs (Figure 4.19) are reported the results for the surveys S6 where two samples were studied, and the Casagrande's plasticity chart for all the boreholes.

Survey S6/C1	
Depth [m]	4.5 – 5.1
Natural humidity [%]	33
Liquid limit [%]	31
Plastic limit [%]	21
Plasticity index [%]	10
USCS classification	CL

Survey S6/C2	
Depth [m]	7.0 – 7.6
Natural humidity [%]	32
Liquid limit [%]	25
Plastic limit [%]	18
Plasticity index [%]	7
USCS classification	CL – ML

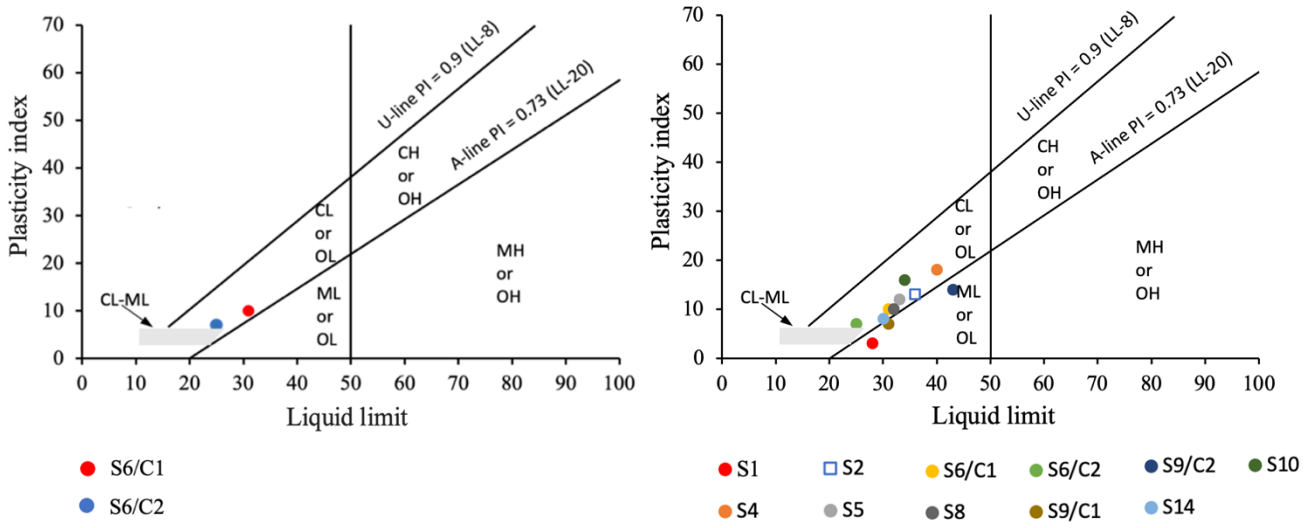

Figure 4.19: Tables with Atterberg limits and Casagrande's plasticity chart for the survey n°6 (left), and total results (right).

4.4.3 Soil consolidation and oedometer test

The soil consolidation is a process on which the soil volume decreases due to a stress induced by a natural load like the sedimentation processes, or anthropogenic loads like the embankment construction. The consolidation process has different duration depending on the soil permeability and compressibility. Typically, this process is very long (years or decades) in clayey soils, while it is faster in sandy soils.

In 1923 Terzaghi developed a mathematical theory to describe the one-dimensional consolidation. Furthermore, the laboratory test used to study it, is called Oedometer test. In this, a saturated soil sample with a cylindrical shape, is subjected to a vertical load, while the lateral expansion is prevented. The load is maintained, generally, for 24 hours during which the soil consolidates. However, the load does not remain constant, but it is increased at stages. The deformations obtained

are then measured to develop a temporal settlement curve. In particular, the deformations are measured at 6, 15 and 30 seconds but also at 1, 2, 4, 8, 16, and 30 minutes and 1, 2, 4, 8 and 24 hours. At the end of the test, also the water content and the final height of the soil sample are measured. The consolidation test allows to obtain different results like the stress-void ratio curve in a semi-logarithmic scale, the swelling index (C_s), the compression index (C_c) and the coefficient of volume compressibility (m_v).

Knowing the water volume (V_w) and the soil volume (V_s) is possible to define the void ratio (e):

$$e = \frac{V_w}{V_s} \qquad \text{Eq. 4.19}$$

The oedometric curve is then obtained considering the relationship between the void ration and the vertical effective stresses (σ'_v).

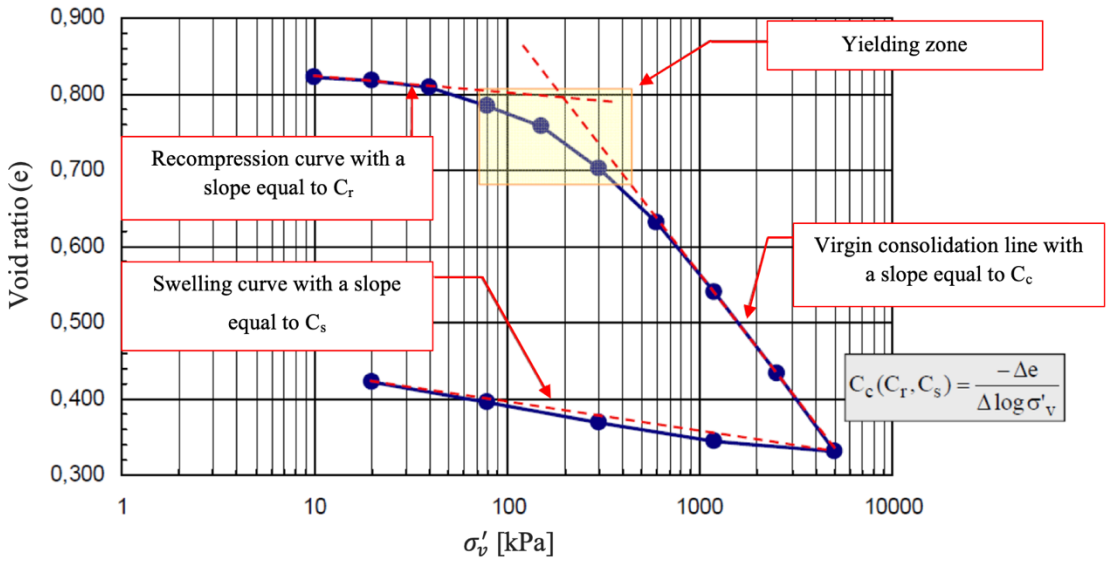

Figure 4.20: Oedometric curve.

This curve can be divided into three sections, a first part of recompression or reloading characterized by a slight slope, an intermediate part of compression or loading, and finally the unloading curve. The slope of these lines is indicated by the recompression index C_r along the initial part of the curve, the compression index C_c along the normal consolidation line (Overconsolidation ratio OCR = 1), and the swelling index (C_s) that characterize the unloading or reloading section.

$$C_r = \frac{\Delta e}{\Delta \log \sigma'_v} \qquad C_c = \frac{\Delta e}{\Delta \log \sigma'_v} \qquad C_s = \frac{\Delta e}{\Delta \log \sigma'_v} \qquad \text{Eq. 4.20}$$

Table 4.4 and Figure 4.21 describe the results of the survey S6 in Sacca degli Scardovari. In particular, the values of the consolidation coefficient (c_v), the permeability coefficient (k), the coefficient of volume compressibility (m_v) and the oedometric modulus (E_{ed}) are summarized. These last ones, knowing the stresses (σ) and the vertical displacement (Δh), are calculated as:

- Coefficient of compressibility: $a_v = \frac{\Delta e}{\Delta \sigma}$ Eq. 4.21
- Coefficient of volume compressibility: $m_v = \frac{a_v}{(1+e)}$ Eq. 4.22
- Oedometric modulus: $E_{ed} = \frac{1}{m_v}$ Eq. 4.23

σ [kPa]	Δh [mm]	ε [%]	e [-]	m_v [m^2/kN]	E_{ed} [kPa]	c_v [m^2/s]	k [m/s]
0	-	-	1,301	-	-	-	-
12,258	0,364	1,82	1,260	1,49E-03	673,521	6,208E-08	9,04E-10
24,517	0,583	2,92	1,234	1,19E-03	841,018	5,366E-08	6,26E-10
49,033	0,940	4,70	1,193	7,55E-04	1332,429	6,400E-08	4,71E-10
98,067	1,563	7,82	1,122	6,63E-04	1500,123	6,403E-08	3,95E-10
196,133	2,352	11,76	1,031	4,38E-04	2291,618	8,881E-08	3,80E-10
392,266	3,310	16,55	0,921	2,75E-04	3613,064	8,792E-08	2,39E-10
784,532	4,298	21,49	0,807	1,53E-04	6626,451	-	-
392,266	4,213	21,07	0,817	1,02E-05	-	-	-
98,067	3,848	19,24	0,859	-	-	-	-
24,517	3,462	17,31	0,903	-	-	-	-

Table 4.4: Results of the oedometer consolidation test, survey n°6 Sacca degli Scardovari.

In this specific case, the oedometric curve obtained is the following:

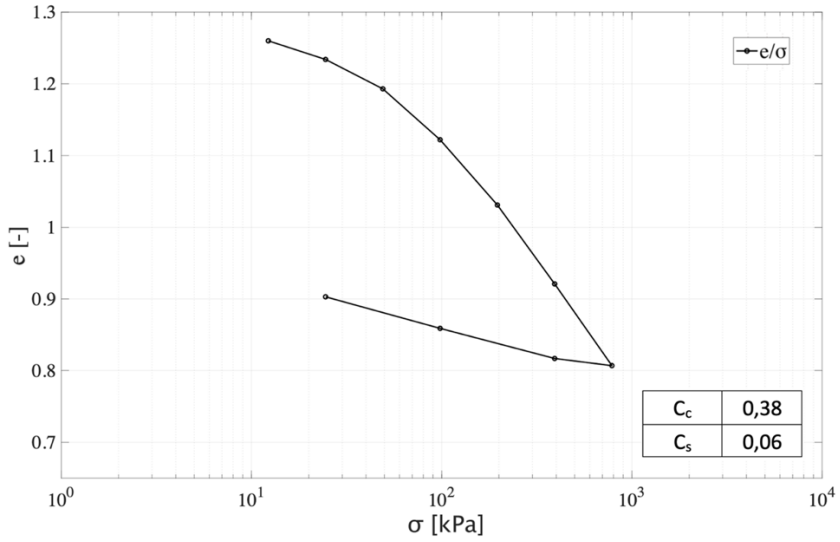

Figure 4.21: Oedometric curve, survey n°6 Sacca degli Scardovari.

In the following graphs are reported all the Oedometric curves, obtained from the tests performed in Sacca degli Scardovari.

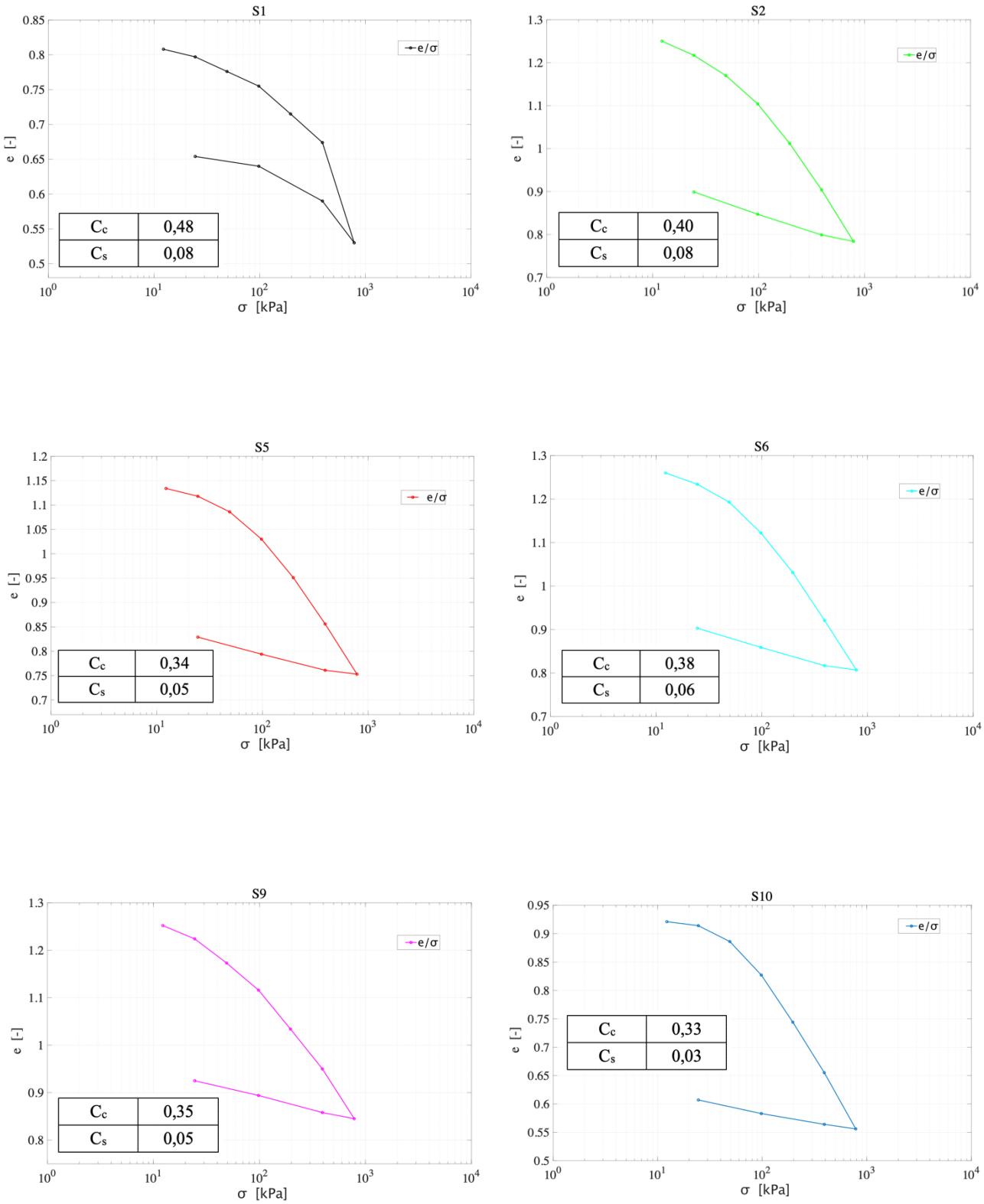

Figure 4.22: Oedometric curves, for Sacca degli Scardovari tests.

4.4.4 Triaxial tests

The triaxial tests have the purpose of define the evolution of the effective stresses until the failure condition is reached. This last one is obtained applying a stress state on the specimen. The effective stress is calculated as the difference between the total stress and the pour water pressure:

$$\sigma' = \sigma - u \qquad \text{Eq. 4.24}$$

In fact, both the variations of pore pressure and the total stress influence the mechanical characteristics of the soil.

During the triaxial tests, the specimen is protected by a latex membrane to prevent the penetration of water into the pores of the soil, and it is located into a Perspex cell. The volume inside the cell is then filled by water in pressure. The aim is to apply different initial state of stress at the specimen. The axial load is then applied through a piston.

This test is subdivided in two phases, a first one, in which an isotropic state of stress is applied, and a second one, in which there is an increment of stress only in the vertical direction. The technical apparatus is that shown in Figure 4.23:

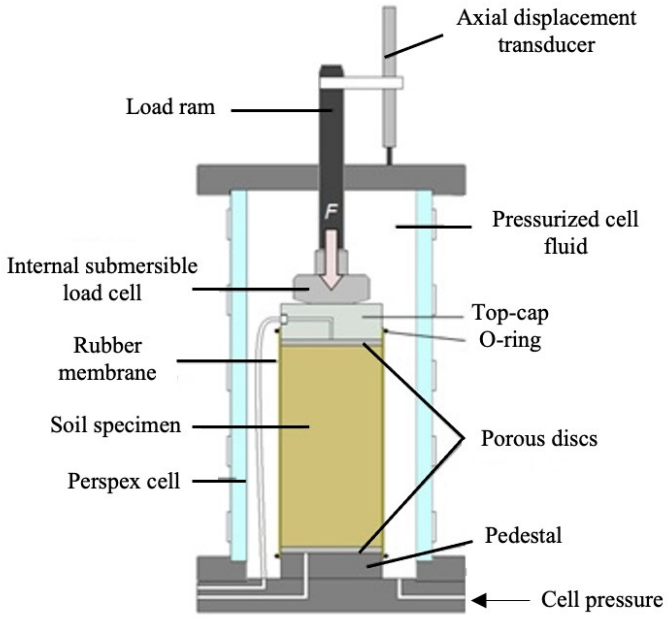

Figure 4.23: Triaxial test apparatus.

This system is equipped with two drains, that may be open or close depending on the test phase. One is generally located at the bottom, while the second is placed at the top of the apparatus. These are

not the only connections between the external environment and the internal part of the cell, because there is also a vent in the upper part and a tube at the bottom that is used to fill the cell with water.

With this kind of test is possible to measure both the volume change of the specimen during a drained test and the pore water pressure during an undrained test. Furthermore, the triaxial tests can be distinguished according to the consolidation and drainage conditions:

- Unconsolidated and undrained test (UU)
- Consolidated and undrained test (CU)
- Consolidated and drained test (CD)

In the UU test the specimen is placed in the triaxial cell with the drainage valves closed during all the experiment. Thus, no consolidation can occur if the sample is completely saturated, even when a confining pressure is applied. This test is a total stress test, and it yields the strength in terms of total stresses, while usually the pore water pressure is not measured. All Mohr circles at failure will have the same diameter and Mohr failure envelope will be a horizontal straight line. In fact, it is important to note that if all the samples have the same water content and void ratio, then they will have the same strength.

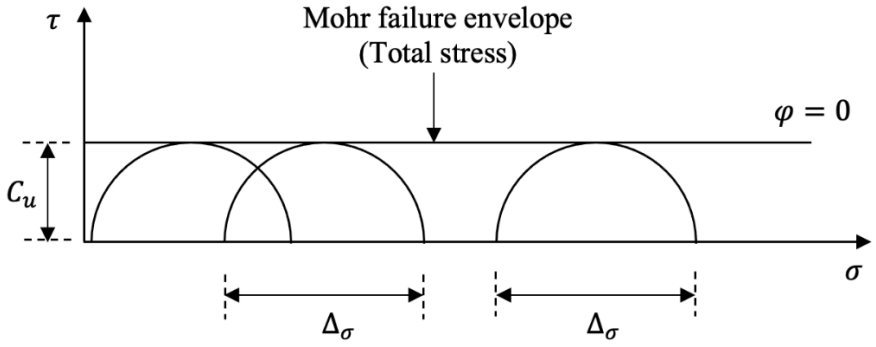

Figure 4.24: Mohr failure envelope in a UU triaxial test.

The intercept of the envelope on the vertical axis defines the intrinsic cohesion parameter (c_u), while the angle of the internal friction (φ') is equal to zero.

The CD triaxial test is characterized by an isotropic consolidation phase and a rupture phase in drained conditions. In this case, the drains are always open, furthermore the breaking occurs very slowly. In this way the pore pressure in the specimens is not altered and volume changes are measured. These tests are then repeated on different samples and with different stress states. At the end it is possible to draw the Mohr circles in terms of effective stresses and define the cohesion parameter (c´) and the

internal friction angle (φ'), starting from the envelope. The problem of this procedure is that the rate of loading must be very slow, to ensure that no excess pore pressure is induced in the specimen. This long time can lead to practical problems in the laboratory and as consequence these tests are not so used. This also because it is possible to measure the induced pore pressures in a consolidated-undrained (CU) test and then calculate the effective stresses in the specimen.

The CU triaxial test is carried out by means of an isotropic consolidation phase but the specimen breaking occurs in undrained conditions. The first phase is characterized by open drains while the second by closed drainage system. Therefore, there is no variation in volume and during the failure phase the variation of the pore water pressure in the specimen is measured. The effective stresses are finally calculated as the difference between the total stresses and the measured pore water pressures.

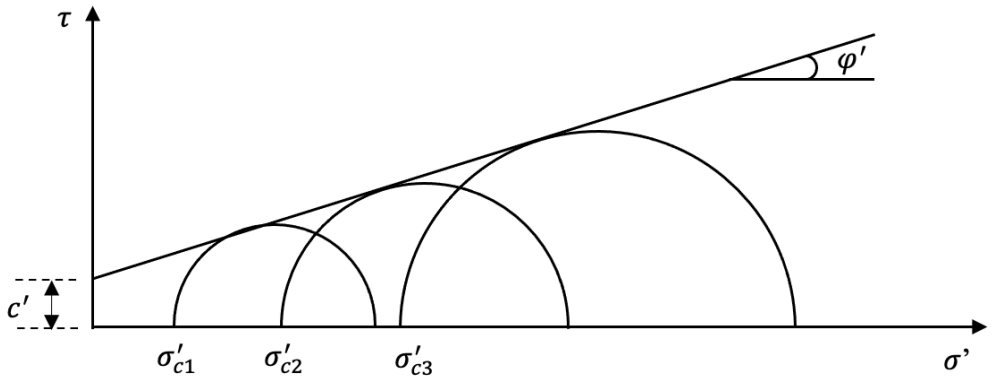

Figure 4.25: Mohr failure envelope in a CU triaxial test.

In the following tables the results, obtained considering the geotechnical survey in Sacca degli Scardovari, are summarized. The number of the boreholes correspond to that in Figure 4.1.

Boreholes	CU triaxial test		
	Depth [m from g.l.]	c’	φ’
S4	4.5 – 5.1	2.47	24
S6	7.0 – 7.6	6.97	22
S9	3.4 – 4.0	13.6	25
S12	4.5 – 5.1	27.5	26
S14	4.5 – 5.1	12.7	23

Table 4.5: CU triaxial tests results.

Boreholes	UU triaxial test		
	Depth [m from g.l.]	c_u	φ
S2	5.0 – 5.5	74.3	0
S5	7.0 – 7.6	52.5	0
S8	6.0 – 6.6	53.5	0
S10	2.4 – 3.0	62.6	0

Table 4.6: UU triaxial tests results.

5. NUMERICAL MODEL RESULTS

In the following chapter, the geotechnical modeling results obtained using the PLAXIS 2D software are presented. Due to the extent of the region analyzed, as regards the Sacca degli Scardovari, only the most critical sections are described in terms of both geotechnical and maritime conditions. For the other lagoons of the Po Delta region, where a geotechnical survey has not been carried out, an approximate solution is obtained. In fact, the same soil characteristics founded in Sacca degli Scardovari are assumed.

5.1 Geotechnical modeling with PLAXIS 2D

PLAXIS 2D is a finite elements package, two-dimensional, developed for the stability, the flow, and the deformation analysis, in different geotechnical problems. The method used is that of finite elements (F.E.M.). This last one is a numerical technique with the aim of approximating the problems solutions, starting from partial differential equations, and reducing them to a system of algebraic equations. In the F.E.M. the domain is made by subdomains of elementary shape, such as triangles and quadrilaterals in the 2D system. For each of these elements, the solution of the problem is expressed through the linear combination of the shape functions.

The software interface is divided into two programs, one for input and one for output. The first is used to define the initial geometry of the problem, the mash, the infiltration conditions, and the different calculation phases. Instead, the output program is useful for viewing the results. Through this, it was possible to characterize the lagoons of the Po Delta, in terms of geotechnical stability and checks on the conditions or mechanisms of rupture. The simulation of the filtration phenomena that affect the stability of the embankment is also very important. Both current (2020) and future (2070) conditions were studied, and not only the stationary but also the extreme tide and wave conditions, were analyzed.

With Plaxis 2D program it is also possible to calculate the safety factors associated with each phase. The approach followed is of the phi/c reduction type, as the parameters of shear strength and tensile strength are decreased until the failure occurs. Then, defined with the subscript 'input' the resistance parameters, referring to the properties entered in the material sets, and with the subscript 'reduced' the parameters referring to the reduced values used in the analysis, the total multiplier ΣMsf is defined in the equation 5.1.

$$\Sigma\text{Msf} = \frac{tan\varphi'_{input}}{tan\varphi'_{reduced}} = \frac{c'_{input}}{c'_{reduced}} = \frac{Tensile\ strength\ _{input}}{Tensile\ strength_{\ reduced}} \quad \text{Eq. 5.1}$$

The incremental multiplier Msf is used to specify the increase of the force reduction starting from the first calculation phase. This is set to 0.1 by default. Furthermore, if a complete failure mechanism has occurred at the end of the process, the safety factor is:

$$SF = \frac{available\ strength}{strength\ at\ failure} = \Sigma\text{Msf at failure} \quad \text{Eq. 5.2}$$

It is important to note that if a failure mechanism is not fully developed, it is necessary to increase the number of steps and repeat the calculation.

The FS values obtained, must then be compared with the limits indicated by the Italian regulation. The information is provided in the "Norme Tecniche per le Costruzioni" (2018). The technical standard introduces three types of partial coefficients, useful for combining actions, reducing geotechnical parameters and resistance. These are indicated with three different letters:

- A: Actions, to amplify the actions
- M: Materials, to reduce the materials strength
- R: Resistance, acting on the overall resistance of the system.

These letters are followed by numbers which indicate specific groups of coefficients. Table 5.1 summarized the partial coefficients regarding the actions.

Loads	Effect	Partial coefficient (γ_F) or (γ_E)	EQU	(A1)	(A2)
Permanent loads (G_1)	Favorable	γ_{G1}	0.9	1.0	1.0
	Unfavorable		1.1	1.3	1.0
Permanent loads (G_2)	Favorable	γ_{G2}	0.8	0.8	0.8
	Unfavorable		1.5	1.5	1.3
Variable loads (Q)	Favorable	γ_{Qi}	0.0	0.0	0.0
	Unfavorable		1.5	1.5	1.3

Table 5.1: Partial coefficients for the actions or for the effect of the actions. (Reproduction of table 6.2.I into the "Norme tecniche per le costruzioni", 2018).

Instead for the resistances:

Parameter	Quantity to which apply the partial factor	Partial coefficient (γ_M)	(M1)	(M2)
Tangent of the shear strength angle	$tan\varphi'_k$	$\gamma_{\varphi'}$	1.0	1.25
Effective cohesion	c'_k	$\gamma_{c'}$	1.0	1.25
Undrained resistance	c_{uk}	γ_{cu}	1.0	1.4
Weight of the unit of volume	γ_γ	γ_γ	1.0	1.0

Table 5.2: Partial coefficients for the geotechnical parameters of the soil. (Reproduction of table 6.2.II into the "Norme tecniche per le costruzioni", 2018).

According to the indications, provided into the paragraph 6.8 "Works of loose materials and excavation fronts", it is necessary to follow the equation:

$$E_d \leq R_d$$

Where E_d is the design value of the action while R_d is the design value of the resistance. Furthermore, the checks must be carried out according to Combination 2 (A2 + M2 + R2) of Approach 1. This last one indicates an approach where the checks are conducted with two different combinations of groups of coefficients. The values of the partial coefficients are reported in Tables 6.2.I, 6.2.II and 6.8.I of the Norme Tecniche per le Costruzioni (NTC), previously summarized.

Table 5.2 indicates to reduce the effective resistance parameters according to $\gamma_{M2} = 1.25$ while Table 6.8.I provides a partial safety coefficient $\gamma_R = 1.1$. Finally, as a consequence, it is necessary to compare the value of FS obtained with a safety factor equal to 1.375.

5.2 Soil characteristics

The soil characteristics depend on the area of interest, however, despite the geotechnical investigations conducted at the Sacca degli Scardovari, it was necessary to introduce some strong assumptions. First of all, due to the limited number of data, it was not possible to exactly identify the mechanical characteristics of the soil, furthermore the tests in situ and in the laboratory were conducted only in the Sacca degli Scardovari and not on the entire area of the Po Delta. This means

that for the lagoons of Caleri, Vallona, Barbamarco and Canarin there are not specific data for the soil characterization from a hydraulic and mechanical point of view.

The mechanical and hydraulic characteristics, for each type of soil, are assumed to be the same for all the sections. This condition may be satisfying for the Sacca degli Scardovari. This is also confirmed by the geotechnical investigations which have shown homogeneity in the soil characteristics. Vice versa, the use of these parameters for modeling the other lagoons of the Po Delta is not confirmed by the geotechnical surveys, as they are missing.

In the analysis, 4 types of soil were considered, one for the superficial clayey layer, one for the intermediate (silty-sandy), one for the deep clayey layer, and finally the material for the embankment. In addition, only for the sections where it is present, the characteristics of the sea protection material have been considered. In particular, the parameters are the friction angle ϕ', the cohesion c', the unsaturated (γ_{unsat}), and saturated (γ_{sat}) specific weight, for all the different types of soil. Furthermore, for the clayey layers, the values of the compression indexes C_c and C_r as well as the value of the hydraulic conductivity at saturation k_{sat} have also been evaluated.

Top clayey layer

- Friction angle: $\phi' = 24°$
- Cohesion: $c' = 2\ kN/m^2$
- Specific weight (unsaturated): $\gamma_{unsat} = 17\ kN/m^3$
- Submerged specific weight (saturated): $\gamma_{sat} = 19\ kN/m^3$
- Hydraulic conductivity at saturation: $k_{sat} = 3.4 \cdot 10^{-9}\ m/s$
- $C_c = 0.35$
- $C_r = 0.05$
- Model: Plaxis soft soil

Sandy silty intermediate layer

- Friction angle: $\phi' = 30°$
- Cohesion: $c' = 2\ kN/m^2$
- Specific weight (unsaturated): $\gamma_{unsat} = 19\ kN/m^3$
- Submerged specific weight (saturated): $\gamma_{sat} = 20\ kN/m^3$
- Young's modulus: $E' = 25000\ kPa$
- Hydraulic conductivity at saturation: $k_{sat} = 8.25 \cdot 10^{-5}\ m/s$
- Model: Plaxis Hardening soil

Deep clayey layer

- Friction angle: $\phi' = 23°$
- Cohesion: $c' = 1\ kN/m^2$
- Specific weight (unsaturated): $\gamma_{unsat} = 16\ kN/m^3$
- Submerged specific weight (saturated): $\gamma_{sat} = 18\ kN/m^3$
- Hydraulic conductivity at saturation: $k_{sat} = 1.0 \cdot 10^{-9}\ m/s$
- $C_c = 0.35$
- $C_r = 0.05$
- Model: Plaxis soft soil

Coastal dike

- Friction angle: $\phi' = 27°$
- Cohesion: $c' = 2\ kN/m^2$
- Specific weight (unsaturated): $\gamma_{unsat} = 18\ kN/m^3$
- Submerged specific weight (saturated): $\gamma_{sat} = 20\ kN/m^3$
- Young's modulus: $E' = 20000\ kPa$
- Hydraulic conductivity at saturation: $k_{sat} = 1.23 \cdot 10^{-5}\ m/s$
- Model: Plaxis Hardening soil

Sea protection

- Friction angle: $\phi' = 40°$
- Cohesion: $c' = 20\ kN/m^2$
- Specific weight (unsaturated): $\gamma_{unsat} = 20\ kN/m^3$
- Submerged specific weight (saturated): $\gamma_{sat} = 22\ kN/m^3$
- Young's modulus: $E' = 22000\ kPa$
- Model: Plaxis Hardening soil

The following pictures (Figures from 5.1 to 5.5) summarize the geometries and the soil types used in PLAXIS 2D. For alle the lagoons, only one is presented. These are the sections that have shown the greatest criticality from a maritime and geotechnical point of view.

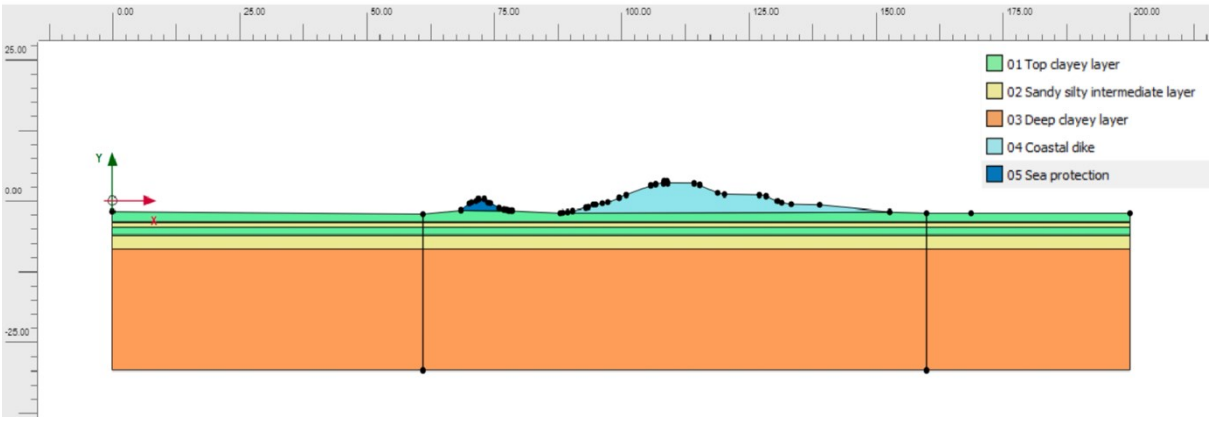

Figure 5.1: Sacca degli Scardovari (Section 18) soil and structure characteristics. Model setup PLAXIS 2D.

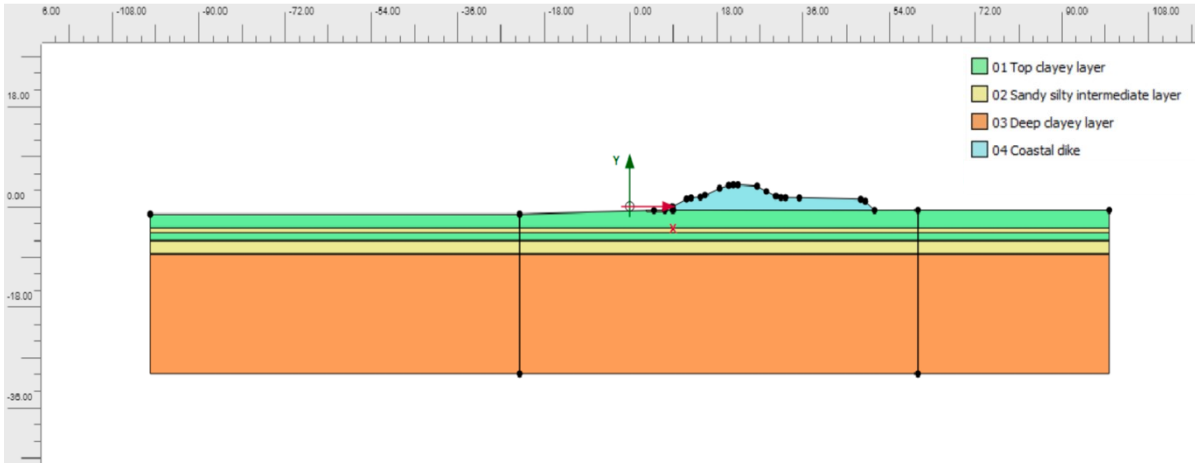

Figure 5.2: Caleri Lagoon soil and structure characteristics. Model setup PLAXIS 2D.

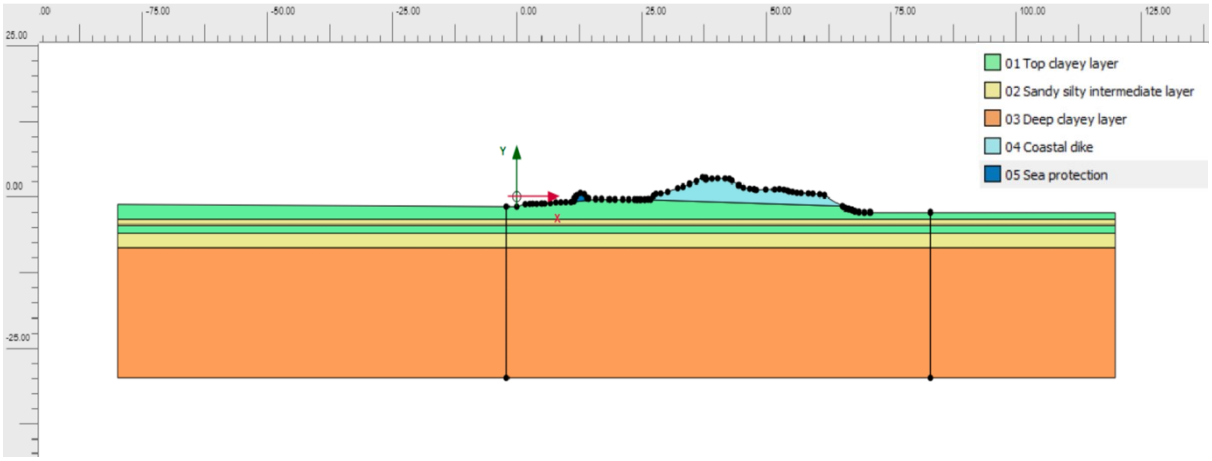

Figure 5.3: Vallona Lagoon soil and structure characteristics. Model setup PLAXIS 2D.

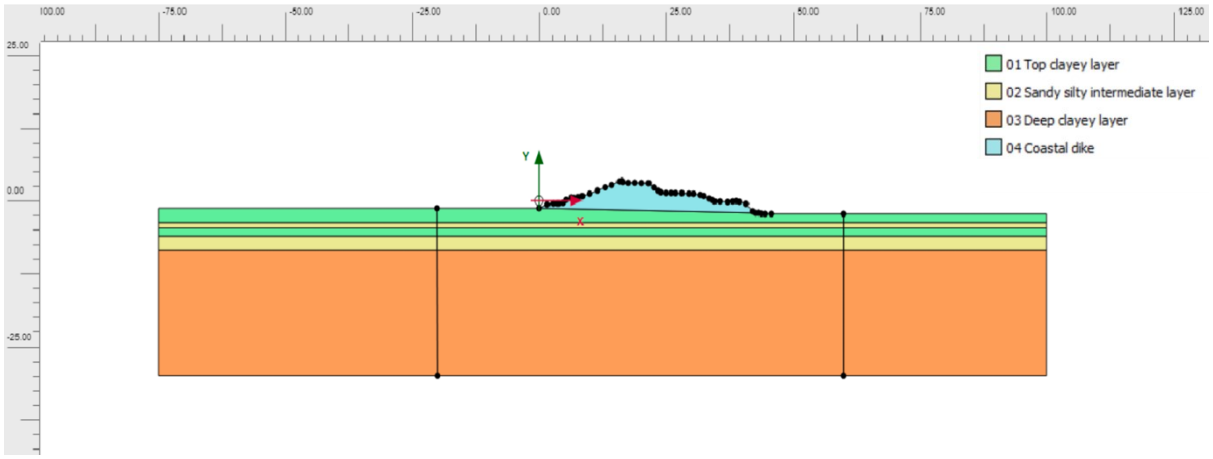

Figure 5.4: Barbamarco Lagoon soil and structure characteristics. Model setup PLAXIS 2D.

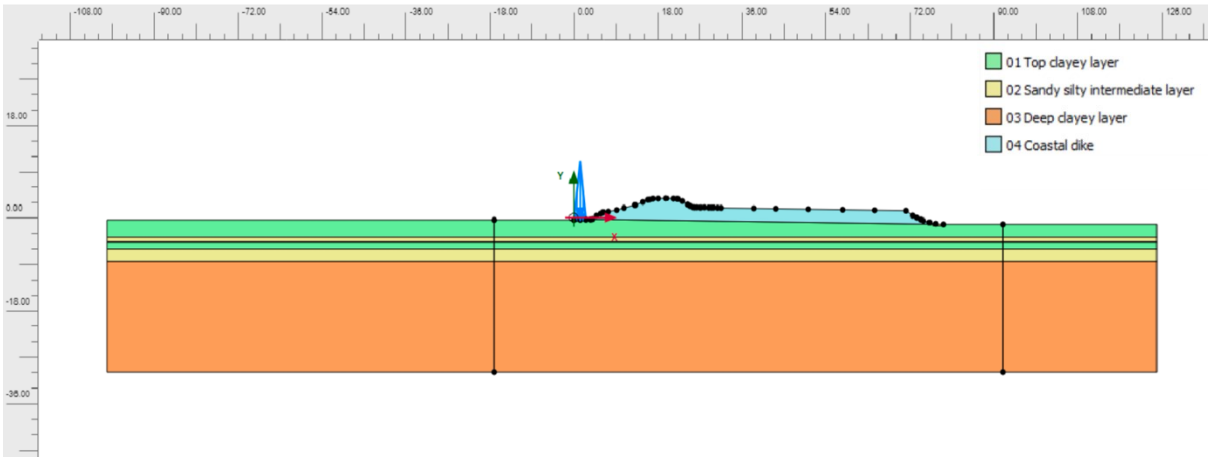

Figure 5.5: Canarin Lagoon soil and structure characteristics. Model setup PLAXIS 2D.

The coastal dikes were built taking as a reference the levels provided by the 2018 Lidar survey, which are more up-to-date and precise than the data of the previous survey carried out in 2009. The zero coincides with the starting point of the surveyed data. It is possible to observe how all the sections analyzed are formed by an upper clayey layer and a silty sand layer, which alternate in the first meters of soil. The deeper layer, on the other hand, is characterized by the presence of clay. In the case of section n° 18 of Sacca degli Scardovari and in the section of the Vallona Lagoon, there is also a sea protection. It is a low crest structure.

Not knowing the mechanical characteristics of the coastal protection, this material in the Canarin lagoon was replaced by a uniform load on the seaside. Furthermore, despite being considered a much more extended section, in such a way as to have a uniformity with all the parts considered, the important portion is delimited by vertical black lines to obtain a more precise mesh in the area of interest.

The modeling is based on the definition of two events: the first one based on the actual sea level condition (2020) and a second one on that expected after 50 years (2070). The return time was set at 300 years. As regards the increase and decrease of the tidal phases, based on the duration of past events, the intervals have been set:

- Growth phase from the initial level (on the mean sea level) to the peak level: 3 hours.
- Peak maintained for: 6 hours
- Time needed to pass from the peak to the final level: 3 hours

The following table summarizes the levels, for each section, for both the current and future events:

Lagoon	*Boreholes*	*Actual event (2020) - Tr 300 years*				*Future event (2070) - Tr 300 years*			
		Initial level	Peak level	Final level (m.s.l.)	Final level (low tide)	Initial level	Peak level	Final level (m.s.l.)	Final level (low tide)
Scardovari (Sec.18)	CPTU 9	0.1	2.19	0.1	-0.4	0.86	2.92	0.86	0.4
Caleri (n° 47)	-	0.1	2.14	0.1	-0.4	0.57	2.59	0.57	0.1
Vallona (n° 35)	-	0.1	2.11	0.1	-0.4	0.57	2.57	0.57	0.1
Barbamarco (n° 28)	-	0.1	1.99	0.1	-0.4	0.57	2.48	0.57	0.1
Canarin (n° 3)	-	0.1	2.06	0.1	-0.4	0.78	2.51	0.78	0.3

Table 5.3: Actual and future scenario levels.

Before analyzing the results, it is necessary to consider some typical characteristics of each section, obtained by the observation of the sampling area:

- Caleri Lagoon (Section n° 47): Section protected by a low cliff, presence of cultivated fields on the landside and a road on the first lateral bank.
- Vallona Lagoon (Section n° 35): Section protected by a low cliff, presence of fishing valleys and a road on the first lateral bank.
- Barbamarco Lagoon (Section n° 28): Section characterized by lateral bank protection on the seaside, fishing valleys and a road on the first lateral bank.
- Canarin Lagoon (Section n° 3): Section characterized by lateral bank protection on the seaside, presence of the canal of the Enel thermoelectric plant, road on the top of the coastal dike.

5.3 Modeling results

The following paragraph describe the results of the modeling carried out in Plaxis 2D. In particular, the trend of the mesh used, the safety factors, the failure surfaces and the effective saturation are represented.

To have an accurate calculation, the finite element mesh follows several criteria. For the numerical stability of the calculation the elements must be regular, while for the accuracy of the calculation, the elements should be sufficiently small, especially in those areas where large increments of deformations and settlements are expected during the analysis. The increase of the number of elements forming the mesh implies greater accuracy but also a higher time consuming. The mesh generation is based on a triangulation procedure. The mesh generator requires a global meshing parameter (l_e), which represents the size of the target element. This last one is calculated as:

$$l_e = r_e \cdot 0.06 \cdot (x_{max} - x_{min})^2 + (y_{max} - y_{min})^2$$

where the Relative Element Size Factor (r_e) is 0.50 for the very fine element distribution, while x_{max}, x_{min}, y_{max} and y_{min} are the outer geometry dimensions.

When a settlement occurs, to observe the localization of the deformations within the soil, the *"Incremental displacement* $|\Delta u|$*"* option, present in the Output program, is used. This contains the incremental components of the calculated displacement.

It is also possible to study the seepage processes both on the body of the embankment and in the soil foundation. These can be one of the main causes for the failure of the structure. In fact, the water flows inside the system, first removing the finer particles and then gradually also those with a larger diameter, until it forms cavities or underground channels through which the water can flow, weakening the structure. This phenomenon can lead to the passage of water from the seaside to the landside, but also to both localized and extensive failure mechanisms.

In the following, results also show the phreatic line that is the surface that separates the zone of saturation and the unsaturated zone.

It is essential also to calculate the safety factor values and compare these with the limits set by the legislation.

In Table 5.4 the safety factors for each condition and lagoon are summarized:

Safety factor $\sum M_{sf}$				
Section	*Actual scenario (2020)*		*Future scenario (2070)*	
	Condition	*Value*	*Condition*	*Value*
Scardovari	Fs +2.19 Peak	2.681	Fs +2.92 Peak	2.343
	Fs +0.10 (m.s.l.)	1.714	Fs +0.86 (m.s.l.)	1.545
	Fs -0.40 (low tide)	1.556	Fs +0.40 (low tide)	1.670
Caleri	Fs +2.14 Peak	1.498	Fs +2.59 Peak	1.430
	Fs +0.10 (m.s.l.)	1.294	Fs +0.57 (m.s.l.)	1.476
	Fs -0.40 (low tide)	1.099	Fs +0.10 (low tide)	1.226
Vallona	Fs +2.11 Peak	1.751	Fs +2.57 Peak	1.715
	Fs +0.10 (m.s.l.)	1.536	Fs +0.57 (m.s.l.)	1.691
	Fs -0.40 (low tide)	1.308	Fs +0.10 (low tide)	1.496
Barbamarco	Fs +1.99 Peak	1.607	Fs +2.48 Peak	1.597
	Fs +0.10 (m.s.l.)	1.636	Fs +0.57 (m.s.l.)	1.640
	Fs -0.40 (low tide)	1.660	Fs +0.10 (low tide)	1.671
Canarin	Fs +2.06 Peak	1.729	Fs +2.51 Peak	1.698
	Fs +0.10 (m.s.l.)	1.287	Fs +0.78 (m.s.l.)	1.707
	Fs -0.40 (low tide)	1.187	Fs +0.30 (low tide)	1.280

Table 5.4: Safety factors obtained in Plaxis 2D.

Considering that the value of the safety factor imposed by the standard is equal to Fs = 1.375, it is possible to observe that in most cases the calculated factors are greater. However, there are differences between one lagoon and another. In particular, for the Sacca degli Scardovari, the values are higher than the limit value, in all scenarios, both current and future. The same thing can be said in the case of the Barbamarco Lagoon. For the Vallona Lagoon, the only value that is less than Fs = 1.375 was calculated for the low tide phase at - 0.40 m above sea level. This, however, is characterized by a safety factor equal to 1.308, therefore very close to the limit value. Finally, the greatest criticalities occur in the Canarin and Caleri Lagoons, with this last one showing the lowest result of the entire analysis and equal to 1.099. This was obtained during the low tide condition at - 0.40 m above sea level, in the current scenario (2020).

5.3.1 Sacca degli Scardovari

The first necessary step is the mesh construction. To obtain a better arrangement of the triangles forming the mesh, at approximately –60.00 m and 160.00 m vertical limits have been inserted.

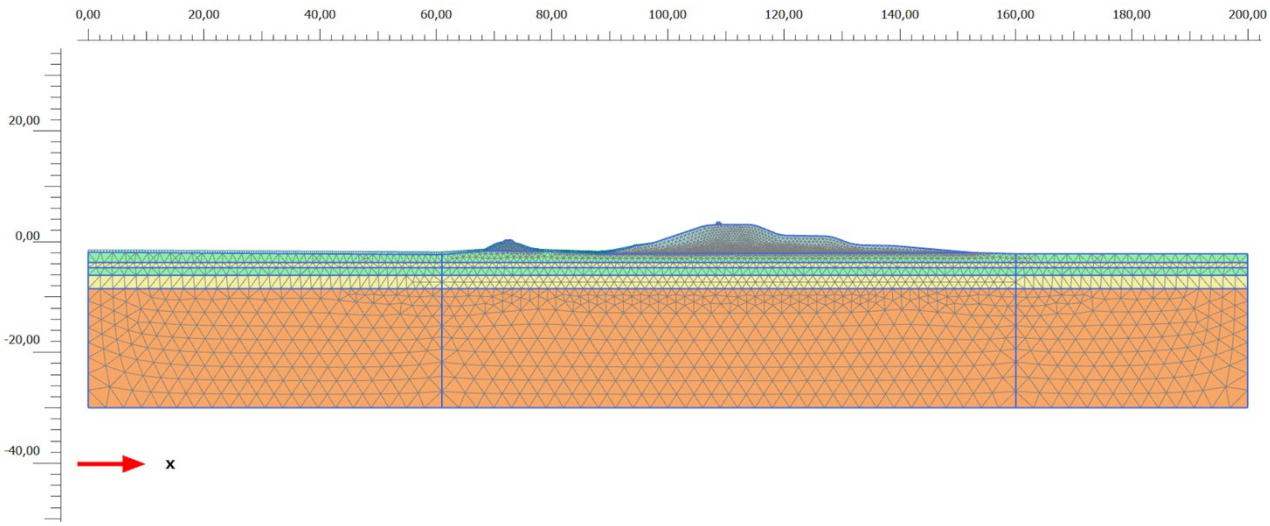

Figure 5.6: Mesh of Sacca degli Scardovari (Section n° 18).

The coastal dike rests first on a top clayey layer, then alternated by a silty sandy layer and finally a deeper layer of clay. The presence of these below the embankment can lead to the hypothesis that most of the filtration processes are related to the area of the body of the embankment. During the peak condition, in the future scenario (+2.92 m from the g.l.) it is possible to observe that the failure mechanisms occur on the landside. This happens not only in the future one but also in the current scenario (+2.19 m from the g.l.).

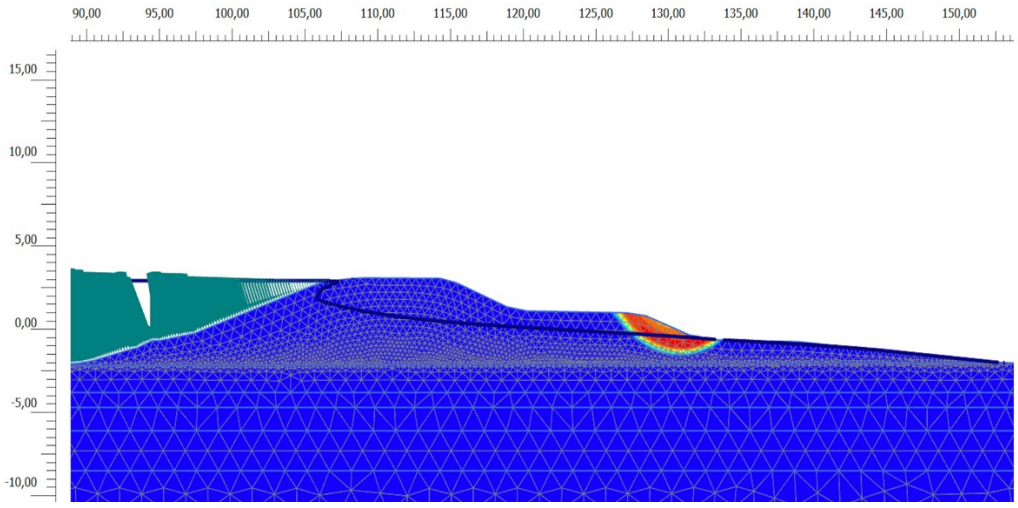

Figure 5.7: Sacca degli Scardovari failure mechanism during the peak condition in the future scenario.

During the decreasing phase, the possible failure surface is different depending on the scenario. All affect the seaside but with different intensity depending on the final level reached. Anyway, is important to note that the safety factors are always greater than those imposed by law.

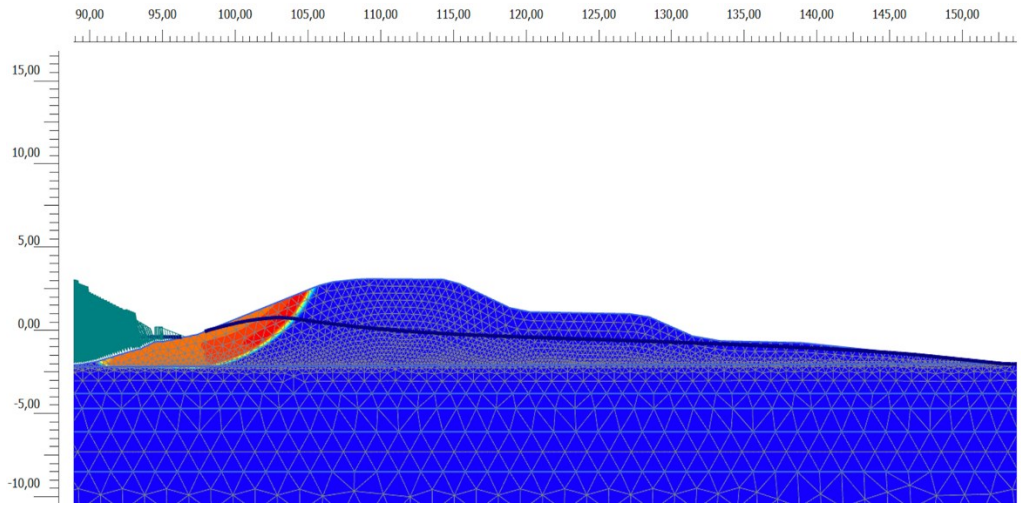

Figure 5.8: Sacca degli Scardovari failure mechanism during the decreasing condition in the actual scenario (-0.40 m from the g.l.).

Figure 5.9 shows the possibility that seepage processes are established through the coastal dike. These can lead to the leakage of water on the landside, and they are the main reason for collapse of the structure during the extreme peak level.

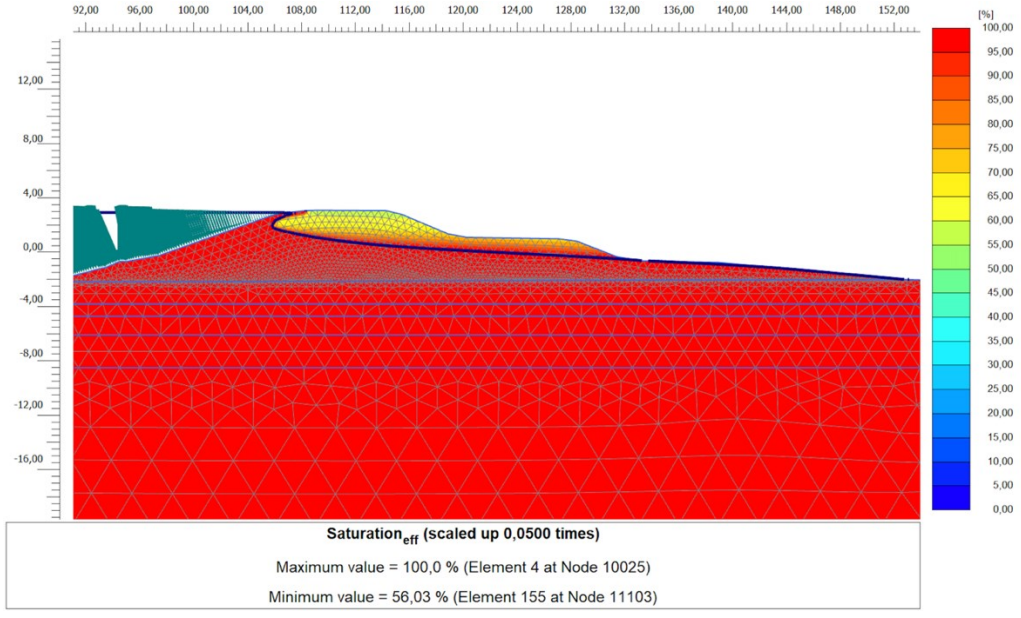

Figure 5.9: Phreatic line behavior and soil effective saturation (Sacca degli Scardovari, future scenario, peak +2.92 m).

In this specific section, the hydraulic gradients are on the order of $0.1 \div 0.2$, so a limited value. This, however, does not exclude the possibility that some piping phenomena occur, inducing an erosional process. Therefore, it would be appropriate to conduct a more detailed analysis.

5.3.2 Caleri Lagoon, Vallona Lagoon, Barbamarco Lagoon and Canarin Lagoon

Starting from the Caleri Lagoon, in Figure 5.10 it is possible to observe the mesh used, being careful to the fact that the origin of the axes was placed in coincidence with the first available embankment point. Furthermore, at approximately –25.00 m and 60.00 m vertical limits have been inserted in order to obtain a better arrangement of the triangles forming the mesh.

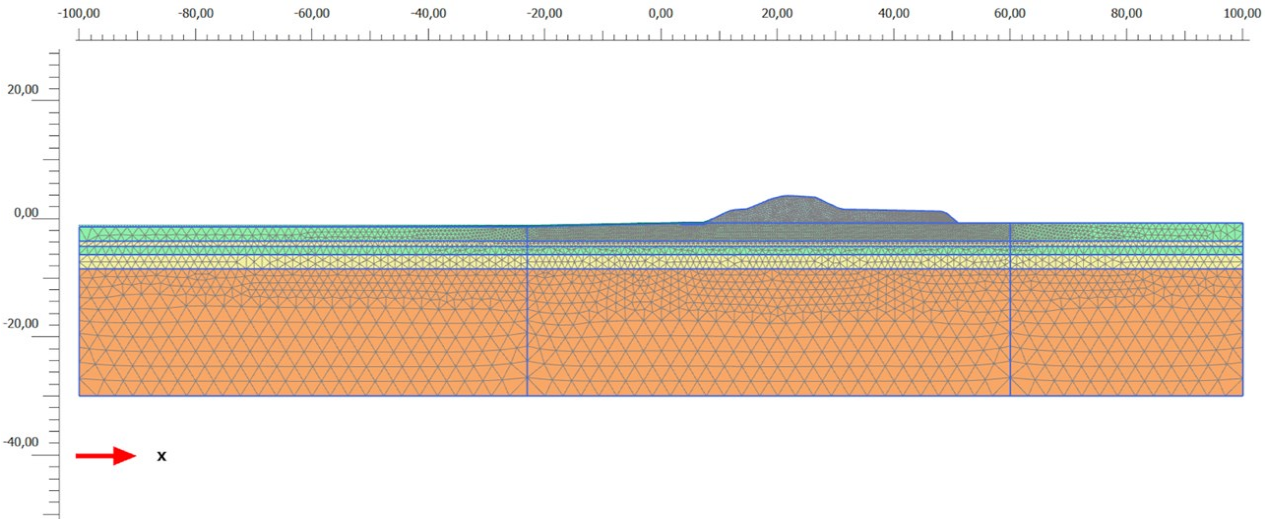

Figure 5.10: Mesh of the Caleri Lagoon (Section n° 47).

The coastal dike rests first on a top clayey layer, then alternated by a silty sandy layer and finally a deeper layer of clay. The presence of these layers below the embankment can lead to the hypothesis that most of the filtration processes can be related to the area of the main body of the embankment. However, it is very important to note that, unlike the Sacca degli Scardovari, in this lagoon it was not possible to carry out on-site analyzes. This is the reason why the profile of each layer is not characterized by the same accuracy. The failure mechanisms differ according to the chosen condition and the scenario. In particular the different failure surfaces can occur both on the landside and on the seaside.

Another result is related to the saturation level that measures the water content in the voids between the solid grains. This is given by the percentage ratio between the volume of water and the total volume of voids. The saturation of the voids varies from a minimum of 0, which corresponds to a sample in which the voids are filled with air (unsaturated soil), to a maximum of 100, in case on which the voids are completely filled with water (saturated soil).

In the future scenario and during the peak conditions (+2.59 m from the g.l.) is possible to observe that the failure mechanisms can occur on the landside. This happens not only in the future scenario but also in the current one (+2.14 m from the g.l.).

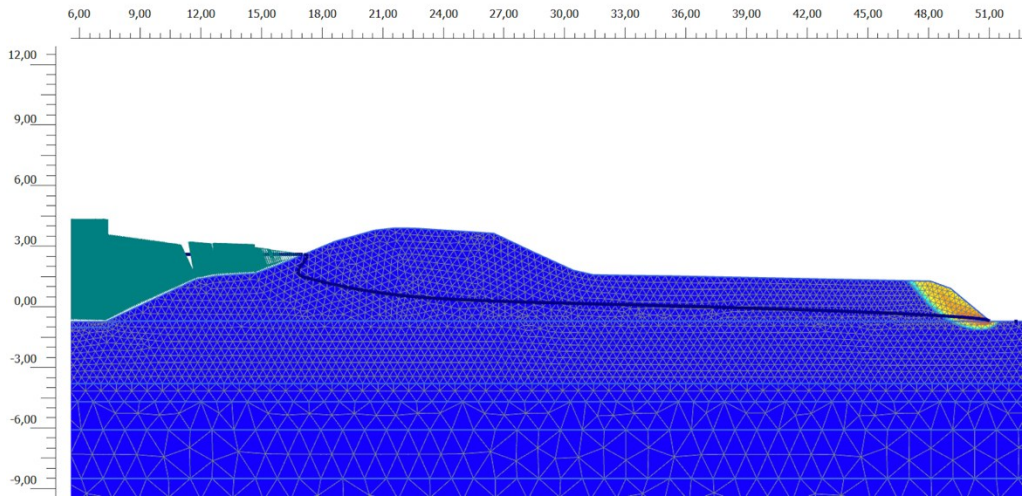

Figure 5.11: Caleri Lagoon failure mechanism during the peak condition in the future scenario.

About the decreasing phase, on the other hand, is possible to distinguish between the condition characterized by a hypothesis of medium sea level and a hypothesis of low tide. Precisely this last one, in the actual scenario (- 0.40 m from the g.l.) shows the lowest safety factor equal to 1.099. As shown in the Figure 5.12 the failure mechanisms occur on the seaside.

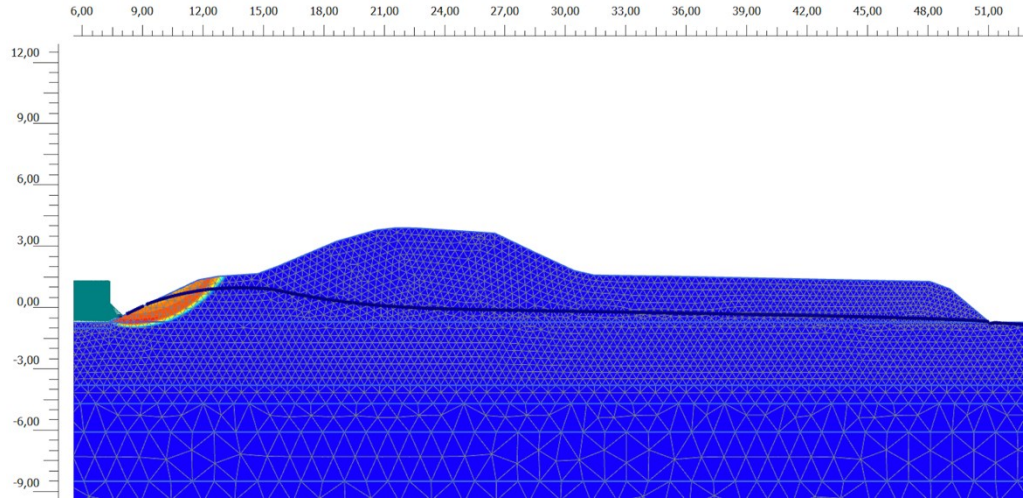

Figure 5.12: Caleri Lagoon failure mechanism during the decreasing condition in the actual scenario (- 0.40 m from the g.l.).

Finally, a particular case is given by the future scenario with a tidal decrease level up to + 0.57 m from the g.l. This in fact shows a failure mechanism not only on the landside but also on the seaside.

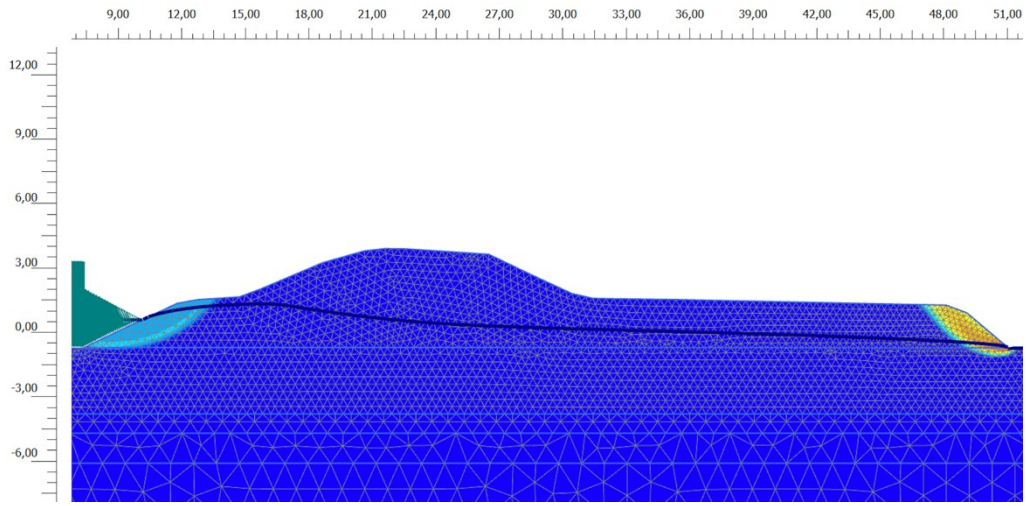

Figure 5.13: Caleri Lagoon failure mechanism during the decreasing condition in the future scenario (+0.57 m from the g.l.).

Figure 5.14 shows the possibility that seepage processes are established through the coastal dike that can lead to the leakage of water on the landside. Furthermore, this phenomenon induces a weakening of the structure and its future collapse.

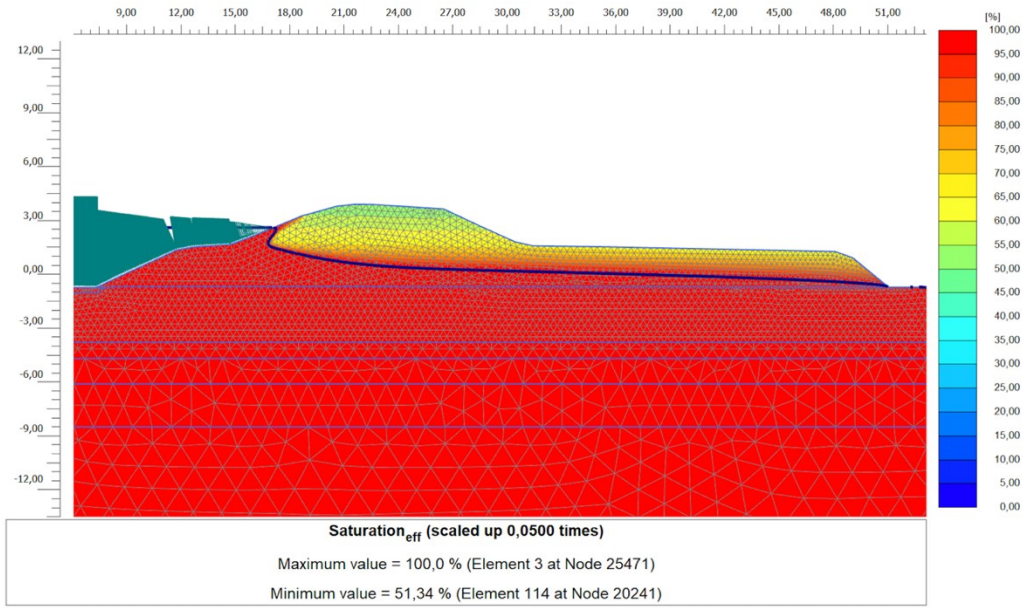

Figure 5.14: Phreatic line behavior and soil effective saturation (Caleri Lagoon, future scenario, peak +2.59 m).

Considering that the hydraulic gradients are on the order of $0.4 \div 0.6$ is possible that some piping phenomena occur, inducing an erosional process. The greatest criticality occurs during the peak condition, and this can be accentuated by the high slope. Therefore, it would be appropriate to conduct a more detailed analysis to assess the extent of this process and provide the possible interventions.

For the Vallona Lagoon, the Figure 5.15 shows the mesh used. Also, in this case the origin of axes was placed in coincidence with the first available embankment point. Approximately at – 2.00 m and 80.00 m vertical limits have been inserted to obtain a better arrangement of the triangles forming the mesh.

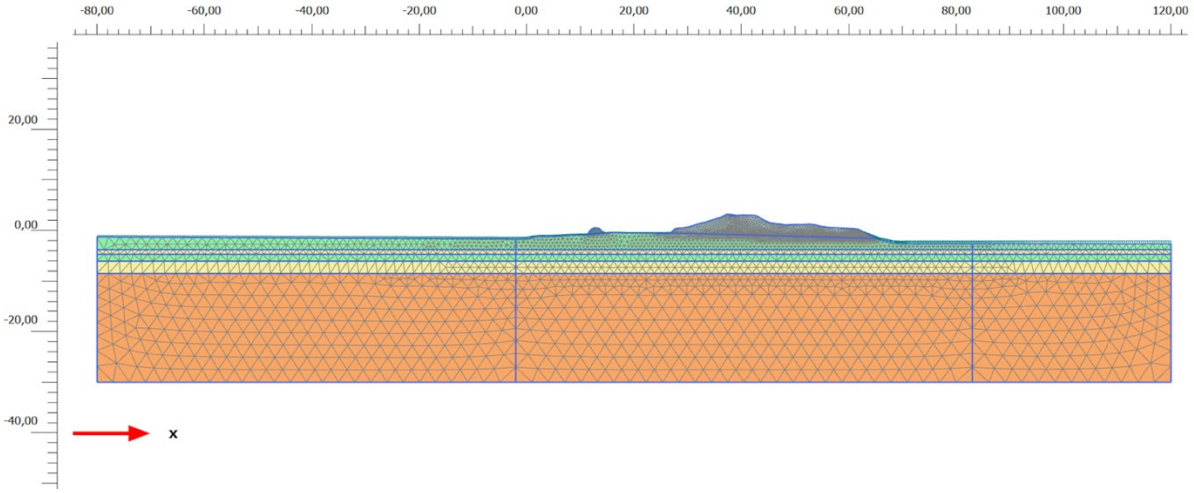

Figure 5.15: Mesh of the Vallona Lagoon (Section n° 35).

The soil stratigraphy follows the same behavior of the Caleri Lagoon, with a top clayey layer, followed by a silty sandy layer and finally a deeper layer of clay. The difference in this case is related to the presence of a low cliff protection on the seaside. These layers below the coastal dike can lead to the hypothesis that most of the filtration processes can be related to the area of the main body of the embankment.

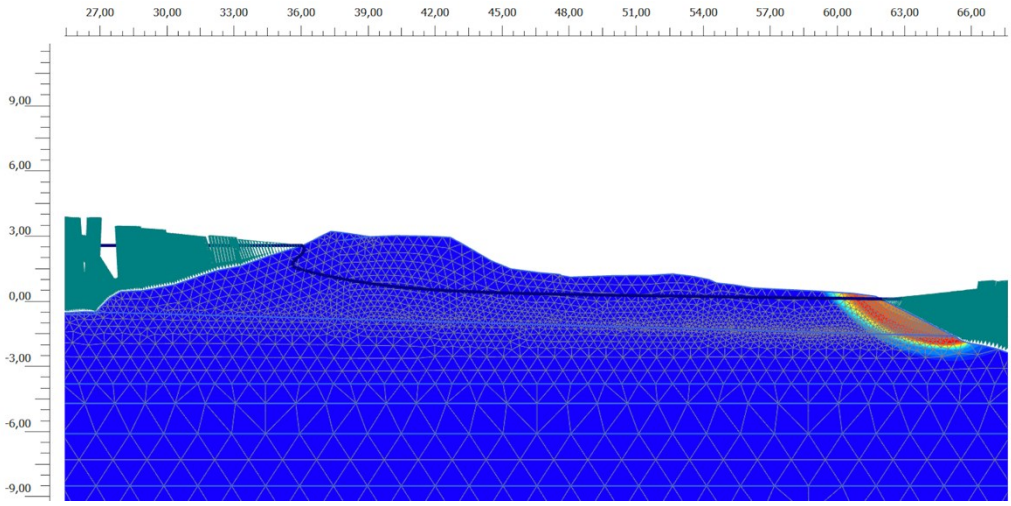

Figure 5.16: Vallona Lagoon failure mechanism during the peak condition in the future scenario.

During the peak conditions, in the future scenario (+2.57 m from the g.l.) is possible to observe that the failure mechanisms can occur on the landside. This happens also in the current one (+2.11 m from the g.l.). About the decreasing phase, is possible to distinguish between a medium sea level and a low tide hypothesis. This last one, in the actual scenario (- 0.40 m from the g.l.) shows the lowest safety factor equal to 1.308. As shown in the Figure 5.17 the failure mechanisms occur on the seaside.

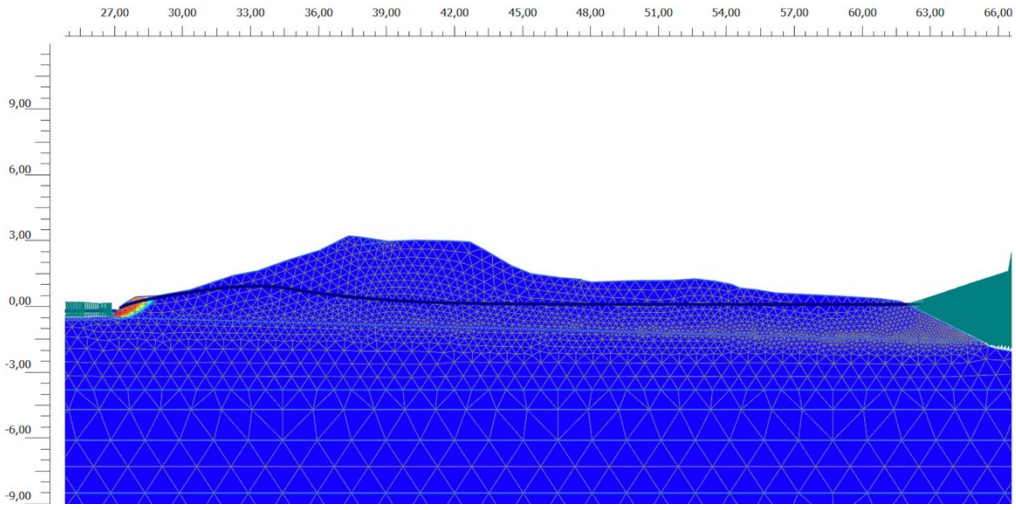

Figure 5.17: Vallona Lagoon failure mechanism during the decreasing condition in the actual scenario (- 0.40 m from the g.l.).

As shown in the previous picture, the failure surface affects a small portion of the coastal dike. Unlike this last one, the condition that could occur in the future scenario affects a significant portion of the system. This considering a low tide condition with a final value of + 0.57 m from the g.l.

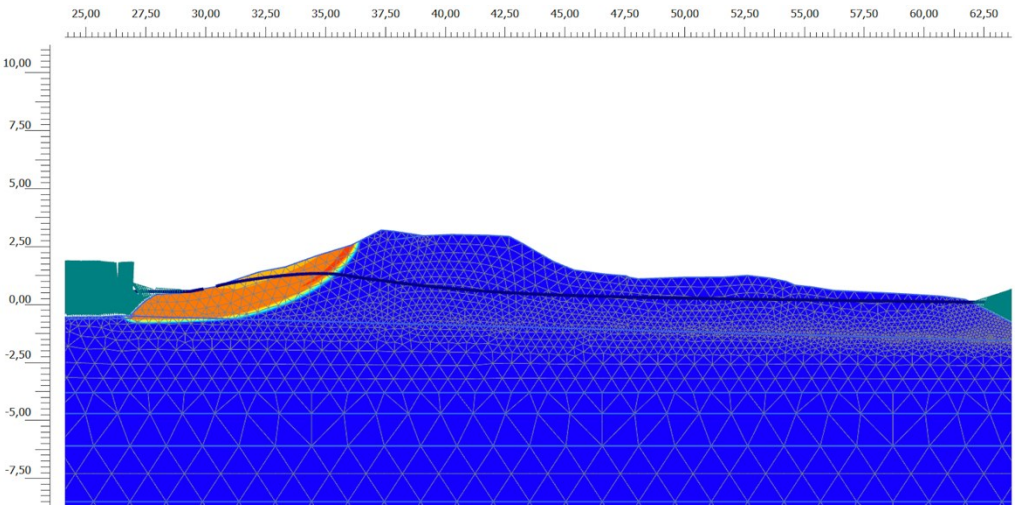

Figure 5.18: Vallona Lagoon failure mechanism during the decreasing condition in the future scenario (+0.57 m from the g.l.).

The possible failure surface occurs on the landside during the peak conditions, while during the low tide conditions the failure mechanism involves the seaside. In almost all the cases, however, the safety factors are higher than those imposed by law.

Figure 5.19 shows the possibility that seepage processes are established through the coastal dike that can lead to the leakage of water on the landside.

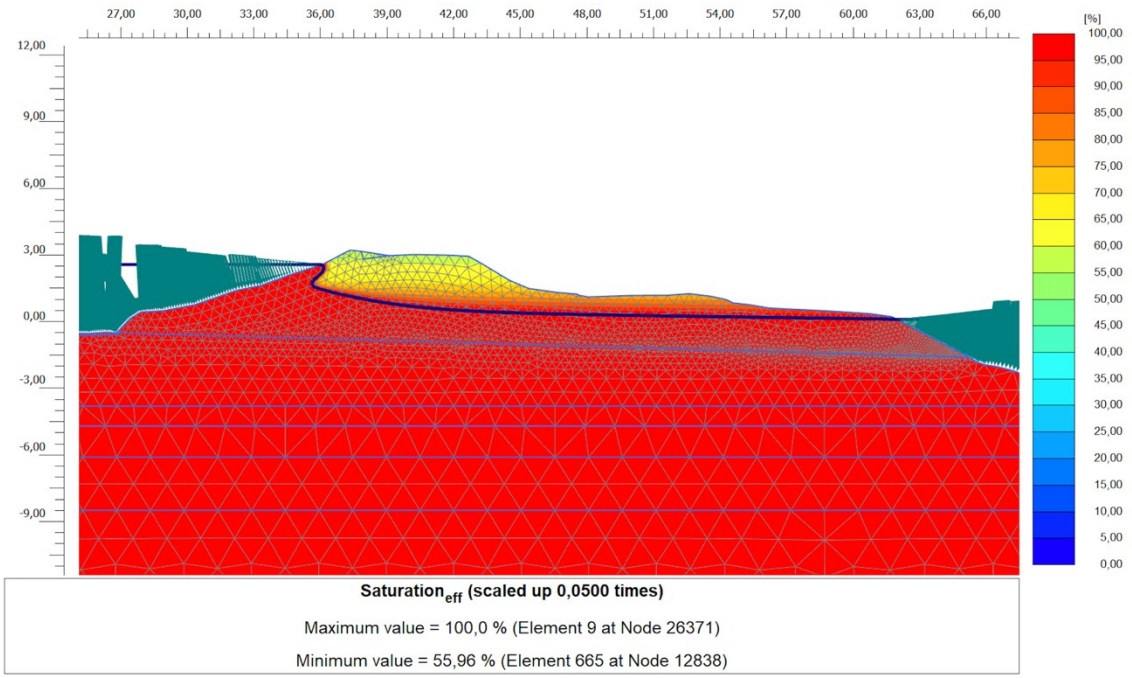

Figure 5.19: Phreatic line behavior and soil effective saturation (Vallona Lagoon, future scenario, peak +2.57 m).

As regards the hydraulic gradient, it is possible to observe how the saturation lines are controlled by the canal of the fishing valleys and therefore the outgoing gradients are low, close to zero.

The mesh used in the Barbamarco Lagoon, is shown in Figure 5.20. Also, in this case the origin of axes was placed in coincidence with the first available embankment point. Approximately at –20.00 m and 60.00 m, vertical limits have been inserted to obtain a better arrangement of the triangles forming the mesh. The soil stratigraphy follows the same behavior of the Caleri and Vallona Lagoons, with a top clayey layer, followed by a silty sandy layer and finally a deeper layer of clay. As in the case of the Caleri Lagoon there isn't a low cliff protection on the seaside. The presence of these layers below the embankment can lead to the hypothesis that most of the filtration processes can be related to the area of the main body of the coastal dike.

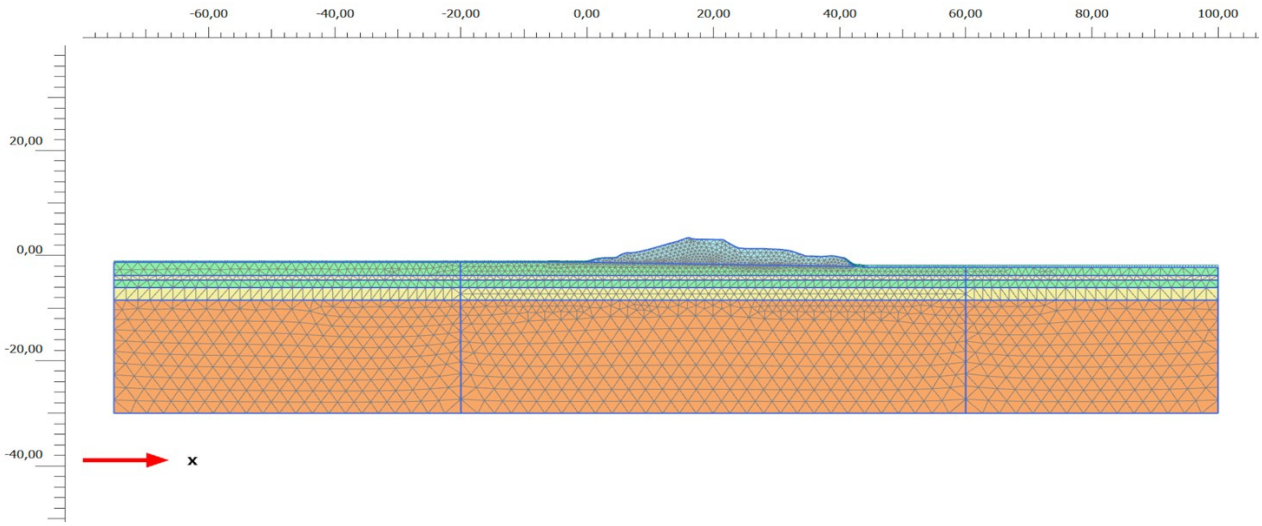

Figure 5.20: Mesh of the Barbamarco Lagoon (Section n° 28).

About the failure mechanisms, the possible failure surface occurs on the landside during the peak conditions, while during the low tide conditions these mechanisms invole the seaside.

During the peak conditions, in the future scenario (+2.48 m from the g.l.) is possible to observe that the failure mechanisms can occur on the landside. This happens not only in the future scenario but also in the current one (+1.99 m from the g.l.).

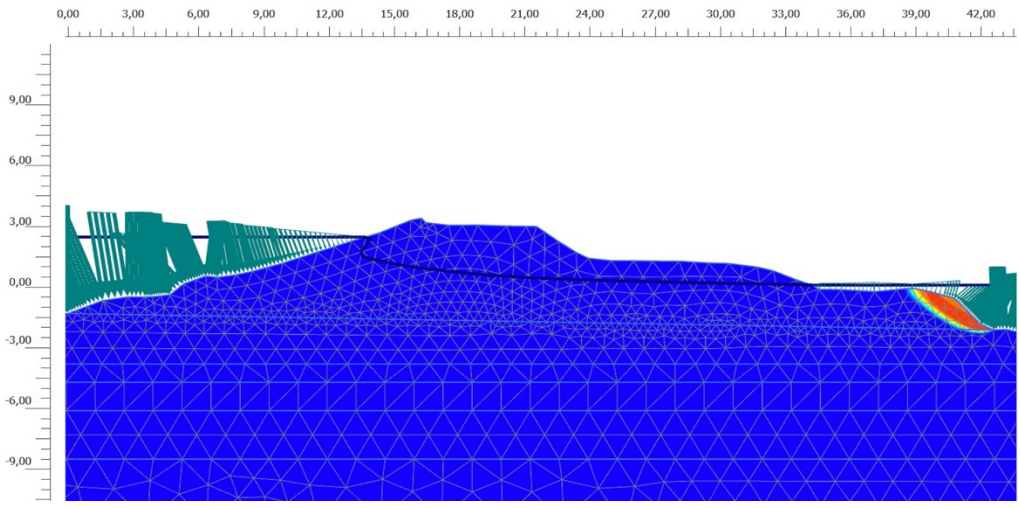

Figure 5.21: Barbamarco Lagoon failure mechanism during the peak condition in the future scenario.

During the decreasing phase, the possible failure surface is different depending on the scenario. This could affect only the landside or both seaside and landside. Is important to note that in all the cases the safety factors are greater than those imposed by law.

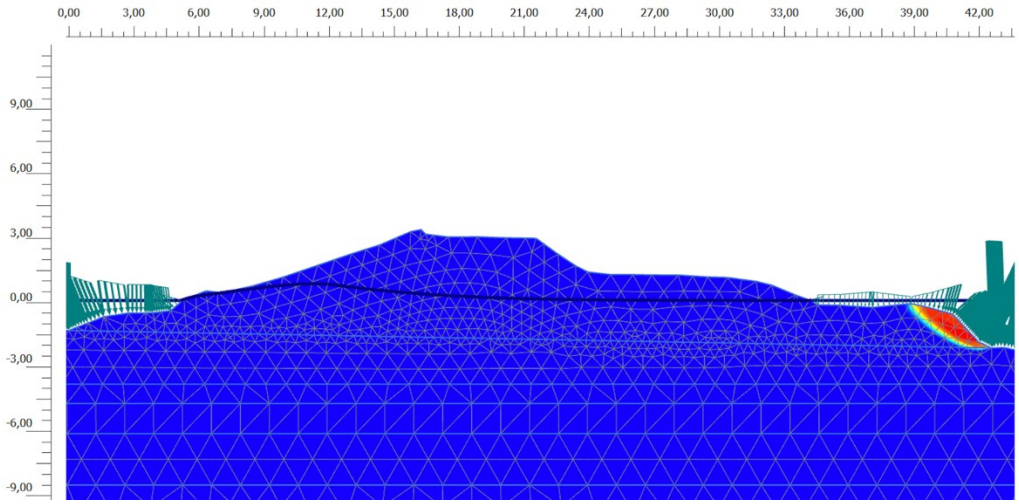

Figure 5.22: Barbamarco Lagoon failure mechanism during the decreasing condition in the actual scenario (+0.10 m from the g.l.).

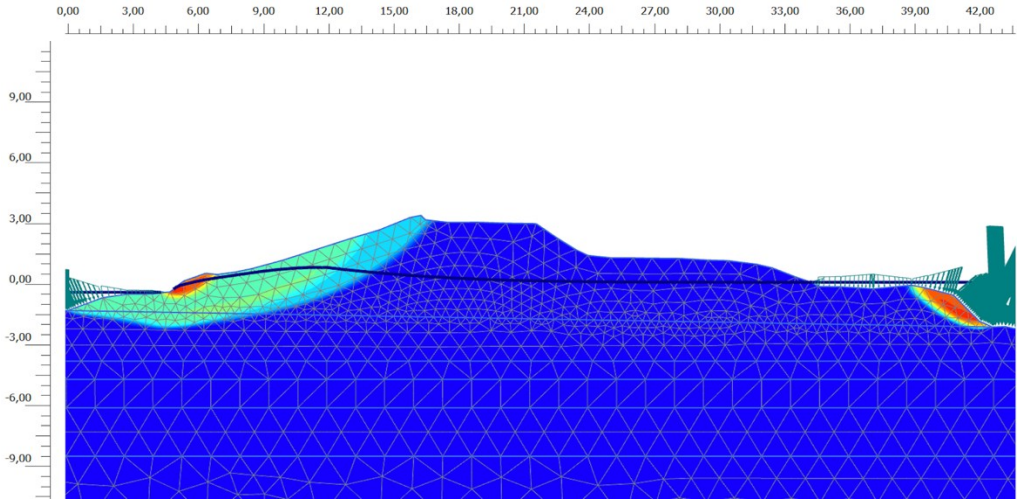

Figure 5.23: Barbamarco Lagoon failure mechanism during the decreasing condition in the actual scenario (- 0.40 m from the g.l.).

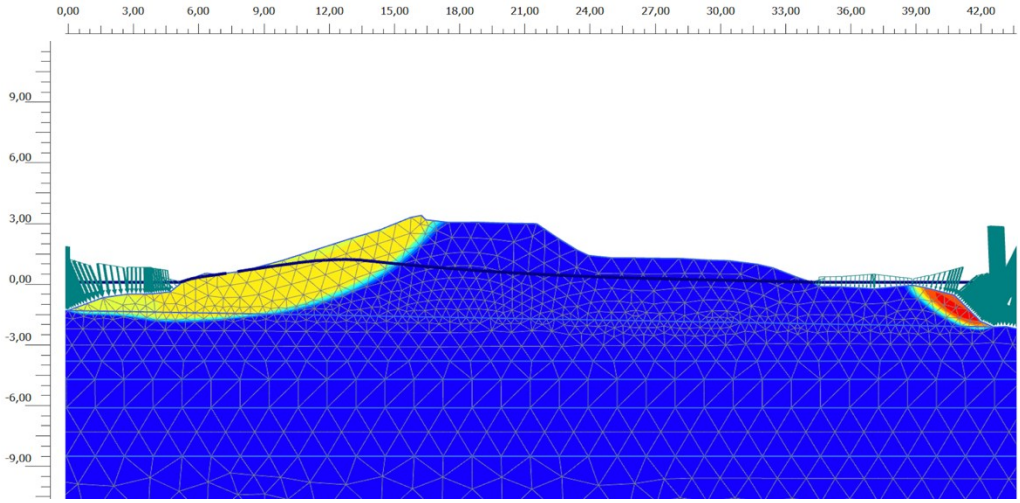

Figure 5.24: Barbamarco Lagoon failure mechanism during the decreasing condition in the future scenario (+0.10 m from the g.l.).

Figure 5.25 shows the possibility that seepage processes are established through the system. This can lead to the leakage of water on the landside.

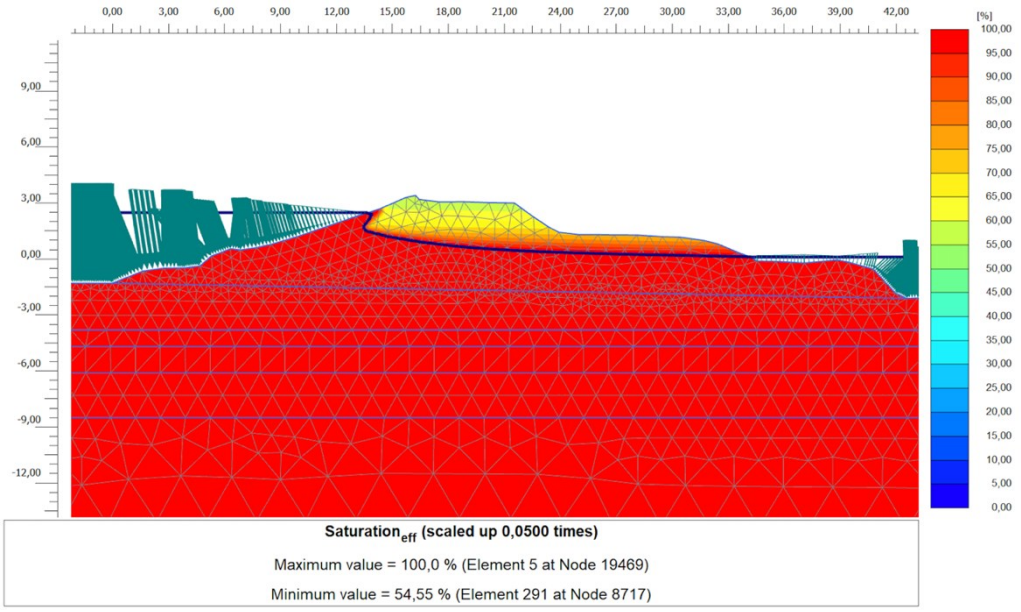

Figure 5.25: Phreatic line behavior and soil effective saturation (Barbamarco Lagoon, future scenario, peak +2.48 m).

Looking at the hydraulic gradient, it is possible to observe that the saturation lines are controlled by the canal of the fishing valleys and therefore the outgoing gradients are low, close to zero.

The last section that was analyzed is that of the Canarin Lagoon whose mesh is shown in Figure 5.26. The soil stratigraphy follows the same behavior of the other lagoons, with a top clayey layer, then alternated by a silty sandy layer and finally a deeper layer of clay. On the seaside, to replace the protection, for which the characteristics are not known, a uniform load is applied.

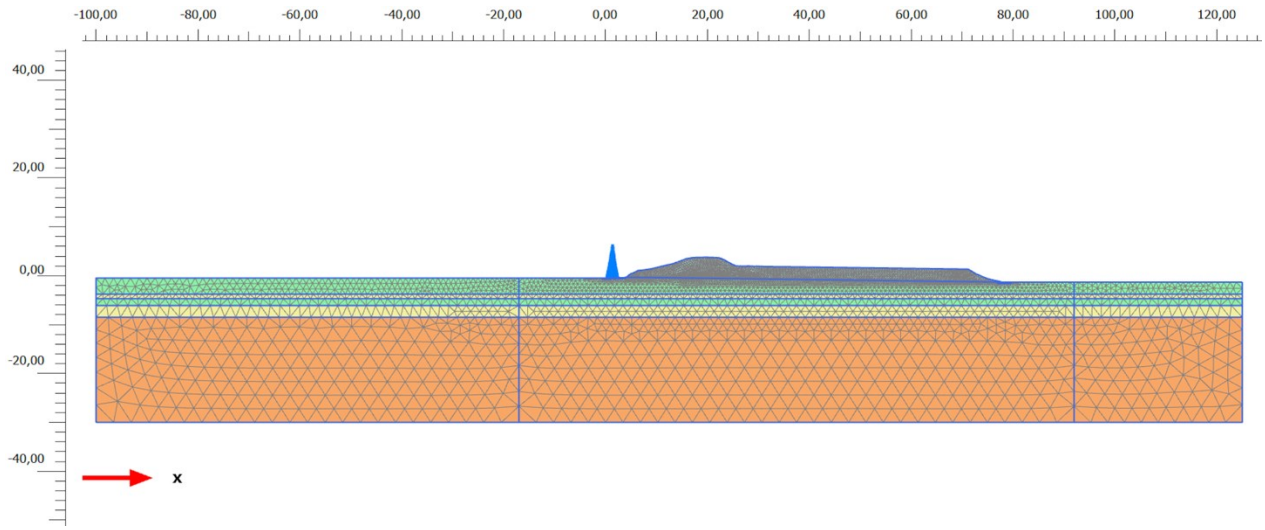

Figure 5.26: Mesh of the Canarin Lagoon (Section n° 3).

In the future scenario and during the peak conditions, with a level of +2.51 from the g.l. it is possible to observe that the failure mechanisms can occur on the landside. This happens not only in the future scenario but also in the current one (+2.06 m from the g.l.).

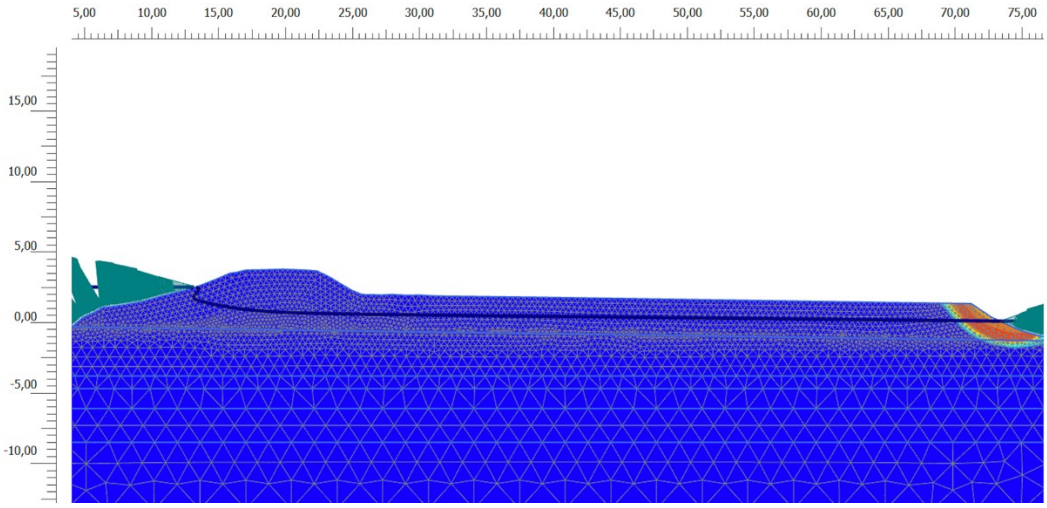

Figure 5.27: Canarin Lagoon failure mechanism during the peak condition in the future scenario.

It may also be interesting to observe what happens during the low tide condition. In the following pictures (Figure 5.28 and 5.29) are represented the different scenario for the actual low tide condition (- 0.40 m from the g.l.) and the future one, with a level of +0.30 m from the ground level.

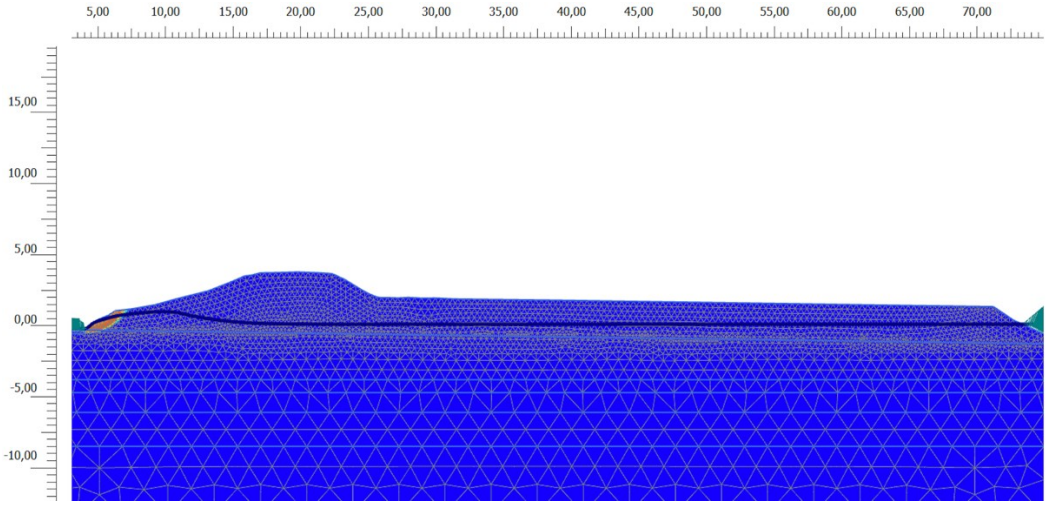

Figure 5.28: Canarin Lagoon failure mechanism during the low tide condition in the actual scenario (- 0.40 m from the g.l.).

In the current condition, the failure surface affects only a limited portion of the embankment, on the seaside. The same thing can be observed also in the future scenario.

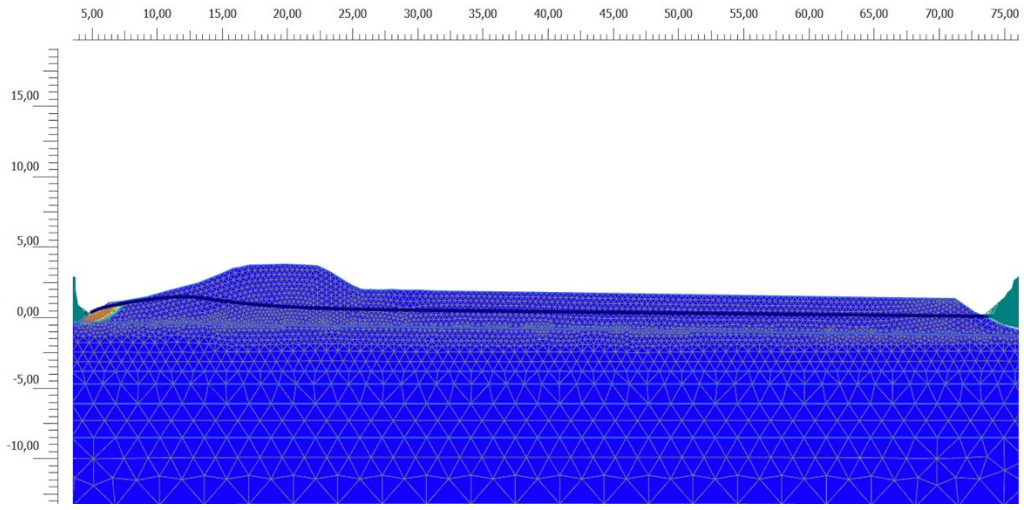

Figure 5.29: Canarin Lagoon failure mechanism during the low tide condition in the future scenario (+0.30 m from the g.l.).

Finally, there is the possibility that seepage processes are established through the coastal dike, with water passing from the seaside to the landside. The behavior of the phreatic line and the effective saturation are represented as follow:

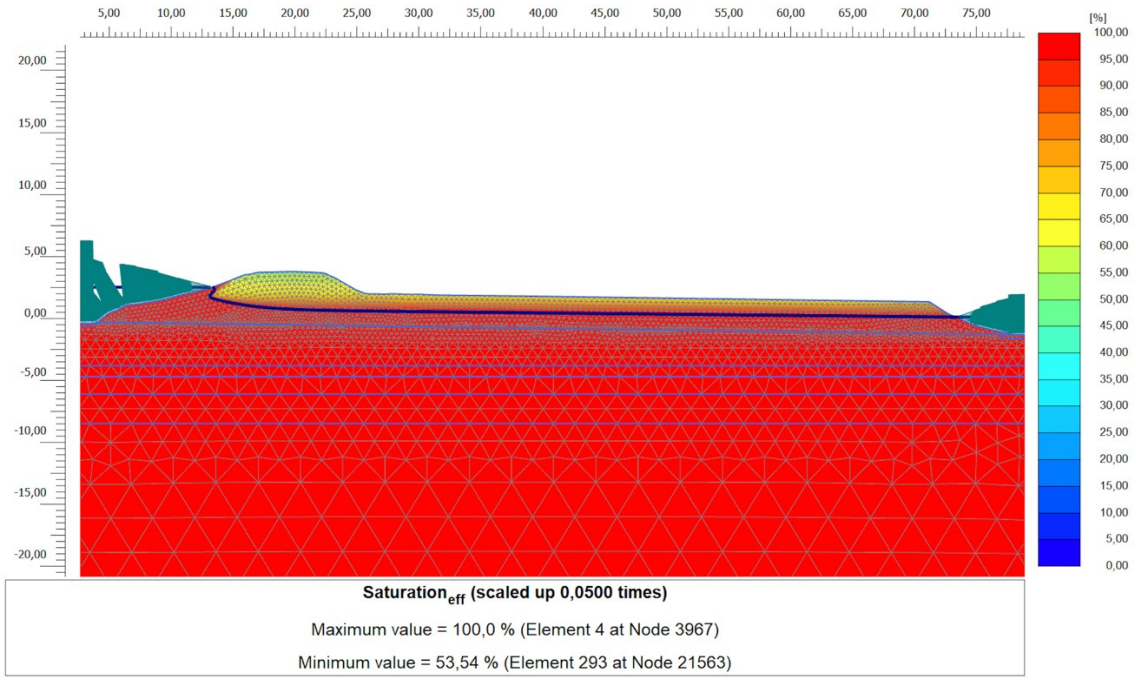

Figure 5.30: Phreatic line behavior and soil effective saturation (Canarin Lagoon, future scenario, peak +2.51 m).

Analyzing the hydraulic gradient, it is possible to observe how the saturation lines are controlled by the presence of the Enel channel behind the coastal dikes and therefore the outgoing gradients are low, close to zero.

5.4 Final considerations

The original structure of the coastal dike in the Po Delta lagoons refers to the requirements introduced by the Superior Council of Public Works (1967). The defense provided a crown of the coastal dike (point at maximum height) of +13.50 m with respect to the absolute value which is the reclamation level (-10.00 m above the mean sea level). Furthermore, the slope is 1:2 on the land side and 1:3 on the seaside. In some section the presence of a rock riprap and the construction of a concrete sea wall is essential to protect the coastal dike against the action of waves and currents.

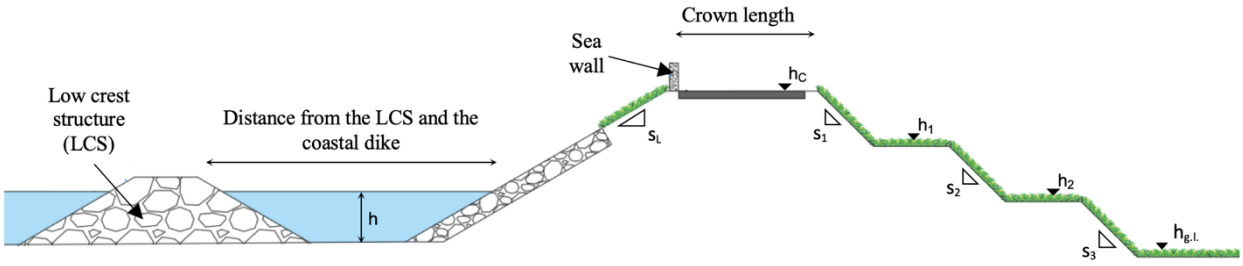

Figure 5.31: Typical section of the coastal embankment in the Po Delta.

It is important to note that not all the embankments are protected by the presence of a low crest structure and consequently they are more exposed to the waves action. Furthermore, very often, to limit costs and speed up the construction of the structures, materials located in the surrounding area have been used. These, however, are not always suitable to reduce the seepage processes. Through geotechnical investigations, in fact, it is possible to identify sandy components both in the central part of the coastal dike and in the soil foundation. The protection against erosion and wave action is instead carried out by stones and bitumen cliff that covers a significant portion of the seaside shore.

Despite some common characteristics, there are several differences in term of structure that characterize the coastal dike, especially if we consider all the lagoons in the Po Delta. These depend on both the geotechnical and maritime aspects of each individual area, as well as on the impacts of storms that during the years affect this area.

Nowadays, the sea dikes are made up of incoherent materials and protected both on the seaside and on the landside. In the latter case, the side banks are covered with topsoil and grass to limit the washout induced by rainfall. On the landside there are also one or more lateral banks where roads have also been built. The seaside, on the other hand, is protected by a mantle to limit the erosion induced by the waves. Furthermore, in some sections there is a low crest structure.

The stability is of great importance. The erosion, the seepage, the sea level rise, the tide level and the phenomenon of subsidence can lead to the overlapping of the structure. All these aspects can then impact on the local economic activities as well as on the intervention and maintenance costs of the structures. For these reasons, the studies should be carried out not only in the Sacca degli Scardovari but also in all the other lagoons where in situ or laboratory tests have not been conducted and therefore the accuracy of the results is lower.

In any case it is possible to distinguish some important phenomena. The main ones are:

- Internal erosion of the coastal dike or foundation soils due to seepage processes
- Decreased stability of the system and possible collapse of the structure
- Erosion of the surface on the seaside due to waves action
- Damages on the structures protecting the coastal dike such as the low crest structure, the rock riprap, and the concrete sea wall.

It is important to distinguish between the current (2020) and the future (2070) conditions. The meteo-marine forcings characterized by a return period of 300 years and the geotechnical characteristics of the analyzed area should be considered. To adapt the coastal dikes to the future events some actions can be defined. First, it is necessary to increase the total height to limit the possibility of an overlap of the system. Furthermore, it is necessary to extend the geotechnical survey already carried out to evaluate more precisely the characteristics of the coastal dike, as well as evaluate the functionality of all the defense systems (mantle, low crest structure, toe protection). A continuous monitoring of the coastal protection to identify the system evolution and promptly recognize the critical conditions is also essential.

6. CONCLUSIONS

The purpose of the present thesis work is to verify the stability of the coastal dikes in the Po Delta region. This is a very vulnerable environment, subject to the variations induced by the river itself and to the action of waves and currents coming from the sea. This analysis covered the meteo-marine and the geotechnical aspects. Due to climate change, this area in the future will be affected by both sea level rise and the presence of increasingly extreme storms with a greater impact of waves on the coastal dikes that protect it. The study, in fact, focused not only on the current scenario (2020) but also on a future one, in 2070.

To simulate the flow inside the coastal lagoons, it is necessary to consider the implementation of two-dimensional or three-dimensional models of shallow waters. For the study of the water level and the wave fields, the 2DEF hydrodynamic model and the SWAN wave model were used. Thanks to the simulations it was possible to identify the distribution of the wave height both offshore and inside the lagoon. For all the lagoons, except for that of Barbamarco, a greater wave height was observed offshore and a decreasing in terms of level as it penetrates the lagoon. Furthermore, thanks to the low sandy barriers, the height of the wave is lower near the sandy island, which therefore acts as a protection for the area behind it. In all the cases analyzed, the water levels increase near the innermost area of the lagoon.

Once the meteo-marine forcings have been identified, it is necessary to study the stability and the seepage processes that occur on the coastal dikes. A geotechnical characterization is therefore needed. Starting from 2021, the AIPO (Interregional Agency for the Po River) has carried out a geotechnical survey with boreholes and CPTus along the coastal dikes of the Sacca degli Scardovari. Several laboratory tests were performed on collected samples. Starting from these data the soils was characterized. However, the surveys were conducted only in the Sacca degli Scardovari and not in the other lagoons of the Po Delta. Performing the test also in these areas would allow to have a better geotechnical characterization and to obtain more accurate results. For the geotechnical modeling PLAXIS 2D was used.

The FEM modeling requires the definition of the soil characteristics; however, despite the geotechnical investigations carried out, strong hypotheses are required. In fact, due to the limited number of data, it is not possible to precisely identify the mechanical characteristics of the soil. Furthermore, the mechanical and hydraulic features, for each type of soil, are assumed to be the same for all the sections. This condition can be satisfied for the Sacca degli Scardovari, where geotechnical

investigations have shown homogeneity of the soil characteristics. Vice versa, the use of these parameters for the modeling of the other lagoons of the Po Delta is not confirmed by the geotechnical boreholes, as they have not been carried out.

As regards the results obtained, the failure mechanisms differ according to the chosen condition. The failure surfaces can occur on the landside or on the seaside. In general, however, it has been shown that during peak conditions, the failure mechanism affect the landside. Vice versa, during low tide conditions the failure mechanisms develops on the seaside. The possibility that seepage processes takes place through the embankment and along the foundation soil was then observed. This leads to the leaching of water from the seaside to the landside. Furthermore, due to processes such as piping there is the possibility that preferential paths are created into the system. The result is that the structure can weaken and collapse.

The current configurations, previously designed by the Superior Council of Public Works, are valid but must be updated to the future scenarios. Among the elements of greater importance, it is necessary to consider the phenomenon of subsidence. In fact, by combining the lowering of the ground level and the mean sea level rise, it is possible that in the future there will be a strong reduction of the freeboard and the possibility of overlapping the structure. To overcome this problem, it will be necessary to consider an enlargement of the coastal dikes and increasing the final level of the crown. From a geotechnical point of view, some critic conditions have occurred. The safety factors in some cases were lower than the value indicated by law (Fs = 1.375). Furthermore, some failure mechanisms were highlighted not only on the landside but also on the seaside. Overall, it is possible to say that, from the analyzes conducted, the actual coastal dikes are suitable but must be adapted to the future scenarios. Updating the structure, without the need to build new systems, allows to significantly reduce the costs and the time. However, it should be emphasized that the critical issues in some sections need to be further investigated. In addition, in all the lagoons it is essential to conduct more geotechnical analyzes to clearly identify the characteristics of the soil foundation and the coastal dike.

In conclusion, it is necessary to raise the coastal dike considering the subsidence effect and the sea level rise. This to create a sufficient freeboard and guarantee a safety condition against the embankment overlap. Then, it will be recommended to proceed with a re-profiling of the coastal dike to achieve geotechnical safety coefficients higher than the limit one. In addition to this, it is appropriate to carry out surveys and boreholes in order to define the soil characteristics along the entire defense system.

REFERENCES

- AGI, (1977). *"Raccomandazioni sulla programmazione ed esecuzione delle indagini geotecniche".*
- Autorità di Bacino del Fiume Po, *"Progetto di Piano stralcio per l'Assetto Idrogeologico (PAI)".*
- Autorità di Bacino del Fiume Po (2016). " *Piano per la valutazione e la gestione del rischio alluvioni*".
- ARPAV, (2006). "*Le lagune del Delta del Po: ecosistemi fragili*".
- *Baldin, G., & Crosato, F. (2017). "L'innalzamento del livello medio del mare a Venezia: eustatismo e subsidenza. ISPRA, Quaderni Ricerca Marina",* 10/2017.
- Consorzio di Bonifica Delta del Po, (2009). "*Quaderni 0 Ca' Vendramin, periodico del laboratorio internazionale delta e lagune*".
- Consorzio di Bonifica Delta del Po, (2011). "*1950-2010, 60 anni di bonifica nel Delta del Po. Emergenza ambientale nel Delta del Po*".
- Consorzio di Bonifica Delta del Po, (2015). "*Atlante lagunare costiero del Delta del Po*".
- D'Alpaos L. & Defina A., (2007). *"Mathematical modeling of tidal hydrodynamics in shallow lagoons: A review of open issues and applications to the Venice lagoon. Computers & Geosciences".*
- Da Deppo L., Datei C., Salandin P., (2019). *"Sistemazione dei corsi d'acqua".*
- Da Deppo L., Datei C., (2022). *"Manuale sulle difese dalle esondazioni e sulla chiusura delle rotte arginali".*
- Favaretto C., Martinelli L., Ruol P., (2021). *"A Spatial Structure Variable Approach to Characterize Storm Events for Coastal Flood Hazard Assessment".* Water, 13 (18), 2556.
- Ferrarin C., Chiggiato J., Bajo M., Schroeder K., Zaggia L., Benetazzo A., (2020). "*VENEZIA: l'acqua alta eccezionale del 12/11/2019. Analisi preliminare dei dati e descrizione della fenomenologia*".
- https://www.isprambiente.gov.it
- https://www.comune.venezia.it
- IPCC, (2019). "*Special Report on the Ocean and the Cryosphere in a Changing Climate*", Ch. 4 "*Sea Level Rise and Implications for Low-Lying Island, Coasts and Communities*".
- IPCC, (2019). "*Special Report on the Ocean and the Cryosphere in a Changing Climate*, *Sintesi per decisori politici*".

- Little A.L., *"Geotechnical investigations for embankment dams"*, International society for soil mechanic and geotechnical engineering.
- Lo Presti D., (2020). *"Use of cone penetration tests for soil profiling and design of shallow and deep foundations".*
- Maicu, F., De Pascalis, F., Ferrarin, C., & Umgiesser, G., (2018). "*Hydrodynamics of the Po River-Delta-Sea system. Journal of Geophysical Research: Oceans*".
- Ministero delle infrastrutture e dei trasporti (2018). *"Aggiornamento delle norme tecniche per le costruzioni".*
- Regione del Veneto (2018). *"Area interna contratto di foce Delta del Po".*
- Ris R.C., Holthuijsen L.H. & Booij N. (1994). "*Coastal Engineering", Ch. 5 "A spectral model for waves in the near shore zone.*".
- Ris R.C., Holthuijsen L.H. & Booij N. (1994). "*Coastal Engineering", Ch. 53 "The SWAN wave model for shallow water.*".
- Robertson P.K., (2010). *"Soil Behavior Type from the CPT: an update".*
- Viero D.P., D'Alpaos A., Carniello L. & Defina A., (2012). "*Un modello idrodinamico accoppiato per la simulazione di rotte arginali in contesti fluviali*", XXXIII Convegno Nazionale di Idraulica e Costruzioni Idrauliche.